

AD6222797

ABSORPTION COEFFICIENTS OF HEATED AIR: A COMPILATION TO 24,000°K

Volume I

D. R. Churchill, B. H. Armstrong,
and K. G. Mueller

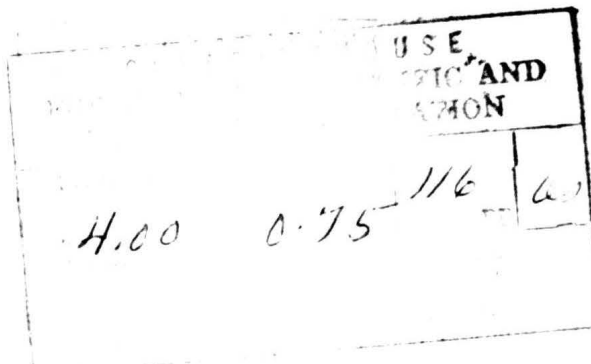
Lockheed Palo Alto Research Laboratory
Lockheed Missiles & Space Company
Palo Alto, California

Contract AF 29(601)-6320

TECHNICAL REPORT NO. AFWL-TR-65-132, Vol. I

October 1965

AIR FORCE WEAPONS LABORATORY
Research and Technology Division
Air Force Systems Command
Kirtland Air Force Base
New Mexico



Research and Technology Division
AIR FORCE WEAPONS LABORATORY
Air Force Systems Command
Kirtland Air Force Base
New Mexico

When U. S. Government drawings, specifications, or other data are used for any purpose other than a definitely related Government procurement operation, the Government thereby incurs no responsibility nor any obligation whatsoever, and the fact that the Government may have formulated, furnished, or in any way supplied the said drawings, specifications, or other data, is not to be regarded by implication or otherwise, as in any manner licensing the holder or any other person or corporation, or conveying any rights or permission to manufacture, use, or sell any patented invention that may in any way be related thereto.

This report is made available for study with the understanding that proprietary interests in and relating thereto will not be impaired. In case of apparent conflict or any other questions between the Government's rights and those of others, notify the Judge Advocate, Air Force Systems Command, Andrews Air Force Base, Washington, D. C. 20331.

DDC release to OTS is authorized.

AFWL-TR-65-132, Vol. I

**ABSORPTION COEFFICIENTS OF HEATED
AIR: A COMPILATION TO 24,000°K**

Final Report

Volume I

**D. R. Churchill, B. H. Armstrong,
and K. G. Mueller**

**Lockheed Palo Alto Research Laboratory
Lockheed Missiles & Space Company
Palo Alto, California
Contract AF 29(601)-6320**

TECHNICAL REPORT NO. AFWL-TR-65-132, Vol. I

FOREWORD

This report was prepared by members of the Physical Sciences Laboratory of Lockheed Missiles and Space Company, Palo Alto, California, under Contract AF 29(601)-6320. The work was performed under Program Element 7.60.06.01.D, Project 5710, Subtask 07.003, and was funded by the Defense Atomic Support Agency (DASA). This effort was carried out at the Palo Alto Research Laboratories during the period from 1 April 1964 to 30 July 1965. The report was submitted on 20 September 1965 by the AFWL Project Officer, Lt Fred J. Reule (WLRTH).

Volume I of this report presents a discussion of absorption processes and an equilibrium code. Volume II is the compilation of the absorption coefficients of heated air.

A list of major contributors to this effort follows:

B. H. Armstrong — Organized and served as consultant on the atomic photoionization calculations and co-authored the report.

D. R. Churchill — Coordinated the various contributions, compiled the tables, calculated the molecular contributions, and co-authored the report.

D. J. Colvin — Programmed portions of the computer code multiplet and obtained the occupation numbers for the multiplet components of the energy levels of atomic nitrogen and oxygen.

S. A. Hagstrom — Served as consultant on molecular radiative processes.

R. R. Johnston — Developed the PIC code which computes the photoionization absorption in atomic nitrogen and oxygen. Developed or adapted the requisite theory.

H. R. McChesney — Carried out the extensive species concentration calculations and obtained the molecular Boltzmann fractions. This work was based in part on that of F. R. Gilmore at Rand (see text).

K. G. Mueller — Provided the absorption coefficients for NO_2 , O^- photodetachment, and free-free processes. (Z. Taulbee carried out the necessary machine computations.) Authored the sections on those contributions.

R. W. Nicholls — Provided the molecular band intensities and served as consultant.

O. R. Platas — Carried out the extensive photoionization calculations with the aid of the PIC program.

This report has been reviewed and is approved.

Fred J. Reule

FRED J. REULE
2Lt USAF
Project Officer

Ralph H. Pennington

RALPH H. PENNINGTON
Lt Colonel USAF
Chief, Theoretical Branch

William H. Stephens

WILLIAM H. STEPHENS
Colonel USAF
Chief, Research Division

ABSTRACT

An extensive tabulation of absorption coefficients of heated air has been carried out with the aid of several large digital computer programs. These tables supersede the previous ones computed at Lockheed by Meyerott, Sokoloff, and Nicholls in 1959. Tables are presented for temperatures at every 1000°K between 1000°K and $24,000^{\circ}\text{K}$ and for eight densities between ten times normal atmospheric to 10^{-6} times normal. Absorption coefficients are individually listed for each of 14 contributing absorbers. The photon energy range is 0.6-10.7 eV with a partition interval of 0.1 eV.

CONTENTS

| Section | | Page |
|---------|---|------|
| I | INTRODUCTION | 1 |
| II | ABSORPTION BY DIATOMIC MOLECULES | 4 |
| | 2. 1 Line Absorption | 4 |
| | 2. 2 The Contributing Band Systems | 14 |
| | 2. 3 The O ₂ Schumann-Runge Continuum | 21 |
| III | ABSORPTION BY ATOMS | 23 |
| | 3. 1 Energy Levels and Occupation Numbers | 23 |
| | 3. 2 Atomic Photoionization Absorption | 34 |
| | 3. 3 The Low-Energy Theory | 39 |
| | 3. 4 The High-Energy Theory | 44 |
| | 3. 5 The Approximate Photoionization Cross Section | 47 |
| IV | MISCELLANEOUS CONTRIBUTIONS TO THE ABSORPTION | 49 |
| | 4. 1 NO ₂ Absorption | 49 |
| | 4. 2 O ⁻ Photo Detachment | 52 |
| | 4. 3 Free-Free Absorption | 56 |
| V | DISCUSSION | 61 |
| | 5. 1 General Remarks | 61 |
| | 5. 2 Comparison With Meyerott, Sokoloff, and Nicholls | 61 |
| | 5. 3 The Atomic Photoionization Contribution | 63 |
| | 5. 4 Recommended Improvements for Future Compilations | 70 |
| VI | REFERENCES | 72 |

| Appendix | | Page |
|---------------------|--|-------------|
| A | AN EQUILIBRIUM CODE | 77 |
| | A. 1 Introduction | 77 |
| | A. 2 Description of the Chemical System | 78 |
| | A. 3 Thermodynamic Relations | 81 |
| | A. 4 Equilibrium Composition | 83 |
| | A. 5 Equilibrium Code | 86 |
| | A. 6 References | 88 |
| | A. 7 Digital Computer Program Listings | 90 |
| DISTRIBUTION | | 105 |

ILLUSTRATIONS

| Figure | | Page |
|--------|---|------|
| 1 | Mass Absorption Coefficient and Cross Section of NO ₂ | 50 |
| 2 | Photodetachment Cross Section of O ⁻ | 54 |
| 3 | Table Grid (Schematic) | 59 |
| 4 | Absorption Coefficient of Heated Air vs. Photon Energy (T = 12,000°K . $\rho/\rho_0 = 1$) | 62 |
| 5 | Linear Spectral Absorption Coefficient of Air vs. Wavelength (T = 12,000°K . $\rho/\rho_0 = 10^0$) | 64 |
| 6 | Linear Spectral Absorption Coefficient of Air vs. Wavelength (T = 6000°K . $\rho/\rho_0 = 10^{-4}$) | 65 |
| 7 | Linear Spectral Absorption Coefficient of Air vs. Wavelength (T = 8000°K . $\rho/\rho_0 = 10^0$) | 66 |
| 8 | Linear Spectral Absorption Coefficient of Air vs. Wavelength (T = 8000°K . $\rho/\rho_0 = 10^{-6}$) | 67 |
| 9 | Linear Spectral Absorption Coefficient of Air vs. Wavelength (T = 24,000°K . $\rho/\rho_0 = 10^{-6}$) | 69 |
| 10 | Photoelectric Cross Section (Sketch) | 69 |

TABLES

| Table | | Page |
|-------|---|------|
| I | Contributors to the Absorption Coefficient of Heated Air | 2 |
| II | Molecular Band Systems Included in the Calculation of the Absorption Coefficient of Heated Air | 14 |
| III | Spectroscopic Constants for the $X^1\Sigma_g^+$ State of N_2 | 17 |
| IV | Spectroscopic Constants for the $b'^1\Sigma_u^+$ State of N_2 | 18 |
| V | Franck-Condon Factors for the $N_2 (b'^1\Sigma_u^+ - X^1\Sigma_g^+)$ Birge-Hopfield No. 1 System | 20 |
| VI | The Absorption Coefficient of Oxygen at Selected Wavelengths | 22 |
| VII | Table of Atomic Core Configurations and Ionization Potentials | 24 |
| VIII | Occupation Number Fractions $p(J, s)$ for the States of Neutral Oxygen in Air. Column 1 lists the Spectroscopic Identification, Column 2 lists the energies, and Columns 3-8 list the Occupation Number Fractions | 29 |
| IX | NO_2 -Absorption Coefficient in cm^2/g | 51 |
| X | Cross Section for O^- Photodetachment | 55 |
| A -I | Molecular Composition of Dry Air | 87 |
| A -II | Thermodynamic Data | 89 |

Section I INTRODUCTION

The tables of absorption coefficients of heated air presented in this report are intended to supersede the previous compilation of Meyerott, Sokoloff, and Nicholls (Ref. 1). Their format for presentation of the absorption coefficients will be followed here, since it allows the user to conveniently select the important contributors from the listed individual absorbers at any temperature, density, and photon energy. Differences between the two calculations are extensive, and reflect the advances made in the field of opacity since the MSN calculations were performed in 1959. Improved digital computer techniques have been used to theoretically reconstruct the line spectra for the molecular band systems which are included in the present tables, where the previous calculation had lumped the entire band contribution at band-head energy. Recent experimental results and analyses have made available improved f numbers and Franck-Condon factors. Atomic photoionization calculations have been advanced significantly since 1959 by the work of a number of investigators, allowing us to greatly improve over the crude version of the hydrogenic model of photoionization employed by MSN.

Since the present tables are the result of a series of large digital computer programs, it has been relatively simple to extend the tables to 24,000°K, thus providing much needed information in regions where little has been available, and to refine the energy partition.

The contributors to the heated air absorption which have been included in our calculation are listed in Table I.

Table I. Contributors to the Absorption Coefficient of Heated Air

- 1. Schumann-Runge bands of O_2
- 2. First positive bands of N_2
- 3. Second positive bands of N_2
- 4. First negative bands of N_2^+
- 5. Beta bands of NO
- 6. Gamma bands of NO
- 7. Vibration-rotation bands of NO
- 8. Birge-Hopfield No. 1 bands of N_2

- 9. Schumann-Runge continuum of O_2
- 10. NO_2
- 11. O^- photodetachment
- 12. Free-free in the presence of ions

- 13. Atomic nitrogen photoionization
- 14. Atomic oxygen photoionization

These may be separated into three groups according to their method of treatment in the calculation. Contributors one through eight arise from bound-bound transitions in diatomic molecules and were treated through the extensive SACHA (Refs. 2-4) digital computer programs. Contributors 13 and 14 were computed with the large PIC computer program (Ref. 5). The rest were entered into the calculation in a semi-empirical fashion and might be called continuum and pseudo-continuum processes, even though discrete transitions may have been included for NO_2 , (Ref. 6). A special computer code was written to collate the results into the desired format and print out the tables.

Theoretical construction of the contributions from bands and continua of diatomic molecules is discussed in Section II, absorption arising from photoionization of atomic nitrogen and oxygen is discussed in Section III, and the remaining processes are covered in Section IV. Comments on the results are contained in Section V. The bulk of the report is contained in the form of tables of absorption coefficients; these appear in Volume II. The equilibrium code which was used in these calculations is discussed in Appendix A.

Section II

ABSORPTION BY DIATOMIC MOLECULES

2.1 LINE ABSORPTION

The line absorption coefficient for a radiative transition between two nondegenerate levels L (lower) and U (upper) may be written (Ref. 7)

$$\mu_{LU}(\nu) = N_L B_{LU} h \nu_{LU} F(\nu) \quad (2.1)$$

where ν_{LU} is the Bohr frequency of the line in cm^{-1} , N_L is the particle number density (number of particles per unit volume) in the lower level, B_{LU} is the Einstein coefficient for absorption, and $F(\nu)$ is a line shape factor normalized such that $\int F(\nu) d\nu = 1$.

To determine the quantities on the right-hand side of Eq. (2.1), the energy levels, selection rules, and wave functions (or transition probabilities) must be found by application of the laws of quantum mechanics to the system under investigation, which in this case is a diatomic molecule. The theoretical approach is to effect a separation of Schrödinger's equation by assuming there to be no interaction between the modes of nuclear vibration, rotation, and electronic motion. This method is known as the Born-Oppenheimer approximation. Once the necessary theoretical expressions are obtained, they may be corrected for small interactions.

Theoretical investigations on diatomic molecules are less complicated than those on polyatomic molecules because of the added vibrational modes, rotational asymmetries, and the larger number of possible electronic states generally associated with the latter. However, purely theoretical approaches yield much less satisfactory results for diatomic molecules than for atoms, particularly when accurate wave functions are desired.

The electronic, vibrational, and rotational energies of a diatomic molecule are quantized (we are not concerned with the unquantized translational energy in the radiation problem). Of the set of quantum numbers which specify a given level, the magnetic quantum number M (the Z component of the total angular momentum quantum number J) may be omitted from the expression for the absorption coefficient which is applicable to a gas of randomly oriented absorbers since the magnetic quantum number specifies the orientation in space and is therefore eliminated by the usual procedure of averaging over initial sub-levels and summing over the final ones. In addition, the spin quantum number S enters in a nonessential way since spin is unaffected in the electric dipole transitions we are considering here.

The Einstein Coefficients B_{LU} . Electronic transitions in diatomic molecules will, in accord with spectroscopic convention (Ref. 8), be labeled by $n', v', J' - n'', v'', J''$, where n denotes the electronic state and v and J are the vibrational and rotational quantum numbers, respectively. Double primes refer to lower levels and single primes to upper levels. As applied to transitions in diatomic molecules, the Einstein coefficient for absorption is given by (Ref. 8)

$$B_{n'', v'', J'', n', v', J'} = \frac{8\pi^3}{3h^2c} \frac{\sum_{M', M''} |R^{M', M''}|^2}{2J'' + 1} \quad (2.2)$$

where

$$R^{M', M''} = \int \bar{\Psi}_{n'', v'', J'', M''}^* \bar{R} \Psi_{n', v', J', M'}^* d\tau \quad (2.3)$$

is the matrix element of the electric dipole moment $\bar{R} = \bar{R}_e + \bar{R}_{nuc.}$ of the electrons and nuclei. M' and M'' label the spatially degenerate components of the upper and lower rotational levels and the summation is over all possible combinations of M' and M'' .

We assume validity of the Born-Oppenheimer approximation in the form wherein the molecular wave function may be expressed as a product of electronic, vibrational, and rotational wave functions, viz:

$$\Psi = \Psi_e \Psi_v \Psi_{\text{rot}} \quad (2.4)$$

with this approximation, the expression for the matrix element becomes

$$\begin{aligned} R^{M', M''} &= \int (\overline{\Psi_e'' \Psi_v'' \Psi_{\text{rot}}''}) \overline{R} (\Psi_e' \Psi_v' \Psi_{\text{rot}}') d\tau \\ &= \int (\overline{\Psi_v'' \Psi_{\text{rot}}''}) \overline{R}_e(r) (\Psi_v' \Psi_{\text{rot}}') d\tau_{v \text{rot}} \end{aligned} \quad (2.5)$$

where $R_e(r) = \int \Psi_e'' \overline{R} \Psi_e' d\tau_e$ is the electronic electric-dipole transition moment, and Ψ_e is assumed to vary slowly with the nuclear separation coordinate, r . Since the electronic wave functions are orthogonal, the nuclear part of \overline{R} does not contribute to $R_e(r)$.

The sum in Eq. (2.2) may now be expressed in the form [cf, Penner (Ref. 9, p. 129)]

$$\sum_{M', M''} |R^{M', M''}|^2 = (v'' | R_e(r) | v')^2 S_{J'', J'} \quad (2.6)$$

where $S_{J'', J'}$ is the so-called Hönl-London factor, which contains all the angular dependence. Following Nicholls and Stewart (Ref. 10), we adopt the term band strength for the other factor, as suggested by Chamberlain (Ref. 11), with the definition

$$S_{v', v''} \equiv (v'' | R_e(r) | v')^2 \quad (2.7)$$

According to Fraser (Ref. 12), it is possible to rewrite this as

$$S_{v', v''} = R_e^2(\bar{r}_{v', v''}) q(v', v'') \quad (2.8)$$

under many circumstances, and for many band systems. In Eq. (2.8),

$$q(v', v'') \equiv |\int \Psi_{v'} \Psi_{v''} dr|^2 \quad (2.9)$$

is the Franck-Condon factor for the band and

$$\bar{r}_{v', v''} = \frac{\int \Psi_{v'} r \Psi_{v''} dr}{\int \Psi_{v'} \Psi_{v''} dr} \quad (2.10)$$

is the corresponding r-centroid (Ref. 13).

Accurate calculations of the electronic transition moments are not available for the molecules of interest to this study. In general, lacking these calculations, recourse must be made to experiment for the determination of the "absolute" values of these quantities. Experimental band strength information is not available for most of the bands present in heated air, however, and the desired $S_{v', v''}$'s must be estimated. These estimates are usually obtained in the following manner.

From the available measurements for one or more bands (v', v'') of a band system, and with the aid of calculated Franck-Condon factors, the $R_e(\bar{r}_{v', v''})$'s are calculated by means of Eq. (2.8). Using these values of R_e , a smooth curve is drawn from which the desired values of $R_e(\bar{r}_{v', v''})$ are obtained for the various bands. Multiplication by the appropriate Franck-Condon factors then yields a corresponding set of band strengths, $S_{v' v''}$. This procedure is practical because $R_e(\bar{r})$ is usually a relatively slowly varying function of \bar{r} . (Franck-Condon factors, on the other hand, vary over several orders of magnitude for each band system considered here.) In a recent

review article, Nicholls (Ref. 14) gave an extensive discussion of the basic theory outlined above and presented tables of band strengths for many band systems of air molecules. We have drawn heavily upon this article for the present study.

The procedure for obtaining the matrix elements [Eq. (2.3)] for vibration-rotation transitions in diatomic molecules differs from that discussed above, and is fully discussed for the one vibration-rotation band system included in the present calculation by Churchill and Hagstrom (Ref. 4).

The number densities or occupation numbers N_L . The particle number density in the lower level (often called the occupation number) is given by the usual expression (Ref. 15)

$$N_{n'', v'', J''} = \frac{N(2J'' + 1)\omega_I \exp \left[\frac{-E_{n'', v'', J''}}{kT} \right]}{Q} \quad (2.11)$$

where N is the total number density for all levels, $E_{n'', v'', J''}$ is the energy of the level and ω_I its nuclear spin statistical weight. Q is the total partition function and may be written as the sum of contributions from all the electronic states:

$$Q = \sum_n Q_n \quad (2.12)$$

Taking into account electronic (orbital + spin), vibrational, rotational, and nuclear (spin only) degrees of freedom, we may write

$$Q_n = Q_{\text{electronic}} Q_{\text{vib-rot}} Q_{\text{nuclear}} \quad (2.13)$$

where

$$Q_{\text{electronic}} = \omega_A (2S + 1) \exp \left[\frac{-\nu_{\text{oo}} hc}{kT} \right] \quad (2.14)$$

$$Q_{\text{vib-rot}} = \sum_{v=0}^{\infty} \exp \left[\frac{-G_o(v)hc}{kT} \right] Q_{\text{rot}}^{(v)} \quad (2.15)$$

$$Q_{\text{rot}}^{(v)} = \int_0^{\infty} (2J + 1) \exp \left[\frac{-F_v(J)hc}{kT} \right] dJ \cong \frac{kT}{hcB_v} \quad (2.16)$$

$$Q_{\text{nuclear}} = \frac{(2I_a + 1)(2I_b + 1)}{\sigma} \quad (2.17)$$

In these formulas ν_{00} is the energy of the $v'' = 0$ to the $v' = 0$ transition of the electronic states in question, $G_o(v)$ is the vibrational term referred to the lowest vibrational level, $F_v(J)$ is the rotational term for the v^{th} vibrational level with B_v its corresponding rotational constant, and S is the total electron spin. ω_{Λ} is the statistical weight for orbital angular momentum Λ about the internuclear axis and takes the value 1 if $\Lambda = 0$ and value 2 if $\Lambda \neq 0$. I_a and I_b are the nuclear spins of the two nuclei and σ is a symmetry number having the value 2 for homonuclear molecules and 1 for heteronuclear systems.

We have made use of an approximate formula for $Q_{\text{vib-rot}}$ that is more convenient for calculation and yet accurate enough for our problem. This formula was developed by Bethe (Ref. 16) and later corrected by Brinkley, et al. (Ref. 17).

$$Q_{\text{vib-rot}} = \frac{1}{1 - \exp \left(\frac{-1.4388\omega_o}{T} \right)} \frac{T}{1.4388B_o} (1 + \gamma T) \quad (2.18)$$

where γ , Bethe's correction factor for anharmonicity and non-rigidity, has the value

$$\gamma = \frac{1}{1.4388\omega_o} \left(\frac{2\omega_o x_o}{\omega_o} + \frac{\alpha_o}{B_o} + \frac{8B_o}{\omega_o} \right) \quad (2.19)$$

Here ω_o and B_o are the vibrational and rotational constants of the $v = 0$ vibrational level, $\omega_o x_o$ is the first anharmonic constant and α_o is the interaction constant for coupling between rotation and vibration.

Returning now to Eq. (2.11), we multiply numerator and denominator by Q_n as given by Eqs. (2.13), (2.14), and (2.17) and obtain after a little algebra

$$N_{n''v''J''} = N_{\text{total}} \frac{Q_{n''}}{Q_{\text{total}}} \frac{\omega_I(2J'' + 1) \exp \left[- \{G_o(v'') + F_{v''}(J'')\} \frac{hc}{kT} \right]}{(2S + 1) \omega_A Q_{\text{nuclear}} Q_{\text{vib-rot}}} \quad (2.20)$$

where use has been made of the relation

$$E_{n''v''J''} = [v_{\infty} + G_o(v'') + F_{v''}(J'')] hc. \quad (2.21)$$

Now let $P_{n''} = Q_{n''}/Q_{\text{total}}$ denote the fractional population of the n''^{th} electronic state and introduce the notation

$$H_{n'n'', v'v', J'J''} = \frac{8\pi^2 L_o}{3hc} \frac{\omega_I}{(2S + 1) \omega_A Q_{\text{nuclear}}} v_{n'n'', J'J'', v'v''} S_{v'}, v'' S_{J''}, J' \quad (2.22)$$

and

$$E_{v''J''} = [G_o(v'') + F_{v''}(J'')] \frac{hc}{k} \quad (2.23)$$

where $L_o = 2.6875 \times 10^{19}$ particles/cm³ is Loschmidt's number.

We now obtain the desired form of Eq. (2.1) by substitution, using Eqs. (2.20), (2.22), and (2.23):

$$\mu(\nu) = \left[\frac{N_{\text{total}} P_{n''}}{L_o Q_{\text{vib-rot}}} \right] H_{n'n'', v'v'', J'J''} \exp \left(\frac{-E_{v''J''}}{T} \right) \pi F(\nu) \quad (2.24)$$

Here the quantities H and E are characteristic of the isolated molecule; i.e., do not depend on the temperature and density. Since the bracketed term in (2.24) is dimensionless, H has dimensions cm^{-2} , and $F(\nu)$ has dimensions cm , the absorption coefficient $\mu(\nu)$ has the required dimension cm^{-1} .

The foregoing equations have been incorporated into the digital computer programs which reconstruct the absorption spectra of the important band systems of heated air. These band systems will be discussed a little further on.

Species concentrations and Boltzmann factors for the electronic states of diatomic air molecules are computed by a separate program known as the Equilibrium code. The results of this computation, which is discussed in Appendix B, are provided to the other programs on a magnetic tape for digital computer use.

The average absorption coefficient and the line shape factor $F(\nu)$. The absorption coefficient, as required in the strict development of the equation of radiative transfer, is a continuous function of frequency. However, it is rarely possible to make use of such monochromatic values of the absorption coefficient in practical problems concerning the flow of radiative energy from one location to another because of the mathematical complexity of such problems. Their practical solution is usually undertaken with the aid of appropriately chosen "average" absorption coefficients which are assumed constant over some suitable frequency interval. In addition, the shape of molecular lines, as represented by the line shape factor $F(\nu)$, are not yet well known as functions of temperature and density. A number of specific line broadening mechanisms have been studied (Ref. 18) both experimentally and theoretically. However, the uncertainties of the general problem are such as to make it inadvisable to include such partial information in an absorption coefficient study which covers such a broad range of temperatures and densities as does the present one. For the reasons outlined above we make use of a frequency averaging procedure in our calculations so that we do not present monochromatic absorption coefficients. Even with this enormous simplification, the amount of data to be computed and presented is very large and requires extensive use

of large digital computer facilities. Again, due to the complexity of the radiative transfer equation, it is not possible to specify a priori the nature and magnitude of the errors which will arise from our frequency averaging procedures. Such errors will, of course, depend on the particular application, and the reader is cautioned to bear in mind the limitations inherent in the use of our results, particularly in connection with problems involving large optical depths.

The averaging procedure. Suppose α denotes a set of numbers which completely specifies the transition from which a given line arises. We are concerned with a large but finite collection of such sets of numbers and so we can order these arbitrarily. Labeling the line L-U with the vector α , Eq. (2.11) may be written

$$\mu_\alpha(\nu) = N_\alpha B_\alpha h\nu_\alpha F_\alpha(\nu) \quad (2.25)$$

The reason for the change in notation becomes clear when we define an average absorption coefficient which pertains to a frequency interval $\Delta\nu$:

$$\bar{\mu}^{\Delta\nu} \equiv \frac{1}{\Delta\nu} \int_{\Delta\nu} \mu(\nu) d\nu \quad (2.26)$$

and, since

$$\mu(\nu) = \sum_{\alpha} \mu_{\alpha}(\nu) + \mu_c(\nu) \quad (2.27)$$

where μ_c is the contribution from continuum transitions, then

$$\begin{aligned} \bar{\mu}^{\Delta\nu} &= \frac{1}{\Delta\nu} \int_{\Delta\nu} \left[\sum_{\alpha} \mu_{\alpha}(\nu) + \mu_c(\nu) \right] d\nu \\ &= \frac{1}{\Delta\nu} \sum_{\alpha} N_{\alpha} B_{\alpha} h\nu_{\alpha} \int_{\Delta\nu} F_{\alpha}(\nu) d\nu + \bar{\mu}_c^{\Delta\nu} \end{aligned} \quad (2.28)$$

We now assume that lines whose Bohr frequencies lie outside the frequency interval $\Delta\nu$ do not contribute to the average absorption coefficient for that interval. The error introduced by this assumption* is reduced by taking $\Delta\nu$ large enough so that many lines are contained therein. Furthermore, the average defined in Eq. (2.26) is generally used only in calculations which apply to optically thin materials where the lines remain relatively narrow, and so do not contribute appreciably to frequencies which differ from the Bohr frequency.

It is then reasonable to assume that

$$\int_{\Delta\nu} F_{\alpha}(\nu) d\nu \cong \int_0^{\infty} F_{\alpha}(\nu) d\nu = 1 \quad (2.29)$$

and Eq. (2.28) takes on the simple form

$$\bar{\mu}^{\Delta\nu} = \frac{1}{\Delta\nu} \sum_{\alpha} N_{\alpha} B_{\alpha} h \nu_{\alpha} + \bar{\mu}_c^{\Delta\nu} \quad (2.30)$$

where the sum is taken over those lines whose maxima fall within $\Delta\nu$.

The sum appearing in the preceding expression may be partitioned into sub-sums according to molecular species, particular band system, etc. In this report we are concerned with contributions from individual band systems and the appropriate partition has been made.

*In the sense of a direct average, not a harmonic average such as, for example, the Rosseland mean. For this latter type of average our procedure actually increases the error.

2.2 THE CONTRIBUTING BAND SYSTEMS

2.2.1 Band Systems Included in the Calculation

The molecular band systems which have been included in the calculation are listed in Table II. Details of the theoretical reconstruction of all of these band systems except one have been given in previous publications (Refs. 2-4) and therefore will not be repeated here. The exception is the Birge-Hopfield No. 1 system of N_2 which will be discussed next. It should be noted, however, that one of the above-cited references (Ref. 3) gives an expression for the line intensity factor, to be applied to the N_2 first positive system, which contains Hönl-London factors that do not apply to that system (i.e., they are incorrect). The correct Hönl-London factors were actually used in the calculations and are given in Ref. 2.

Table II. Molecular Band Systems Included in the Calculation of the Absorption Coefficient of Heated Air

| Band System Number | Molecular Species and System Name | Transition in Spectroscopic Notation | Total Number of Lines Included in the Calculation for This Band System |
|--------------------|-----------------------------------|--------------------------------------|--|
| 1 | O_2 Schumann-Runge | $B^3\Sigma_u^- - X^3\Sigma_g^-$ | 4,611 |
| 2 | N_2 first positive | $B^3\Pi_g - A^3\Sigma_u^-$ | 48,785 |
| 3 | N_2 second positive | $C^3\Pi_u - B^3\Pi_g$ | 20,369 |
| 4 | N_2^+ first negative | $B^2\Sigma_u^+ - X^2\Sigma_g^+$ | 3,216 |
| 5 | NO beta | $B^2\Pi - X^2\Pi$ | 18,518 |
| 6 | NO gamma | $A^2\Sigma - X^2\Pi$ | 31,429 |
| 7 | NO vibration-rotation | $X^2\Pi - X^2\Pi$ | 25,610 |
| 8 | N_2 Birge-Hopfield No. 1 | $b'^1\Sigma_u^+ - X^1\Sigma_g^+$ | 38,983 |

The spectral atlases for all of these systems have been merged into a master air atlas to be used in this and other calculations. This atlas contains the following information for each line to be included in the air computation: the frequency, H factor (described previously), and identification vector. The identification vector permits lines to be selected according to their band system so that the proper temperature-density dependent factor may be applied to account for the particle population density in the lower state of the transition.

The band strengths which were used in the reconstruction of the first 6 systems listed in Table II were taken directly from a compilation by Nicholls (Ref. 14). Otherwise, the spectroscopic constants used in the reconstruction of the first seven listed systems remain the same as for previous calculations (Refs. 2-4).

2.2.2 The Birge-Hopfield No. 1 Band System of N_2

The vacuum ultraviolet spectrum of N_2 is very complicated, with a large number of band systems having been identified (Ref. 19). Spectroscopic constants are available for some of these, including the Birge-Hopfield No. 1 bands (Ref. 20) which arise from transitions between the ground electronic state $X^1\Sigma_g^+$ and the excited state $b^1\Sigma_u^+$. Since these bands are relatively strong in absorption and extend to longer wavelengths ($\sim 1650 \text{ \AA}$) than most of the others, they were included in the present calculation. The Birge-Hopfield No. 2 band system, which lies in the same frequency region, was not included. Further remarks on this omission will be reserved for Section V.

Since both states involved in the Birge-Hopfield No. 1 transitions are $^1\Sigma$'s, the structure of the band system is simple. Each band consists of a single R and a single P branch (since $\Delta J = 0$ is forbidden for $\Sigma - \Sigma$ transitions, there is no Q branch).

Line frequencies for these bands may be calculated by use of the relation

$$\nu_{n'n'', v'v'', J'J''} = \nu_{\infty} + [G_o(v') - G_o(v'')] + [F_v(J') - F_{v''}(J'')] \quad (2.31)$$

where ν_{∞} is the term* for the $v'' = 0 \rightarrow v' = 0$ rotationless transition, $G_o(v)$ is the vibrational term of the v^{th} level where the first vibrational level is $v = 0$, and $F_v(J)$ is the rotational term for the v^{th} level. For the R branch terms, $J' = J + 1$; for the P branch terms, $J' = J'' - 1$.

Rotational terms are computed for both states from the expression (Ref. 8)

$$F_v(J) = B_v J(J + 1) - D_v J^2(J + 1)^2 \quad (2.32)$$

Observed and calculated values of the rotational constants B_v and D_v are given by Lofthus (Ref. 20) for the $X^1\Sigma_g^+$ state up to $v'' = 15$. He also gives $G_o(v)$ up to $v'' = 20$.

We have used the formula of Wilkinson as given by Lofthus (Ref. 20) to obtain values of B_v for v'' up to 27 for the $X^1\Sigma_g^+$ state, and we have used the formula of Lofthus (Ref. 20) to obtain values of $G_o(v)$, also to $v'' = 27$. D_v was assumed constant (at the observed value of $6 \times 10^{-6} \text{ cm}^{-1}$ for $v'' = 15$) for all $v'' \geq 15$.

Table III lists the spectroscopic constants for the $X^1\Sigma_g^+$ electronic state which were used in our calculation. ν_{∞} was taken to be $103,672.1 \text{ cm}^{-1}$ as given by Lofthus (Ref. 20). The maximum allowable value of J was set to 100 for our calculation.

*The word "term" is used in molecular spectroscopy to denote an energy expressed in the dimension cm^{-1} .

Table III. Spectroscopic Constants for the $X^1\Sigma_g^+$ State of N_2

| v | $G_0(v)$ (cm $^{-1}$) | B_v (cm $^{-1}$) | D_v (cm $^{-1}$) |
|-----|---------------------------|------------------------|------------------------|
| 0 | 00.00 | 1.9898 | 6.4×10^{-6} * |
| 1 | 2329.66 | 1.9720 | 5.0×10^{-6} |
| 2 | 4630.83 | 1.9548 | 5.0×10^{-6} |
| 3 | 6903.44 | 1.9364 | 5.5×10^{-6} |
| 4 | 9147.41 | 1.9186 | 5.5×10^{-6} |
| 5 | 11362.67 | 1.9008 | 5.5×10^{-6} |
| 6 | 13549.14 | 1.8829 | 5.0×10^{-6} |
| 7 | 15706.76 | 1.8651 | 5.0×10^{-6} |
| 8 | 17835.44 | 1.8473 | 5.0×10^{-6} |
| 9 | 19935.11 | 1.8295 | 5.0×10^{-6} |
| 10 | 22005.70 | 1.8117 | 5.0×10^{-6} |
| 11 | 24047.13 | 1.7939 | 5.3×10^{-6} |
| 12 | 26059.33 | 1.7761 | 5.5×10^{-6} |
| 13 | 28042.23 | 1.7583 | 5.5×10^{-6} |
| 14 | 29995.74 | 1.7405 | 6.0×10^{-6} |
| 15 | 31919.80 | 1.7227 | 6.0×10^{-6} |
| 16 | 33814.33 | 1.7048 | 6.0×10^{-6} |
| 17 | 35679.26 | 1.6870 | 6.0×10^{-6} |
| 18 | 37514.51 | 1.6692 | 6.0×10^{-6} |
| 19 | 39320.01 | 1.6514 | 6.0×10^{-6} |
| 20 | 41095.68 | 1.6336 | 6.0×10^{-6} |
| 21 | 42841.45 | 1.6158 | 6.0×10^{-6} |
| 22 | 44557.25 | 1.5980 | 6.0×10^{-6} |
| 23 | 46242.99 | 1.5802 | 6.0×10^{-6} |
| 24 | 47898.61 | 1.5624 | 6.0×10^{-6} |
| -5 | 49524.03 | 1.5446 | 6.0×10^{-6} |
| 26 | 51119.17 | 1.5267 | 6.0×10^{-6} |
| 27 | 52683.97 | 1.5089 | 6.0×10^{-6} |

*Observed value.

For the $b' 1\Sigma_u^+$ upper electronic state, the spectroscopic constants were calculated from formulas due to Lofthus (Ref. 20), which give good agreement with the available experimental data. Of the eight observed vibrational levels in this state, seven have been included in our calculation.

The single omission is the highest ($v'' = 7$) observed level; no Franck-Condon factors were available for this level. Table IV lists the constants employed in the calculations for this state.

Table IV. Spectroscopic Constants for the $b' 1\Sigma_u^+$ State of N_2

| v | $G_0(v)$ (cm $^{-1}$) | B_v (cm $^{-1}$) | D_v (cm $^{-1}$) |
|-----|---------------------------|------------------------|------------------------|
| 0 | 0.0 | 1.1515 | 1.104×10^{-5} |
| 1 | 742.0 | 1.146 | 1.137×10^{-5} |
| 2 | 1474.4 | 1.142 | 1.169×10^{-5} |
| 3 | 2196.7 | 1.137 | 1.202×10^{-5} |
| 4 | 2909.8 | 1.132 | 1.234×10^{-5} |
| 5 | 3613.2 | 1.128 | 1.267×10^{-5} |
| 6 | 4307.0 | 1.123 | 1.299×10^{-5} |

We now turn to a discussion of the line intensities associated with these bands.

Since nitrogen nuclei obey Bose statistics ($I = 1$), the symmetric levels will have the higher statistical weight (Ref. 8)

$$W_I(s) = (2I + 1)(I + 1) = 6$$

and the antisymmetric levels will have the lower statistical weight

$$W_I(a) = (2I + 1)I = 3$$

For the $^1\Sigma$ state, rotational levels belonging to even J are symmetric and those belonging to odd J are antisymmetric. Consequently, there is an intensity alternation with the progression of J .

The value of Q_{nuclear} for this band system is $9/2$, so the final expressions for the H function become:

$$H_{v'v'', J'J''} = \frac{16\pi^2 L_0}{9hc} \nu_{v'v'', J'J''} |R_e|^2 q(v'v'') S_{J'J''} \quad (2.33)$$

where $|R_e|^2 q(v'v'')$ replaces $S_{v'v''}$ to indicate the lack of band strength information, and $S_{J'J''}$ takes on the appropriate value from the following list:

- J'' even, R branch - $2(J'' + 1)$
- J'' odd, R branch - $(J'' + 1)$
- J'' even, P branch - $2J''$
- J'' odd, P branch - J''

The Franck-Condon factors used in this calculation were provided by Nicholls (Ref. 21) and are based on Morse potentials. Table V gives these values.

The value of $|R_e|^2$ used in this calculation was assumed to be that corresponding to an f-number of 0.1, solely on indirect experimental evidence (see discussion by Gilmore (Ref. 22)).

Equations 2.31 - 2.33 and 2.23 were incorporated into a digital computer code which was used to construct a spectral atlas for this system. This atlas was also merged into the SACHA air atlas mentioned previously.

Table V. Franck-Condon Factors For The N_2 ($b, ^1\Sigma_u^+ - X, ^1\Sigma_g^+$)
Birge-Hopfield No. 1 System

| v' | v'' | | | | | | | |
|----|----------|----------|----------|----------|----------|----------|----------|--|
| | 0 | 1 | 2 | 3 | 4 | 5 | 6 | |
| 0 | 2.1190-7 | 2.9921-6 | 2.1884-5 | 1.0971-4 | 4.2151-4 | 1.3171-3 | 3.4716-3 | |
| 1 | 2.7849-6 | 3.4604-5 | 2.2112-4 | 9.5936-4 | 3.1524-3 | 8.3013-3 | 1.8101-2 | |
| 2 | 1.8669-5 | 2.0290-4 | 1.1238-3 | 4.1742-3 | 1.1554-2 | 2.5089-2 | 4.3828-2 | |
| 3 | 8.5095-5 | 8.0341-4 | 3.8204-3 | 1.1986-2 | 2.7389-2 | 4.7522-2 | 6.3144-2 | |
| 4 | 2.9664-6 | 2.4137-3 | 9.7434-3 | 2.5373-2 | 4.6537-2 | 6.1416-2 | 5.6360-2 | |
| 5 | 8.4338-4 | 5.8603-3 | 1.9804-2 | 4.1831-2 | 5.9053-2 | 5.4340-2 | 2.7371-2 | |
| 6 | 2.0367-3 | 1.1957-2 | 3.3239-2 | 5.5152-2 | 5.5978-5 | 2.9782-2 | 3.0393-3 | |
| | 7 | 8 | 9 | 10 | 11 | 12 | 13 | |
| 0 | 7.9072-3 | 1.5831-2 | 2.8210-2 | 4.5158-2 | 6.5404-2 | 8.6174-2 | 1.0372-1 | |
| 1 | 3.3321-2 | 5.2317-2 | 7.0244-2 | 8.0177-2 | 7.6375-2 | 5.8193-2 | 3.1969-2 | |
| 2 | 6.2072-2 | 7.0591-2 | 6.2211-2 | 3.8661-2 | 1.2476-2 | 5.3382-5 | 9.5731-3 | |
| 3 | 6.2689-2 | 4.2684-2 | 1.4943-2 | 1.4776-4 | 9.7782-3 | 3.3398-2 | 4.6879-2 | |
| 4 | 3.1176-2 | 5.4214-3 | 2.1711-3 | 2.2324-2 | 4.0811-2 | 3.4640-2 | 1.1261-2 | |
| 5 | 2.7340-3 | 5.3553-3 | 2.8169-2 | 3.8433-2 | 2.1321-2 | 1.3800-3 | 7.4268-3 | |
| 6 | 5.8297-3 | 2.9014-2 | 3.4894-2 | 1.3957-2 | 1.7964-5 | 1.5049-2 | 3.2478-2 | |
| | 14 | 15 | 16 | 17 | 18 | 19 | 20 | |
| 0 | 1.1442-1 | 1.1595-1 | 1.0613-1 | 9.2899-2 | 7.3580-2 | 5.3735-2 | 3.6175-2 | |
| 1 | 8.9762-3 | 2.1381-6 | 9.6578-3 | 3.3955-2 | 6.2614-2 | 8.4465-2 | 9.2570-2 | |
| 2 | 3.3555-2 | 5.3490-2 | 5.3909-2 | 3.4531-2 | 1.0367-2 | 1.0483-5 | 1.2100-2 | |
| 3 | 3.6128-2 | 1.2112-2 | 2.4528-6 | 1.2953-2 | 3.8361-2 | 5.1042-2 | 3.8781-2 | |
| 4 | 1.1900-4 | 1.5406-2 | 3.7429-2 | 3.7755-2 | 1.5946-2 | 1.6971-4 | 1.1410-2 | |
| 5 | 2.9736-2 | 3.4215-2 | 1.3956-2 | 9.4965-9 | 1.4218-2 | 3.5984-2 | 3.3118-2 | |
| 6 | 2.2115-2 | 1.8886-3 | 7.0055-3 | 2.8850-2 | 2.9672-2 | 7.9907-3 | 1.4963-3 | |
| | 21 | 22 | 23 | 24 | 25 | 26 | 27 | |
| 0 | 2.2435-2 | 1.2804-2 | 6.7151-3 | 3.2302-3 | 1.4220-3 | 5.7133-4 | 2.0881-4 | |
| 1 | 8.6338-2 | 7.0204-2 | 5.0455-2 | 3.2307-2 | 1.8514-2 | 9.5167-3 | 4.3901-3 | |
| 2 | 4.0365-2 | 6.9563-2 | 8.6062-2 | 8.4950-2 | 7.0140-2 | 4.9651-2 | 3.0553-2 | |
| 3 | 1.3774-2 | 5.5983-5 | 1.1550-2 | 4.1815-2 | 7.1932-2 | 8.5977-2 | 8.0219-2 | |
| 4 | 3.7500-2 | 4.8499-2 | 3.2247-2 | 7.2453-3 | 1.2946-3 | 2.3401-2 | 5.8100-2 | |
| 5 | 9.8604-3 | 6.3770-4 | 2.0551-2 | 4.4396-2 | 4.2193-2 | 1.6791-2 | 8.9475-5 | |
| 6 | 2.2638-2 | 3.7228-2 | 2.1406-2 | 1.0002-3 | 1.0148-2 | 3.8019-2 | 4.5685-2 | |

2.3 THE O₂ SCHUMANN-RUNGE CONTINUUM

The B $^3\Sigma_u^-$ - X $^3\Sigma_g^-$ (Schumann-Runge) continuum of O₂ is a strongly absorbing system in the ultraviolet and is an important contributor to the absorption of heated air up to about 10,000°K. Evans and Schexnayder (Ref. 23) have performed a combined experimental and theoretical study of this continuum and have presented results which are readily adapted to our compilation. These results, which are listed in Table VI, give values of a reduced absorption coefficient, \hat{K} , where $\hat{K} = \frac{K}{K_{\max}}$. Here K_{\max} is the value of the maximum spectral absorption coefficient of a standard sample of pure O₂ at 300°, and K is the spectral absorption coefficient of the same sample at some other wavelength and temperature.

The values of the average absorption coefficient presented in the tables for air in appendix A were obtained by use of the expression

$$\bar{\mu}_{O_2 \text{ S-R cont.}}^{\Delta\nu} = C(O_2) \cdot \left(\frac{\rho}{\rho_0}\right)_{\text{air}} \cdot \hat{K}_{\Delta\nu} \cdot 400 \quad (2.34)$$

where C(O₂) is the O₂ concentration in moles per mole of original cold air and $\hat{K}_{\Delta\nu}$ has been obtained by interpolating linearly with photon energy. The average value of \hat{K} was assumed to be the value at the center of the energy interval. Since \hat{K} is a slowly varying function of photon energy, the error introduced may be neglected here. The 400(cm⁻¹) contained in the above expression is the best estimate for K_{\max} .

Table VI. The Absorption Coefficient of Oxygen at Selected Wave Lengths and Temperature

| Photon Energy (eV) | 9.54 | 9.18 | 8.86 | 8.55 | 8.43 | 8.27 |
|--------------------|--|-----------------------------|-----------------------------|-----------------------------|-----------------------------|-----------------------------|
| Wave Length | $\lambda = 1,300\text{\AA}$ | $\lambda = 1,350\text{\AA}$ | $\lambda = 1,400\text{\AA}$ | $\lambda = 1,450\text{\AA}$ | $\lambda = 1,470\text{\AA}$ | $\lambda = 1,500\text{\AA}$ |
| T($^{\circ}$ K) | $\hat{\kappa}$, Best estimate; all states excited | | | | | |
| 300 | 0.000 | 0.425 | 0.985 | 0.995 | 0.940 | 0.822 |
| 1,000 | — | 0.424 | 0.937 | 0.903 | 0.847 | 0.744 |
| 2,000 | — | 0.400 | 0.808 | 0.715 | 0.670 | 0.590 |
| 3,000 | — | 0.359 | 0.674 | 0.580 | 0.543 | 0.495 |
| 4,000 | 0.207 | 0.304 | 0.559 | 0.483 | 0.457 | 0.422 |
| 5,000 | 0.185 | 0.251 | 0.466 | 0.404 | 0.385 | 0.358 |
| 6,000 | 0.158 | 0.216 | 0.394 | 0.343 | 0.332 | 0.307 |
| 7,000 | 0.130 | 0.189 | 0.335 | 0.296 | 0.288 | 0.270 |
| 8,000 | 0.105 | 0.168 | 0.291 | 0.260 | 0.253 | 0.243 |
| 9,000 | 0.081 | 0.153 | 0.255 | 0.228 | 0.224 | 0.218 |
| 10,000 | 0.058 | 0.140 | 0.227 | 0.202 | 0.200 | 0.197 |
| Photon Energy (eV) | 8.00 | 7.75 | 7.47 | 7.29 | 7.09 | |
| Wave Length | $\lambda = 1,550\text{\AA}$ | $\lambda = 1,600\text{\AA}$ | $\lambda = 1,660\text{\AA}$ | $\lambda = 1,700\text{\AA}$ | $\lambda = 1,750\text{\AA}$ | |
| 300 | 0.583 | 0.335 | 0.135 | 0.060 | 0.018 | |
| 1,000 | 0.549 | 0.351 | 0.180 | 0.104 | 0.053 | |
| 2,000 | 0.471 | 0.353 | 0.229 | 0.170 | 0.112 | |
| 3,000 | 0.407 | 0.330 | 0.242 | 0.198 | 0.143 | |
| 4,000 | 0.360 | 0.303 | 0.237 | 0.197 | 0.153 | |
| 5,000 | 0.316 | 0.272 | 0.222 | 0.189 | 0.153 | |
| 6,000 | 0.275 | 0.240 | 0.200 | 0.175 | 0.148 | |
| 7,000 | 0.245 | 0.217 | 0.180 | 0.163 | 0.138 | |
| 8,000 | 0.221 | 0.197 | 0.170 | 0.153 | 0.132 | |
| 9,000 | 0.200 | 0.182 | 0.158 | 0.144 | 0.125 | |
| 10,000 | 0.182 | 0.169 | 0.147 | 0.135 | 0.119 | |

Section III
ABSORPTION BY ATOMS

3.1 ENERGY LEVELS AND OCCUPATION NUMBERS

In order to calculate photoionization absorption, one must specify the set of atomic states or energy levels present in the gas under given equilibrium conditions and compute the absorption from each of these states individually. The contribution to the absorption coefficient from an individual atomic state i can be expressed, for calculational purposes, as

$$\mu_i(\epsilon) = N_i \sum_j \sigma_{ij}(\epsilon) \quad \text{cm}^{-1} \quad (3.1)$$

where N_i is the number density (in atoms/cm³) of atoms in the state i , and $\sigma_{ij}(\epsilon)$ is the photoionization cross section.

The subscript j arises from the fact that each atomic state will, in general, give rise to several different photoionization transitions, corresponding to different states of the residual atom. For each of these different final states j there is a separate cross section $\sigma_{ij}(\epsilon)$ and different energy threshold ϵ_{ij}^T such that, to obtain the total cross section for all final states, the sum over j as indicated in Eq. (3.1) must be performed for all states j for which $\epsilon \geq \epsilon_{ij}^T$.

The theory whereby the cross sections $\sigma_{ij}(\epsilon)$ are obtained is described in the next section. The present section is devoted to a brief discussion of the number densities, or occupation numbers, N_i which, together with the $\sigma_{ij}(\epsilon)$, make up the absorption coefficient according to Eq. (3.1).

The computer code PIC which was employed to calculate the atomic photoionization absorption coefficients as defined by Eq. (3.1) was devised to use as input data a set of occupation number fractions $p_i = N_i/N_v$ evaluated at 6 different density values for any group of states i which one wishes to consider at a given temperature (N_v is the total particle number density, $\sum_i N_i$). For the code to calculate the cross sections for the relevant transitions, a spectroscopic identification of the state i including its energy must be given with each set of 6 values of p_i . Each atomic state is, therefore, specified by an identification number ($i \gamma n \ell S L$) and the energy of the state (in eV relative to the ground state of the neutral atom of the species):

- i is a two-digit designation of the species and charge state: 01, 02, etc., for oxygen I, oxygen II, etc.; and 11, 12, etc., for nitrogen I, nitrogen II, etc.
- γ is the two-digit designation of the core, and is listed in Table VII, along with the relevant ionizatio. potentials.
- n (two digits) is the principal quantum number of the excited electron or outermost populated shell.
- ℓ is the orbital angular momentum of the excited electron or outermost populated shell (summation conventions III and IV).
- $(2S + 1)$ is the spin multiplicity (summation convention II).
- L is the total orbital angular momentum (summation convention I and II).

Table VII. Table of Atomic Core Configurations and Ionization Potentials*

| Species | State | Core Designation | Ioniz. Potentials(eV) | |
|---------|---------------------------------------|------------------|-----------------------|---|
| | | | O | N |
| O-I | $1s^2 2s^2 2p^3 (^4S) n\ell (2S+1 L)$ | $\gamma = 1$ | 13.617 | |
| | | 2 | 16.942 | |
| | | 3 | 18.631 | |
| | | 4 | 28.42 | |
| | $2s^2 2p^4 (^4P) (2D)$ | 5 | 34.19 | |
| | | 6 | 37.88 | |
| | | 7 | 39.99 | |
| | | 8 | 52.11 | |

*Ionization potentials are given to lowest state of lowest term of next stage of ionization.

Table VII (Cont'd.)

| Species | State | Core Designation | Ioniz. Potentials (eV)* | |
|-------------|--|------------------|-------------------------|---------|
| | | | O | N |
| O-II, N-I | $1s^2 2s^2 2p^2 ({}^3P) n\ell ({}^{2S+1}L)$ $2s \quad 2p^3 ({}^5S)$ | $\gamma = 1$ | 35. 154 | 14. 548 |
| | | | 37. 659 | 16. 447 |
| | | | 40. 50 | 18. 601 |
| | | | 42. 623 | 20. 400 |
| | | | 50. 028 | 25. 989 |
| | | | 52. 793 | 28. 094 |
| | | | 58. 336 | 32. 430 |
| | | | 59. 580 | 33. 787 |
| | | | 61. 238 | 35. 230 |
| | | | 70. 339 | 42. 3 |
| | | | 72. 127 | 43. 1 |
| | | | 77. 708 | 47. 4 |
| O-III, N-II | $1s^2 2s^2 2p ({}^2P) n\ell ({}^{2S+1}L)$ $2s \quad 2p^2 ({}^4P)$ | $\gamma = 1$ | 54. 946 | 29. 617 |
| | | | 63. 758 | 36. 703 |
| | | | 70. 671 | 42. 145 |
| | | | 75. 312 | 45. 861 |
| | | | 77. 309 | 47. 716 |
| | | | 83. 607 | 52. 781 |
| | | | 86. 568 | 54. 799 |
| | | | 90. 642 | 58. 188 |
| | | | 77. 411 | 47. 426 |
| | | | 87. 575 | 55. 757 |
| | | | 97. 081 | 63. 629 |
| | | | 103. 881 | 69. 189 |
| O-IV, N-III | $1s^2 2s^2 ({}^1S) n\ell ({}^{2S+1}L)$ $2s \quad 2p ({}^3P)$ | $\gamma = 1$ | 106. 122 | 70. 843 |
| | | | 113. 088 | 76. 606 |
| O-V, N-IV | $1s^2 2s ({}^2S) n\ell ({}^{2S+1}L)$ $2p ({}^2P)$ | $\gamma = 1$ | 113. 898 | 77. 450 |
| | | | 125. 821 | 87. 442 |
| O-VI, N-V | $1s^2 ({}^1S) n\ell ({}^{2S+1}L)$ | $\gamma = 1$ | 138. 110 | 97. 863 |

*Ionization potentials are given to lowest state of lowest term of next stage of ionization.

The input to the PIC code then consists of cards with the following information:

1, γ , n, ℓ , $2S+1$, L Energy (eV) p(1), p(2), p(3), p(4), p(5), p(6)

The arguments for p indicate the different density values chosen. Since the number of atomic energy levels is essentially infinite, various conventions, lumpings, and simplifications had to be adopted to hold the number of levels within tractable limits.

As the occupation number calculation depends only on the energy of an atomic state it is convenient to combine states of nearly equal energy and exploit the well-known sum rules over Wigner coefficients in the evaluation of the optical transition probabilities. The following conventions were adopted:

| | |
|--------------------|--|
| (i) n = 3 | L and S specified for each atomic term. Exception: Levels summed over total angular momentum L for given multiplicity ($2S + 1$) when experimentally the L-splitting of the levels is much less than the S-splitting or when the energies are poorly known (Labelled: L = 9) |
| (ii) n ≥ 4 | Summed over all L-S terms (Labelled: $2S + 1 = 0$, L = 0) |
| (iii) 6 ≤ n < 9 | Summed over electron angular momentum $\ell \geq 4$ (Labelled: $\ell = 4$) |
| (iv) n > 9 | Summed over all values of the electron angular momentum (Labelled: $\ell = 0$) |
| (v) n > 17 | Not included |

The original calculations performed with the PIC code (Ref. 5) employed a set of such occupation number fractions obtained from earlier calculations (Ref. 24) and given (in abbreviated form) in AFSWC TR-61-72 (Ref. 25). Since this original set of occupation numbers covered only the temperature range $kT = 2$ eV to $kT = 20$ eV it was inadequate for the present calculation and a new set of occupation numbers having the required format had to be computed.

The thermodynamic functions (fractional electronic populations, or "Boltzmann fractions") needed to compute atomic occupation numbers, once the total atomic concentrations are known, have been calculated by Gilmore (Ref. 26). These calculations were, of course, performed for a particular selection of atomic energy levels with different identification and lumping conventions than those chosen for the PIC code.

Because of the existence of these results due to Gilmore, our occupation-number calculations were confined to unfolding the Gilmore Boltzmann fractions, in a manner appropriate for PIC input, and to devising a code (the "Equilibrium Code," see Appendix B), for computing the atomic and molecular mole fractions, or species concentrations. Thereupon, by multiplying these two results (Boltzmann fractions \times mole fractions) the occupation number fractions were obtained in the required form.

A computer code was devised to unfold the Gilmore Boltzmann fractions, attach the atomic identification required by PIC, and multiply by the species concentrations obtained from the equilibrium code. This code called "Multiplet ID Split" produces, as its output, a set of cards in the PIC input format (previously described) with occupation numbers, fractions, and spectroscopic identifications as required.

In the unfolding process, the original average energy of the combined levels was retained for each of the unfolded levels and the occupation numbers were split in proportion to the statistical weights of the unfolded subgroups of levels of which the original "level" was constituted. For example, if Gilmore had lumped all $n = 3$ levels of a given configuration together, these were split by the fractions $(2l + 1)/2r^2$ ($l = 0, 1, 2$) to give occupation numbers for the separate l values. These were then further split by the ratios $(2S_c + 2)/2(2S_c + 1)$ and $2S_c/2(2S_c + 1)$ to account for the two spin multiplicities involved when the outer $n = 3$ electron is attached to a core of spin S_c . Since the PIC code accepts levels summed over L-values, the Gilmore fractions were not split into subfractions for the various appropriate L-values.* As stated above, the average energy as originally assigned

*Some of these fractions for the lower levels are already given by Gilmore for individual atomic terms, with L and S specified as needed for PIC. These were, of course, left as is.

by Gilmore was retained for the unfolded levels and the occupation numbers of the unfolded levels computed only from their statistical weights. Thus, the Boltzmann factors $\exp(-\Delta E_i/kT)$, where ΔE_i is an energy difference between the average energy \bar{E} as assigned by Gilmore and the actual sublevel energy E_i , have been neglected. In addition, this procedure will cause errors in the photoelectric edge positions of amount ΔE_i . However, both these errors should be less than the uncertainties in the total calculation arising from other sources.* (It perhaps should be emphasized that the extrapolation on the energies of the bound states required in the Burgess-Seaton theory to obtain the phase shift at the edge is not carried out in the PIC code by use of the input state energies. It is done, rather, from tabular state energies stored in the code.)

Table VIII lists a sample set of unfolded occupation number fractions produced by the Multiplet ID Split code. The values listed are for the states of neutral oxygen present in air at 10,000°K and densities** from 10 to 10^6 normal air density, denoted by $\alpha(1)$, $\alpha(2)$, etc. The identification index, which we have labelled i in this section, is actually carried in the code as two indices, J and s . The atomic state is defined by J , and the species by s . Column 1 of Table VIII lists the spectroscopic identification of the state, Column 2 lists the energy of the state (in eV), and Columns 3-8 list the occupation number fractions $p_i = N_i/N_v$ for the 6 density values, where N_i is the number density of particles in the state i and N is the total number density. As indicated above, they are normalized such that multiplication of these occupation number fractions p_i by the total particle number density $N_v = \sum_i N_i$ (electrons - and molecules, of course - are included in N_v as separate species) yields the actual occupation number N_i . (A table of the values of N_v for the required temperatures and densities therefore forms part of the input information to the PIC code.) All the levels for which Boltzmann fractions were computed by Gilmore have not been included

*Particularly the matrix-element values.

**It will be seen that a second card has been inserted after each primary card to carry the two additional density columns, since the PIC code can accept a maximum of six density columns at one time.

Table VIII. Occupation No. Fractions (μ J.s) for States of Neutral Oxygen in Air. Col. 1 lists the Spectroscopic Identification, Col. 2 lists the energies, and Cols. 3-8 list the Occupation No. Fractions

Table VIII (Cont'd.)

Table VIII (Cont'd.)

Table VIII (Cont'd.)

UXF211 - FRACTIONAL ACCUMULATION NUMBERS P (J, S) 1 = 0.6170e-01 11013

Table VIII (Cont'd.).

UNIVERSITY OF TORONTO LIBRARIES

in that states of principal quantum number $n \geq 5$ have been neglected for some excited cores. These levels have generally very low population at the temperatures of this study, and are, therefore, not important.

3.2 ATOMIC PHOTOIONIZATION ABSORPTION

Within the limits of the present study it was not practical to include the effects of atomic lines. The manner in which these can be included and an estimate of the effects of such line contributions can be obtained from a previous study (Ref. 5). The primary atomic effect which, it will be seen, becomes very important toward the high-temperature low-density region of our calculations is that of photoionization.

A computer code called PIC (photoionization calculation) developed under the previously referenced study (Ref. 5) was used in the present work to compute the photoionization contribution (except for the O^- photodetachment contribution, which is considered separately in Section IV). A brief summary of the calculational basis of this code (due to R. R. Johnston, and taken from Ref. 5, with appropriate modifications) is included below for completeness. For further details of this calculation and an actual listing of the code, the reader should consult Ref. 5.

The atomic energy levels included in the present calculation (from which photoionization transitions take place) and the concentrations, or occupation numbers, of these states have been described in the preceding section.

As stated previously, the absorption coefficient for photoionization transitions can be expressed in terms of the total photoionization cross sections $\sigma_{ij}(\epsilon)$ from initial states i to final states j .

The general initial state* (iγnSL) treated in the present calculation may be written

$$2s^{n_s} 2p^{n_p} \left(S_{12} L_{12} \right) n \left(S_L \right)$$

with the K-shell $1s^2$ understood and the configuration

$$2s^{n_s} 2p^{n_p} \left(S_{12} L_{12} \right)$$

specified by the core index γ (Table VII). A general photoionization transition from such an initial state may be written

$$2s^{n_s} 2p^{n_p} \left(S_{12} L_{12} \right) n \left(S_L \right) \rightarrow 2s^{n'_s} 2p^{n'_p} \left(S_c L_c \right) n' l' \left(S' L' \right) e^+ \left(S' L' \right) \quad (3.2)$$

where the final state consists of a free electron with energy e and orbital angular momentum l' and a residual atom

$$2s^{n'_s} 2p^{n'_p} \left(S_c L_c \right) n' l' \left(S' L' \right)$$

In the one-electron, electric-dipole approximation considered here the possible final states are limited by selection rules:

- (a) $S' = S$, for electric multipole transitions in LS coupling.
- (b) $L' = L - 1, L, L + 1$ only, for dipole transitions.
- (c) $l' = l_0 + 1 \geq 0$, where l_0 is the initial orbital angular momentum of the electron being ejected.

*As defined in the preceding section, i and γ are code numbers representing, respectively, the ionic species and core coupling for the state involved. The remaining symbols nSL are standard atomic spectroscopic notation for principal quantum number, orbital single-electron angular momentum, total spin, and total orbital angular momentum, respectively.

For the photoionization from a multiply-occupied initial state, a parentage expansion (Ref. 27) will give rise in general to several possible states of the residual atom — each with a different energy threshold ϵ^T and coefficient of fractional parentage F_p . An enumeration of the possibilities follows:

(a) Ejection of an outer (n, l) electron

$$2s^{n_s} 2p^{n_p} (S_{12} L_{12}) M(S_L) = 2s^{n'_s} 2p^{n'_p} (S_{12} L_{12}) M'(S_{L'})$$

Here $n'_s = n_s$, $n'_p = n_p$, $S_c = S' = S_{12}$, $L_c = L' = L_{12}$.
 $l' = l \pm 1 \geq 0$.

(b) Ejection of a 2p outer electron: Decomposing the initial state into parents:

$$2s^{n_s} 2p^{n_p} (S_L) = \sum_p F_p \left[2s^{n_s} 2p^{n_p-1} (S_{pL_p}) 2p(S_L) \right]$$

every pair (S_{pL_p}) for which

$$F_p = \left| \left(p^{n_p} S_L \left\{ \left| p^{n_p-1} (S_{pL_p}) pSL \right| \right\} \right) \right|^2$$

is nonvanishing constitutes a possible final state of the residual atom with $n'_s = n_s$, $n'_p = n_p - 1$, $S_c = S_p$, $L_c = L_p$ and $l' = 0$ or 2 .

(c) Ejection of a 2s outer electron: Decomposing the initial state into parents.

$$2s^{n_s} (S_L) = \sum_p F_p \left[2s^{n_s-1} (S_{pL_p}) 2s (S_L) \right]$$

the only possible states are

$$n_s = 2 : S = 0, L = 0; S_p = \frac{1}{2}, L_p = L = 0, F_p = 2$$

or

$$n_s = 1 : S = \frac{1}{2}, L = 0; S_p = 0, L_p = L = 0, F_p = 1.$$

in both of which

$$n'_s = n_s - 1, S_c = S_p, L_c = L_p, F' = 1.$$

(d) Ejection of a 2p inner electron. Decoupling one 2p electron from the rest

$$2s^{n_s} 2p^{n_p} \left(\begin{smallmatrix} S_{12} \\ L_{12} \end{smallmatrix} \right) M(S_L) = \sum_p F'_p \left[2s^{n_s} 2p^{n_p-1} \left(\begin{smallmatrix} S_{pL_p} \\ L_p \end{smallmatrix} \right) 2p \left(\begin{smallmatrix} S_{12} \\ L_{12} \end{smallmatrix} \right) M(S_L) \right]$$

$$F'_p = \left| \left(\begin{smallmatrix} n_p \\ p \end{smallmatrix} \right) S_{12} L_{12} \left(\begin{smallmatrix} n_p-1 \\ p \end{smallmatrix} \right) (S_{pL_p}) p S_{12} L_{12} \right|^2$$

the outer (n, l) electron must be coupled to $\left(\begin{smallmatrix} S_{pL_p} \\ L_p \end{smallmatrix} \right)$. so the recoupled initial state may be written

$$\sum_{pS''L''} F_p(S''L'') \left[2s^{n_s} 2p^{n_p-1} \left(\begin{smallmatrix} S_{pL_p} \\ L_p \end{smallmatrix} \right) M(S''L'') \right] 2p(S_L)$$

where $F_p = F'_p U^2(lL_p L_1 : L''L_{12}) U^2(\frac{1}{2} S_p S \frac{1}{2} : S''S_{12})$ and the U-functions are the Jahn coefficients of Ref. 28. Experimentally, the energies of states with different values of $(S''L'')$ usually vary much less than do the energies of states with different $\left(\begin{smallmatrix} S_{pL_p} \\ L_p \end{smallmatrix} \right)$. Therefore the $(S''L'')$ -splitting of the photoionization edges is ignored and the sum over $(S''L'')$ is carried out directly, leading to final states $2s^{n_s} 2p^{n_p-1} \left(\begin{smallmatrix} S_{pL_p} \\ L_p \end{smallmatrix} \right) M$ with probability F'_p . So $n'_s = n_s, n'_p = n_p - 1, S_c = S_p, L_c = L_p, F' = 0, 2$.

(c) Ejection of a 2s inner electron. Decomposing the initial state as in Case (d)

$$2s^{n_s} 2p^{n_p} (s_{12} L_{12}) m(s_L) = \sum_{pS'} F_p(s') \left[2s^{n_s-1} 2p^{n_p} (s_p L_{12}) m(s'_L) \right] 2s(s_L)$$

$$F_p(s') = F'_p U^2 \left(\frac{1}{2} s_p s \frac{1}{2} : s' s_{12} \right) . F'_p = \left(\frac{2s_p + 1}{2s + 1} \right)$$

As in Case (d), the sum over S' is carried out directly, leading to final states $2s^{n_s-1} 2p^{n_p} (s_p L_{12}) m(L)$ with probability F'_p . So $n'_s = n_s - 1$, $n'_p = n_p \cdot s_c = s_p \cdot L_c = L_{12}$, and $l' = 1$.

Such a decomposition of the initial state into substates each with a different ionization potential results in a splitting of the photoionization edges. For calculations, e.g., of Planck mean opacities at high temperatures, this splitting should yield results only slightly different from a calculation in which splitting is ignored. However, the splitting of the 2p-edges is typically a few electron volts in magnitude and therefore should affect the present low-temperature absorption coefficients significantly.

Once the initial atomic state i is decomposed into all possible final states of the residual ion, the photoionization cross section σ_{ij} is evaluated in the one-electron, electric-dipole approximation. For a transition from an initial bound electronic state (n, l) to a final state of the free electron with energy ϵ , the photoionization cross section may be written (Ref. 24)

$$\sigma_{ij}(\epsilon) = \frac{16\pi^3 e^2 \omega}{3c} F_p \left[\left(\frac{\epsilon}{2l+1} \right) (R_{nl}^{\epsilon, l-1})^2 + \left(\frac{\epsilon+1}{2l+1} \right) (R_{nl}^{\epsilon, l+1})^2 \right] \quad (3.3)$$

for photon frequency ω . In terms of the integrals $R_{nl}^{\epsilon l'}$ over the radial wave functions

$$R_{nl}^{\epsilon \ell'} = \int_0^{\infty} r^2 dr R_{\epsilon, \ell}(r) r R_{nl}(\epsilon') \quad (3.4)$$

This result has been derived assuming L-S coupling with the neglect of spin-orbit interaction, and assuming that the wave function of the final free electron state, $R_{\epsilon'}(r)$, is normalized on the energy scale

$$\int_0^{\infty} r^2 dr R_{\epsilon', \ell'}(r) R_{\epsilon'}(r) = \delta(\epsilon' - \epsilon) \quad (3.5)$$

Thus the only unknown quantities in Eq. (3.3) are the radial matrix elements $R_{nl}^{\epsilon \ell'}$. In most previous work (Refs. 24, 29, and 30) these matrix elements have been approximated by hydrogenic values.

For electrons with initial state principal quantum number $n \geq 6$ or orbital angular momentum $\ell \geq 2$ hydrogenic results have been used here. For smaller values of these quantum numbers, some recently obtained, and significantly more accurate expressions for the radial matrix elements are used. For small values of the electron final energy, the approximation of Burgess and Seaton (Ref. 32) is used and is discussed in the first of the subsequent subsections. An approximation valid for high-energy electrons is described in the second, and the third presents the method whereby the two approximations were joined.

3.3 THE LOW-ENERGY THEORY

Recently, Burgess and Seaton (Ref. 32) have presented an approximation to the radial matrix elements in terms of the asymptotically correct wave functions. This approximation derives from the observation of Bates and Damgaard (Ref. 33) that the major contribution to the radial integral for bound-bound transitions usually comes from values of r sufficiently large that the effective potential is a Coulomb potential. Replacing the actual one-electron wave function by its asymptotic form - a linear

combination of the regular and irregular Coulomb wave functions for the observed value of the energy, modified for small r to ensure convergence of the radial integrals - Bates and Damgaard evaluated the radial matrix elements $R_{nl}^{n'l'}$ and presented their results in tabular form.

Burgess and Seaton (Ref. 32) applied similar considerations to the evaluation of the radial matrix elements $R_{nl}^{el'}$ for bound-free transitions. Whereas the asymptotic behavior of the bound-state wave function is determined by the physically observed energy of the bound state, the large-radius behavior of the free-electron wave function, at a given energy, is determined by a phase shift $\delta_{l'}(L', \epsilon)$. In the approximation of asymptotically correct wave functions, Burgess and Seaton numerically evaluated the radial matrix elements and parameterized the resulting photoionization cross section [Eq. (3.3)] in the form

$$\sigma(\epsilon) = \sigma_0 \sum_{l'=l+1} C_{ll'}(L') \frac{G_{ll'}^2(\nu) \cos^2 [\varphi(l, l', \nu; \epsilon) + \delta_{l'}(L', \epsilon)]}{2\gamma_{ll'}(\epsilon) - 1} \frac{1}{(1 + \epsilon\nu^2)} \quad (3.6)$$

where L' is the orbital angular momentum of the total system in the final state. The quantities $C_{ll'}(L')$ are the results of the angular integrations and may be simply expressed in terms of Racah coefficients as described in Ref. 32. G , γ , and φ are tabulated by Burgess and Seaton as functions of ν for various combinations of l and l' , and ϵ is the electron kinetic energy in rydbergs divided by Z^2 . The basic variable of the theory, ν , is defined by

$$\nu = Z \left(\frac{1/\lambda_H}{1/\lambda'' - 1/\lambda} \right)^{1/2} \quad (3.7)$$

where

$$1/\lambda_H = 1 \text{ Ry cm}^{-1} = 109,737.3 \text{ cm}^{-1}$$

$$1/\lambda = \text{term value of the initial state (cm}^{-1}\text{)}$$

$1/\lambda''$ = term limit obtained by removing the initial (n, l) electron and leaving the residual ion in its final state (cm^{-1})

Z = charge of the residual ion

The dimensional constant σ_0 of Eq. (3.6) is given in terms of the Bohr radius a_0 by

$$\sigma_0 = \frac{4\pi}{3} \alpha a_0^2 \left(\frac{\nu^2}{Z^2} \right) [\xi(\nu)]^{-1} = \frac{8.559 \times 10^{-19} \text{ cm}^2}{\xi(\nu)} \left(\frac{\nu^2}{Z^2} \right) \quad (3.8)$$

where $\xi(\nu)$ is a normalization correction to the asymptotic bound-state wave function and may be estimated from knowledge of the physical bound states of the system. For example, the evaluation of $\xi(\nu)$ for the outer electron in the configuration

$1s^2 2s^2 2p^2 \left(\begin{smallmatrix} S \\ C \\ L \\ C \end{smallmatrix} \right) n^2 \left(\begin{smallmatrix} S \\ L \end{smallmatrix} \right)$ is obtained from consideration of the series obtained by varying n with everything else fixed. The observed energies, $\epsilon_{n'l}$, of the terms in the resulting series, relative to the series ionization limit $I_f = \lim_{n' \rightarrow \infty} \epsilon_{n'l}$, are written

$$(\epsilon_{n'l} - I_f) = -1/\nu_{n'l}^2 \quad (3.9)$$

in terms of their effective quantum number $\nu_{n'l}$. and the quantum defect, $\mu_{n'l}$, is defined by

$$\mu_{n'l} = n' - \nu_{n'l} \quad (3.10)$$

Seaton (Ref. 34) has shown that the so-defined quantum defect $\mu_{n'l}$ is a continuous, analytic function of the energy (for fixed l) which may be written $\mu_f - 1/\nu^2$. Further, $\mu_f - 1/\nu^2$ must tend to an integer as ν tends to any one of the integers $0, 1, \dots, l$. Then $\xi(\nu)$ of Eq. (3.8) is given by

$$\xi(\nu) = 1 + \frac{d\mu_f}{d\nu} = 1 + \frac{2}{\nu^3} \frac{d\mu_f(\nu)}{d\nu} \Big|_{\nu \rightarrow \infty} : \quad (3.11)$$

evaluated at the observed physical energy ϵ_{nl} of the state (nl) whose normalization is required.

Thus, to estimate $\xi(\nu)$, the observed energy of at least one additional term of the $(n'l)$ series of the initial state (n, l) is required. For outer (n, l) electrons, such states are usually known - at least upon relaxation of the condition that the outer coupling S_L be fixed. For inner electrons, however, in the presence of an excited outer electron [e.g., the $2p$ orbital in the state $2s^2 2p^2 (3p) 3s$ of Ni], the excited state necessary to estimate $\xi(\nu)$ is a doubly excited state - $2s^2 2p (2p) 3s 3p$ in the preceding example. The energies of such states are generally not known. The present calculation uses an approximation of Seaton (Ref. 34) for such inner $2p$ -orbitals

$$\xi(\nu) = \frac{(\nu - 1)(\nu + 2)}{4(\nu + 1)}$$

and chooses $\xi = 1.0$ for inner $2s$ -orbitals. Some comparisons with Hartree-Fock solutions indicate that this approximation is reasonable.

For the phase shift $\delta_p(L', \epsilon)$ of the free-electron final state, Seaton (Ref. 34) has shown that a low-energy approximation is given by extrapolating the quantum defect $\mu_p(\epsilon)$, Eq. (3.10), of the series containing the final state to small positive energies according to the formula (cf. also Ref. 35)

$$\delta_p(\epsilon, L') = \pi \mu_p(\epsilon) \quad (3.12)$$

For electrons with principal quantum number $n > 3$, the initial-state occupation numbers are summed over the total orbital angular momentum of the atom; the decomposition into final L' values is therefore ignored, and the phase shift is taken to be zero and $C_{ll'} = l_>/(2l + 1)$, where $l_>$ is the greater of l and l' . Since electrons with orbital angular momentum $l' \geq 2$ in the final state have small phase shifts at low energies, the present calculation again assumes the phase shift to vanish.

For photonionization of an outer electron to a final s or p state the zero energy phase shift is obtained by Eq. (3.12), extrapolating linearly from the physical bound states with high principal quantum numbers.* However, in the photoionization of an inner electron in the presence of an outer excited electron a difficulty occurs similar to that encountered for such states in the normalization procedure. Again, the physical states required are doubly excited states and are unknown; the extrapolation of the quantum defect is therefore impossible. The present calculation sets the phase shift to zero for such states. Generally, the most significant low-energy phase shift is for final s-states, thus the $2p \rightarrow \epsilon s$ photoionization cross section in the presence of an outer excited electron is in question. However, the $2p \rightarrow \epsilon d$ transition, with small d-state phase shift, usually dominates the $2p \rightarrow \epsilon s$, so this uncertainty is probably not too great. A more serious difficulty is the neglect of the p-state phase shift in the $2s \rightarrow \epsilon p$ transition in the presence of the excited outer electron. The uncertainty due to this approximation can probably only be resolved by detailed electron scattering calculations or Hartree-Fock calculations of the continuum state.

A low-energy expansion of the Burgess-Seaton cross section, Eq. (3.6), for integer ν and to first order in ϵ agrees with a corresponding expansion of the exact hydrogenic results. Thus, the Burgess-Seaton theory is to be considered a valid approximation when the electron kinetic energy is much less than Z^2 rydbergs. Furthermore, when sufficient information regarding the physical bound states is available, the result of Burgess and Seaton is probably more reliable than continuum Hartree-Fock calculations (Refs. 36 and 37) as some effects due to exchange and polarization of the core are reflected in the physical energies of the states with large principal quantum number used in the extrapolation for the phase shift.

Thus we conclude that the Burgess-Seaton approximation is a reasonably valid and useful approximation near the photoionization threshold, except for the aforementioned inner-shell transitions in the presence of an excited outer electron. The simplicity of

*The bound-state energies required are tabulated in the computer code so that high accuracy is not required of the input state energies.

the resulting expression for the photoionization cross section renders it particularly suitable for evaluation of the large number of initial states present in a calculation of this type.

3.4 THE HIGH-ENERGY THEORY

For energies of the final state free electron much greater than zero, the Burgess-Scaton approximation is inapplicable. An approximation of frequent utility in high-energy scattering calculations is the Born approximation. However, a straightforward application of the Born approximation to calculation of the photoionization cross section leads to an incorrect result, as discussed in Ref. 5.

The basic expression for a radiative transition - in the electric dipole approximation - between atomic states $|i\rangle$ and $|f\rangle$ is

$$\sigma_{fi} = \frac{4\pi^2 e^2 \omega}{c} |\langle f | \vec{r} | i \rangle|^2 \quad (3.13)$$

from which Eq. (3.3) is obtained upon performing the angular integrations and the average over the polarization directions of the incident radiation. As shown by Bethe and Salpeter (Ref. 38), forms equivalent to Eq. (3.13) are given by

$$\sigma_{fi} = \frac{4\pi^2 e^2}{m^2 c \omega} |\langle f | \vec{p} | i \rangle|^2 = \frac{4\pi^2 Z^2 e^6}{m^2 c \omega^3} \left| \langle f | \frac{\vec{r}}{r^3} | i \rangle \right|^2 \quad (3.14)$$

These are the dipole-velocity and dipole-acceleration forms, respectively: Z is the nuclear charge, and m the electron mass. It can be shown (Ref. 5) that a use of the acceleration form of the matrix element in a high-energy Born approximation gains one iterate of the Born series over the use of the dipole-velocity form. Accordingly, the present calculation evaluates the photoionization cross section for high-electron energy by the dipole-acceleration Born approximation.

When the angular integrations and polarization averages are performed in Eq. (3.14), a result analogous to Eq. (3.3) is obtained, namely,

$$\sigma_{ij}(\epsilon) = \frac{16\pi^3 Z^2 e^6}{3m^2 \omega^3 c} F_p \left[\left(\frac{l}{2l+1} \right) \left(R_{nl}^{\epsilon, l-1} \right)^2 + \left(\frac{l+1}{2l+1} \right) \left(R_{nl}^{\epsilon, l+1} \right)^2 \right] \quad (3.15)$$

with

$$R_{nl}^{\epsilon l'} = \int_0^{\infty} R_{\epsilon l'}(r) \frac{1}{r^2} R_{nl}(r) r^2 dr \quad (3.16)$$

In the first Born approximation the properly normalized free-electron wave function is the plane wave $-(k/2\pi)^{1/2} \exp(i\vec{k} \cdot \vec{r})$ - so that Eq. (3.16) becomes

$$R_{nl}^{\epsilon l'} = \sqrt{\frac{k}{2\pi^2}} \int_0^{\infty} j_{l'}(kr) R_{nl}(r) dr \quad (3.17)$$

in terms of the spherical Bessel functions $j_l(kr)$, where k^2 = electron kinetic energy in rydbergs.

Through use of a generalization of the HFS code of Hermann and Skillman (Ref. 39), wave functions have been generated for the many atomic states present in the gas. The resulting numerical wave functions have been fitted by analytic functions of the form

$$R_{nl}(r) = \sum_{n=1}^N C_n r^{\beta_n} e^{-\alpha_n r} \quad (3.18)$$

with integer values of β_n . From comparison of the numerical results, the following conventions were adopted in order to reduce the number of orbitals required while still retaining accuracy suitable to the present application:

- (a) For ground-state cores - $2s^{n_s} 2p^{n_p} n \ell$, the orbital (n, ℓ) was calculated for $3 \leq n \leq 8$ and $\ell = 0, 1, 2, 3$ only. For all values of (n, ℓ) the core orbitals are approximated by those calculated with $(n = 3, \ell)$ unless $\ell = 3$, when the core orbitals used are those calculated with $(n = 4, \ell = 3)$.
- (b) For excited cores with one or more 2s-electrons excited to a 2p-orbit, the orbital (n, ℓ) is calculated for $n = 3, 4, 5$ and $\ell = 0, 1, 3$ and for $n = 3, 4$ for $\ell = 2$. For larger n the (n, ℓ) orbital is approximated by those calculated in the presence of the ground-state core. The core orbitals are subject to the same conventions as in Case (a).

In terms of the bound orbitals, Eq. (3.18), Eq. (3.15) for the cross section becomes

$$\sigma_{nl}^{el} = (1.712 \times 10^{-18}) \frac{Z^2}{\omega^3 k} F_p C_{ll'} \left[\sum_{n=1}^N C_n \left(\frac{1}{k} \right)^{\beta_n} I_{l'} \left(\frac{\alpha_n}{k}, \beta_n \right) \right]^2 \text{cm}^2 \quad (3.19)$$

where

$$C_{ll'} = (l'/2l + 1)$$

and

$$I_l(\alpha, \beta) = \int_0^\infty e^{-\alpha z} z^\beta j_l(z) dz$$

$$= \frac{\Gamma(\frac{l}{2}) \Gamma(l + \beta + 1)}{z^{l+1} \Gamma(l + \frac{3}{2})} \frac{F \left(\frac{l + \beta + 1}{2}, \frac{l - \beta + 1}{2} \mid l + \frac{3}{2} \right)}{(1 + \alpha^2)^{1/2(l + \beta + 1)}} \quad (3.20)$$

These are most easily evaluated using the recursion relations

$$\left. \begin{aligned}
 I_l(\alpha, \beta) &= \delta_{\beta 0} \delta_{l1} - \alpha I_{l-1}(\alpha, \beta) + (\beta + l - 1) I_{l-1}(\alpha, \beta - 1) \\
 I_0(\alpha, \beta) &= \Gamma(\beta)(1 + \alpha^2)^{-\beta/2} \sin [\beta \tan^{-1}(1/\alpha)] \\
 I_l(\alpha, 0) &= \delta_{l1} - \alpha \left(\frac{2l-1}{l} \right) I_{l-1}(\alpha, 0) - \left(\frac{l-1}{l} \right) I_{l-2}(\alpha, 0) \\
 I_0(\alpha, 0) &= \tan^{-1}(1/\alpha)
 \end{aligned} \right\} \quad (3.21)$$

As discussed by Chandrasekhar (Ref. 40) the three expressions [Eqs. (3.13) and (3.14)] are equivalent for exact wave functions but for approximate wave functions the fact that they weight different regions of configuration space differently leads to different results. Thus the Burgess-Seaton approximation of wave functions correct for large r starts from Eq. (3.13) and conforms to the familiar uncertainty principle arguments that low-energy scattering states preferentially sample the long-range parts of the bound state. Similarly the high-energy scattering state weights more heavily the short-range part (the high-momentum Fourier components) of the bound state, as does the acceleration form of the matrix element. Variationally determined wave functions are usually less reliable for small than for intermediate values of r , so the accuracy at short distances of the HFS wave functions represents a source of uncertainty in the present results.

3.3 THE APPROXIMATE PHOTOIONIZATION CROSS SECTION

The occurrence of the spherical Bessel function in Eq. (3.17) represents an approximation to the more correct positive-energy regular Coulomb function valid if $k \gg Z$ — a domain of validity opposite to that of the Burgess-Seaton approximation, as discussed at the end of the first subsection. For the present calculation, an exponential interpolation formula is used.

$$\sigma(\epsilon) = \sigma_{BS}(\epsilon) e^{-\alpha r} + \sigma_{HE}(\epsilon)(1 - e^{-\alpha r}) \quad (3.22)$$

where σ_{BS} and σ_{HE} are the photoionization cross sections calculated according to the Burgess-Seaton and high-energy approximations, respectively. The parameter α was chosen to weight the two approximations equally at $\epsilon = Z^2$ rydbergs.

Comparisons of the photoionization cross section for OI and NII obtained from Eq. (3.22) with Hartree-Fock calculations obtained with the computer program of Daigarno, Henry, and Stewart (Ref. 36) and with hydrogenic results, are presented in Ref. 5 and will not be repeated here. It is seen from these comparisons that the hydrogenic approximation for the 2p edges consistently underestimates the Hartree-Fock results and agreement improves for states of higher degree of ionization. Thus, the hydrogenic approximation is most suitable at high temperatures and low densities. Comparing continuum Planck means obtained by Stewart and Pyatt (Ref. 29) with those obtained in Ref. 5 bears out this observation.

To account for bound-bound transitions with upper level above the merging limit, the photoionization cross section is extrapolated linearly to a value (Z^2/n_m^2) rydbergs below the vacuum edge, where n_m is the principal quantum number where merging of the lines occurs. This is discussed further in Ref. 5 where the formula for n_m is given.

Section IV
MISCELLANEOUS CONTRIBUTIONS TO THE ABSORPTION

4.1 NO₂ - ABSORPTION

4.1.1 Experimental Data

Mueller (Ref. 6) has compiled the available experimental data on the absorption coefficient of NO₂. Since experimental data exist only in a very narrow range of wavelengths, 1000°K ≤ T ≤ 2000°K, Mueller extrapolated the data to cover the range 2500 Å ≤ λ ≤ 8000 Å and 300°K ≤ T ≤ 3000°K. Using the measurements of Wurster and Marrone (Ref. 41), Gilmore (Ref. 42) corrected some of these predicted values and gave a prediction up to 8000°K.

In our application we use the values of Mueller as corrected and enlarged by Gilmore. (See Figure 1 and Table IX.)

4.1.2 Calculation

The absorption coefficient μ_{NO_2} in cm^{-1} is calculated within the range of parameters:

$$1000^{\circ}K \leq T \leq 8,000^{\circ}K$$

$$\text{Range I} \quad 10 \geq \rho/\rho_0 \geq 10^{-6}$$

$$19,837 \text{ \AA} \geq \lambda \geq 1,167 \text{ \AA} \text{ (in linear steps of 0.1 eV)}$$

where the temperature and the relative density ρ/ρ_0 of the air sample are provided by the equilibrium code (Appendix B).

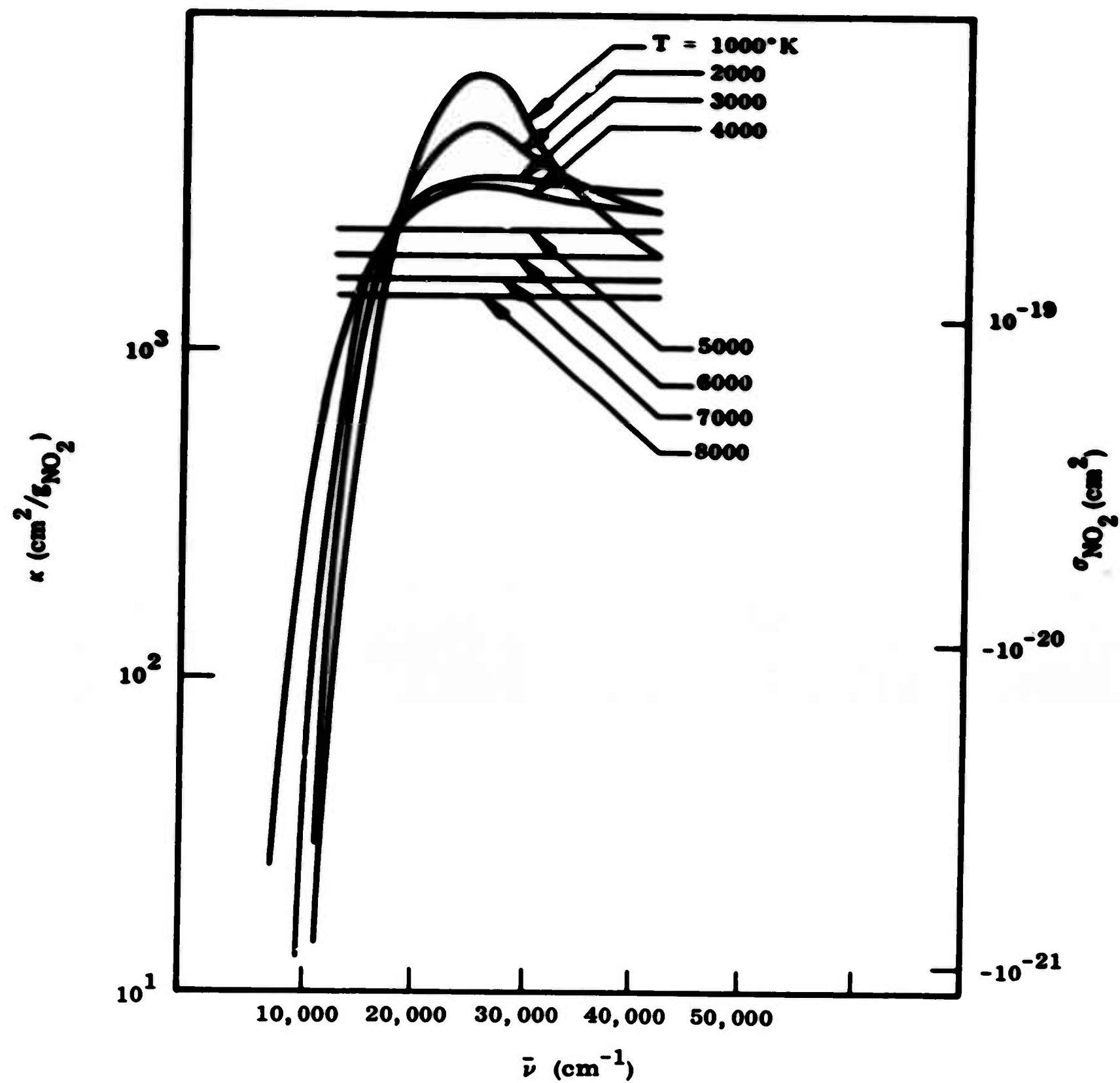


Figure 1 Mass Absorption Coefficient and Cross Section of NO_2

Table IX. NO_2 - Absorption Coefficient in cm^2/g

| Wave-length λ (μ) | Wave Number $\bar{\nu}$ (cm^{-1}) | Temperature (°K) | | | | | | | |
|---------------------------------------|--|------------------|-------------------|-------------------|-------------------|------------------|------------------|------------------|------------------|
| | | 1000 | 2000 | 3000 | 4000 | 5000 | 6000 | 7000 | 8000 |
| 1.9837 | 5041 | 0 | 0 | 0 | 0 | 0 | 0 | 0 | 0 |
| 1.4168 | 7058 | 0 | 0 | 0 | 2.8 ¹ | 0 | 0 | 0 | 0 |
| 1.1020 | 9074 | 0 | 0 | 1.1 ¹ | 1.6 ² | 0 | 0 | 0 | 0 |
| 0.9016 | 11091 | 1.4 ¹ | 2.9 ¹ | 1.4 ² | 4.9 ² | 0 | 0 | 0 | 0 |
| 0.8000 | 12500 | 7.5 ¹ | 2.3 ² | 4.2 ² | 8.2 ² | 2.4 ³ | 2.0 ³ | 1.7 ³ | 1.5 ³ |
| 0.7630 | 13108 | 1.4 ² | 3.6 ² | 6.0 ² | 1.0 ³ | 2.4 ³ | 2.0 ³ | 1.7 ³ | 1.5 ³ |
| 0.6612 | 15124 | 6.0 ² | 1.1 ³ | 1.5 ³ | 1.7 ³ | 2.4 ³ | 2.0 ³ | 1.7 ³ | 1.5 ³ |
| 0.5834 | 17141 | 1.7 ³ | 2.2 ³ | 2.3 | 2.25 ³ | 2.4 ³ | 2.0 ³ | 1.7 ³ | 1.5 ³ |
| 0.5220 | 19157 | 3.4 ³ | 3.2 ³ | 2.8 ³ | 2.7 ³ | 2.4 ³ | 2.0 ³ | 1.7 ³ | 1.5 ³ |
| 0.4723 | 21173 | 4.9 ³ | 4.0 ³ | 3.1 ³ | 3.0 ³ | 2.4 ³ | 2.0 ³ | 1.7 ³ | 1.5 ³ |
| 0.4312 | 23191 | 6.2 ³ | 4.6 ³ | 3.3 ³ | 3.15 ³ | 2.4 ³ | 2.0 ³ | 1.7 ³ | 1.5 ³ |
| 0.3967 | 25208 | 6.7 ³ | 4.9 ³ | 3.38 ³ | 3.25 ³ | 2.4 ³ | 2.0 ³ | 1.7 ³ | 1.5 ³ |
| 0.3673 | 27226 | 6.4 ³ | 4.6 ³ | 3.40 ³ | 3.2 ³ | 2.4 ³ | 2.0 ³ | 1.7 ³ | 1.5 ³ |
| 0.3420 | 29240 | 5.0 ³ | 4.1 ³ | 3.35 ³ | 3.1 ³ | 2.4 ³ | 2.0 ³ | 1.7 ³ | 1.5 ³ |
| 0.3199 | 31260 | 4.0 ³ | 3.7 ³ | 3.30 ³ | 3.0 ³ | 2.4 ³ | 2.0 ³ | 1.7 ³ | 1.5 ³ |
| 0.3006 | 33267 | 3.3 ³ | 3.4 ³ | 3.25 ³ | 2.94 ³ | 2.4 ³ | 2.0 ³ | 1.7 ³ | 1.5 ³ |
| 0.2834 | 35286 | 2.8 ³ | 3.2 ³ | 3.20 ³ | 2.85 ³ | 2.4 ³ | 2.0 ³ | 1.7 ³ | 1.5 ³ |
| 0.2681 | 37306 | 2.5 ³ | 3.0 ³ | 3.16 ³ | 2.80 ³ | 2.4 ³ | 2.0 ³ | 1.7 ³ | 1.5 ³ |
| 0.2543 | 39324 | 2.2 ³ | 2.83 ³ | 3.12 ³ | 2.75 ³ | 2.4 ³ | 2.0 ³ | 1.7 ³ | 1.5 ³ |
| 0.2419 | 41339 | 2.0 ³ | 2.6 ³ | 3.10 ³ | 2.70 ³ | 2.4 ³ | 2.0 ³ | 1.7 ³ | 1.5 ³ |

The experimental values of the absorption coefficient κ are given in cm^2/gm of NO_2 . From this we can find the absorption coefficient μ_{NO_2} in cm^{-1} by multiplying by the mass of NO_2 per cm^3 :

$$\mu_{\text{NO}_2} = \kappa \cdot X(\text{NO}_2) \cdot M(\text{NO}_2) \cdot \frac{P}{RT} \quad (4.1)$$

with the molecular weight $M(\text{NO}_2) = 46.01 \text{ g mole}^{-1}$, the gas constant $R = 82.053 \text{ atm deg}^{-1} \text{ mole}^{-1}$ and the temperature T . The mole fraction $X(\text{NO}_2)$ and the pressure P can be taken from the equilibrium code.

In Table IX, the experimental data for κ cover the range of parameters:

$$1000^\circ\text{K} \leq T \leq 8000^\circ\text{K}$$

Range II

$$19,857 \text{ \AA} \geq \lambda \geq 2419 \text{ \AA}$$

In that part of Range I, which is not covered by Range II, μ_{NO_2} is set to zero.

To find the values of κ for values of λ between the λ -grid of Table IX, the following interpolation method is applied. Let λ_1 and λ_2 be two tabulated values of λ in Table IX, adjacent to a given λ . Then $\kappa(\lambda)$ is found by use of the expression

$$\log \kappa(\lambda) = \log \kappa(\lambda_1) + [\log \kappa(\lambda_2) - \log \kappa(\lambda_1)] \frac{\lambda - \lambda_1}{\lambda_2 - \lambda_1} \quad (4.2)$$

4.2 O⁻ PHOTO-DETACHMENT

4.2.1 Experimental and Theoretical Data

The cross section σ_{PD} for O⁻ photodetachment up to 3 eV has been measured by Smith (Ref. 43). For this energy range only the transition to the ³P-oxygen level with the threshold energy 1.456 eV contributes. The energy region above 3 eV, where, in addition, transitions to the ¹D and ³D levels contribute with threshold energies of 3.43 eV and 5.66 eV respectively, has not yet been investigated experimentally.

Theoretical derivations of the cross section σ_{PD} as made by Klein and Brueckner (Ref. 44) and Martin and Cooper (Ref. 45) do not give results which match the experimental values in the energy region above 5 eV. The values calculated in Ref. 45 are assumed to be accurate only within 60 - 70 percent.

Smith (Ref. 43) gave a prediction of the cross section σ_{PD} for the range $3 \text{ eV} \leq h\nu \leq 7.5 \text{ eV}$. He assumed that the contributions of the $3P$, $1D$, $1S$ components are proportional to the product of statistical weight and photon energy according to Bates and Massey (Ref. 46). In addition, he used the experimental threshold energies.

For our application, we took the data measured ($\leq 3 \text{ eV}$) and predicted ($\geq 3 \text{ eV}$) by Smith. For $7.5 \text{ eV} \leq h\nu \leq 10.625 \text{ eV}$, we extrapolated Smith's curve. (See Figure 2 and Table X.)

4.2.2 Calculation

The absorption coefficient

$$\mu_{PD} = \sigma_{PD} \cdot N_V(O^-) \quad (4.3)$$

is calculated within the range

$$1000^\circ\text{K} \leq T \leq 24,000^\circ\text{K}$$

$$10 \geq \rho/\rho_0 \geq 10^{-6}$$

$$19,837 \text{ \AA} \geq \lambda \geq 1,167 \text{ \AA}$$

$$(0.625 \text{ eV} \leq h\nu \leq 10,625 \text{ eV} \text{ in linear steps of } 0.1 \text{ eV})$$

where the temperature T and the relative density ρ/ρ_0 are provided by the equilibrium code.

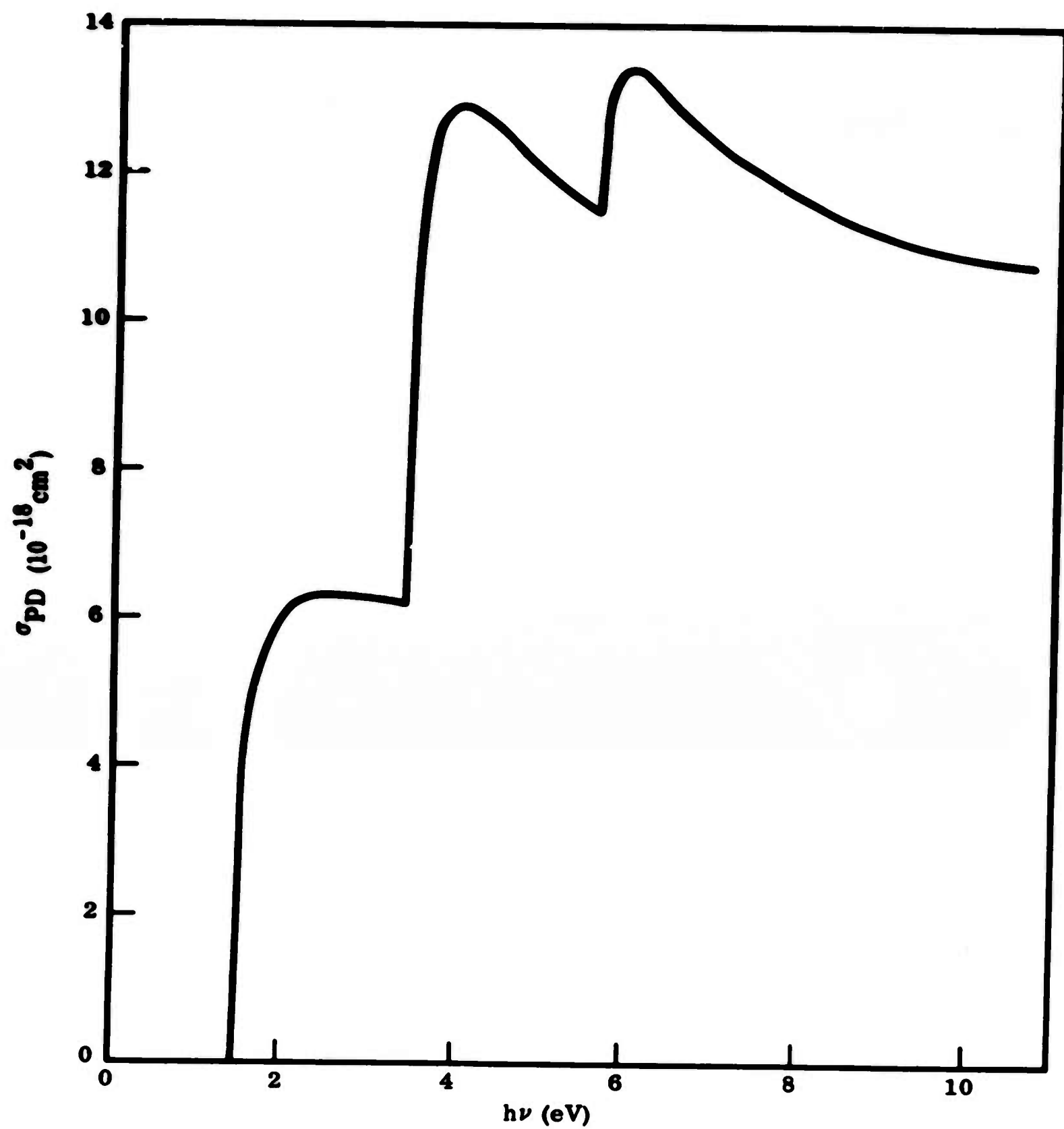


Figure 2 Photodetachment Cross Section of O^-

Table X. Cross Section for O⁻ Photodetachment

| Photon Energy (eV) | Cross Section (cm ² × 10 ⁻¹⁸) | Photon Energy (eV) | Cross Section (cm ² × 10 ⁻¹⁸) |
|-----------------------|---|-----------------------|---|
| 1.45 | 0 | 3.70 | 12.6 |
| 1.46 | 0.4 | 3.80 | 12.8 |
| 1.47 | 0.8 | 4.0 | 12.9 |
| 1.48 | 1.2 | 4.2 | 12.8 |
| 1.49 | 1.6 | 4.4 | 12.6 |
| 1.50 | 2.0 | 4.6 | 12.4 |
| 1.52 | 2.8 | 4.8 | 12.2 |
| 1.54 | 3.6 | 5.0 | 12.0 |
| 1.56 | 4.0 | 5.2 | 11.8 |
| 1.60 | 4.4 | 5.4 | 11.65 |
| 1.625 | 4.8 | 5.65 | 11.5 |
| 1.70 | 5.2 | 5.7 | 12.4 |
| 1.825 | 5.6 | 5.75 | 13.0 |
| 2.0 | 6.0 | 5.8 | 13.2 |
| 2.1 | 6.2 | 5.9 | 13.4 |
| 2.3 | 6.25 | 6.0 | 13.4 |
| 2.4 | 6.30 | 6.4 | 13.0 |
| 2.8 | 6.30 | 6.8 | 12.6 |
| 3.0 | 6.28 | 7.2 | 12.2 |
| 3.2 | 6.25 | 7.5 | 12.0 |
| 3.4 | 6.23 | 8.0 | 11.7 |
| 3.42 | 6.8 | 8.5 | 11.4 |
| 3.44 | 8.0 | 9.0 | 11.2 |
| 3.45 | 8.8 | 9.5 | 11.0 |
| 3.48 | 9.6 | 10.0 | 10.9 |
| 3.50 | 10.8 | 10.7 | 10.8 |
| 3.60 | 11.8 | | |

The number density

$$N_V(O^-) = N_V \cdot X(O^-) \quad (4.4)$$

is a product of the total number density N_V and the mole fraction $X(O^-)$, generated by the equilibrium code.

Linear interpolation is applied to find $\sigma_{PD}(h\nu)$ for the values of $h\nu$, not given in Table X. This yields the expression

$$\sigma_{PD}(h\nu) = \sigma_{PD}(h\nu_1) + \sigma_{PD}(h\nu_2) - \sigma_{PD}(h\nu_1) \frac{\nu - \nu_1}{\nu_2 - \nu_1} \quad (4.5)$$

where $h\nu_1$ and $h\nu_2$ are the tabular points of Table X, adjacent to $h\nu$.

4.3 FREE-FREE ABSORPTION

4.3.1 Basic Equations

We consider an air sample consisting of neutrals, ions, and electrons. Let $N_V(Z)$ and $N_V(e)$ be the number density of Z-fold charged positive ions and of electrons, respectively for a given sample in equilibrium, these number densities depend on the temperature T and the relative density ρ/ρ_0 and may be taken from the equilibrium code. The positive ions are assumed to have a pure Coulomb field of charge Z .

The absorption coefficient μ_{FF} in cm^{-1} for free-free transitions of the electrons in the field of the positive ions can be written as (Refs. 7, 30):

$$\mu_{FF} = \sum_Z N_V(e) N_V(Z) g K(Z) \cdot \quad (4.6)$$

Kramer's semiclassical absorption coefficient $K(Z)$ per electron per cm^3 per ion per cm^3 in Eq. (4.6) is given by

$$K(Z) = \frac{4}{3\sqrt{6\pi}} \left(\frac{2\pi e^2}{hc} \right) \left(\frac{e^2}{mc^2} \right)^2 \frac{1}{\nu^3} \left(\frac{mc^2}{kT} \right)^{1/2} \quad (4.7)$$

and \bar{g} is the Gaunt factor averaged over the (non-relativistic, non-degenerate) Boltzmann velocity distribution of the electrons. The quantity $\bar{\nu}$ is the wave number in cm^{-1} , and m the mass of the electrons; the other physical constants used are in standard notation.

The Gaunt factor \bar{g} as a function of the dimensionless quantities

$$u = \frac{hc\bar{\nu}}{kT} \quad (4.8)$$

$$\gamma^2 = Z^2 \frac{hcR_\infty}{kT} \quad (R_\infty: \text{Rydberg constant}) \quad (4.9)$$

has been given by Karzas and Latter (Ref. 47).

4.3.2 Calculation

The absorption coefficient μ_{FF} in cm^{-1} is calculated for the range of parameters

$$1,000^\circ \leq T \leq 24,000^\circ\text{K}$$

$$\text{Range I} \quad 10 \geq \rho/\rho_0 \geq 10^{-6}$$

$$19,837 \text{ \AA} \geq \lambda = \frac{1}{\bar{\nu}} \geq 1,167 \text{ \AA} \text{ (in linear steps of 0.1 eV)}$$

where the temperature T and the relative density ρ/ρ_0 are provided by the equilibrium code. The necessary physical constants and conversion factors are (Chemical Rubber Handbook, 1962-63):

Fine Structure Constant $\alpha = \left(\frac{2\pi e^2}{hc} \right) = 7.2972 \times 10^{-3}$

Classical Electron Radius $r_0 = \frac{e^2}{mc^2} = 2.81776 \times 10^{-13} \text{ cm}$

Rest Energy of Electron $mc^2 = 511,005.8 \text{ eV}$

Rydberg Energy $hcR_\infty = 13.6058 \text{ eV}$

Temperature Equivalent of 1 eV $= 11,604.9^\circ\text{K}$

Wave Number Equivalent of 1 eV $= 8,065.79 \text{ cm}^{-1}$

The number densities $N_V(e)$, $N_V(Z)$ can be found from the total number density N_V and the mole fractions X_i generated by the equilibrium code by use of the formulas:

$$N_V(e) = N_V \cdot \kappa(e) \quad (4.10)$$

$$N_V(1) = N_V \cdot [X(N_2^+) + X(O_2^+) + X(CO^+) + X(NO^+) + X(N^+) + X(O^+) + X(C^+) + X(A^+) + X(Ne^+)] \quad (4.11)$$

$$N_V(2) = N_V \cdot [X(N^{++}) + X(O^{++}) + X(C^{++}) + X(A^{++}) + X(Ne^{++})] \quad (4.12)$$

where the sums in (4.11) and (4.12) are taken over all single and double charged ions.

A two-dimensional array of Gaunt factors $\bar{g}(u_1 \gamma^2)$ over the range

Range II $\gamma^2 = 3, 10, 100, 1000$
 $0.25 \leq u \leq 30$

is taken from Karzas and Latter (see Table XI). The u -steps are chosen such that the following linear interpolation of \bar{g} as a function of $\log u$ and $\log \gamma^2$ can be made.

Let $(u_a \gamma_1^2)$, $(u_a \gamma_2^2)$, $(u_b \gamma_1^2)$, and $(u_b \gamma_2^2)$ be the four points of the $(u\gamma^2)$ -grid of Table XI which are adjacent to an arbitrary point $(u\gamma^2)$ of Range II (Figure 3).

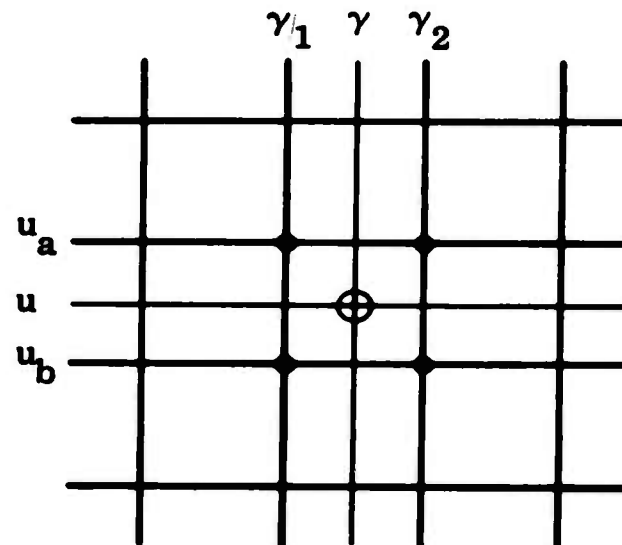


Figure 3 Table Grid (Schematic)

The first interpolation step results in the formula

$$\bar{g}(u\gamma_1^2) = \bar{g}(u_a \gamma_1^2) + [\bar{g}(u_b \gamma_1^2) - \bar{g}(u_a \gamma_1^2)] \frac{\log u - \log u_a}{\log u_b - \log u_a} \quad (4.13)$$

with $i = 1, 2$. From these values $\bar{g}(u\gamma_i^2)$, the final value $\bar{g}(u\gamma^2)$ is obtained:

$$\bar{g}(u\gamma^2) = \bar{g}(u\gamma_1^2) + [\bar{g}(u\gamma_2^2) - \bar{g}(u\gamma_1^2)] \frac{\log \gamma^2 - \log \gamma_1^2}{\log \gamma_2^2 - \log \gamma_1^2} \quad (4.14)$$

In that part of Range I, which is not covered by Range II, μ_{FF} is set to zero.

Table XI. Gaunt Factors $\bar{g}(u_1, \gamma^2)$

| u_1 | $\gamma^2 = 3$ | $\gamma^2 = 10$ | $\gamma^2 = 100$ | $\gamma^2 = 1000$ |
|-------|----------------|-----------------|------------------|-------------------|
| 0.2 | 1.50 | 1.38 | 1.20 | 1.100 |
| 0.3 | 1.425 | 1.325 | 1.16 | 1.090 |
| 0.4 | 1.375 | 1.285 | 1.14 | 1.070 |
| 0.6 | 1.320 | 1.240 | 1.13 | 1.060 |
| 0.8 | 1.280 | 1.23 | 1.11 | 1.055 |
| 1.0 | 1.265 | 1.20 | 1.105 | 1.050 |
| 1.2 | 1.25 | 1.1925 | 1.100 | 1.048 |
| 1.4 | 1.235 | 1.1825 | 1.095 | 1.047 |
| 1.6 | 1.225 | 1.1770 | 1.0925 | 1.045 |
| 1.8 | 1.215 | 1.170 | 1.090 | 1.044 |
| 2.0 | 1.2075 | 1.166 | 1.086 | 1.0425 |
| 2.4 | 1.195 | 1.160 | 1.085 | 1.0413 |
| 2.8 | 1.185 | 1.155 | 1.082 | 1.040 |
| 3.2 | 1.176 | 1.150 | 1.080 | 1.0390 |
| 3.6 | 1.170 | 1.1475 | 1.079 | 1.0380 |
| 4.2 | 1.160 | 1.1450 | 1.0785 | 1.0370 |
| 5.0 | 1.150 | 1.140 | 1.079 | 1.0365 |
| 5.8 | 1.140 | 1.1375 | 1.0795 | 1.0375 |
| 6.2 | 1.135 | 1.1350 | 1.0798 | 1.0380 |
| 7.2 | 1.125 | 1.1340 | 1.080 | 1.0390 |
| 8.2 | 1.115 | 1.1325 | 1.0805 | 1.0395 |
| 9.2 | 1.105 | 1.1300 | 1.081 | 1.0400 |
| 10.2 | 1.095 | 1.128 | 1.0815 | 1.0410 |
| 12.0 | 1.078 | 1.125 | 1.084 | 1.0420 |
| 14.2 | 1.060 | 1.120 | 1.0855 | 1.0435 |
| 16.2 | 1.045 | 1.117 | 1.0870 | 1.0450 |
| 18.0 | 1.030 | 1.114 | 1.0885 | 1.0460 |
| 20.6 | 1.015 | 1.1075 | 1.0905 | 1.0465 |
| 23.0 | 1.000 | 1.1020 | 1.0910 | 1.0475 |
| 25.4 | 0.985 | 1.0975 | 1.0925 | 1.0485 |
| 26.4 | 0.980 | 1.0950 | 1.0936 | 1.0490 |
| 28.0 | 0.970 | 1.090 | 1.0940 | 1.0495 |
| 30.0 | 0.960 | 1.086 | 1.0950 | 1.0500 |

Section V DISCUSSION

5.1 GENERAL REMARKS

A survey of the tables leads to the observation that the region of the temperature-density plane covered by these calculations cannot be readily partitioned into subregions where either atomic transitions or molecular transitions are clearly dominant. In fact, our results indicate the existence of a large region where both atomic and molecular transitions contribute appreciably to the absorption, with the relative contribution depending on photon energy (or the equivalent frequency). Certain general conclusions, however, can be drawn on the basis of the calculation:

- (1) Atomic photoionization contributions are more important at lower temperatures than has been frequently assumed
- (2) Ultraviolet molecular bands of N_2 are very important up to about 15,000°K at the higher densities
- (3) Much more experimental work and analyses are needed in all areas covered by the calculation.

5.2 COMPARISON WITH MEYEROTT, SOKOLOFF, AND NICHOLLS

Considering the differences between the present work and that of MSN (Ref. 1), the agreement between them is certainly acceptable. As an example, a graph from Ref. 1 is presented in Figure 4 with our results for the total air absorption plotted thereon. In our results, some of the prominent band characteristics exhibited by their curve are suppressed, with the largest disagreement centered on the $N_2^+ 1^-$ bands at about 3.1 eV. Our curve rises above theirs both in the ultraviolet and in the infrared. The former effect is due to enhancement of the ultraviolet absorption by the Birge-Hopfield bands of N_2 which were not included in the MSN compilation. The difference

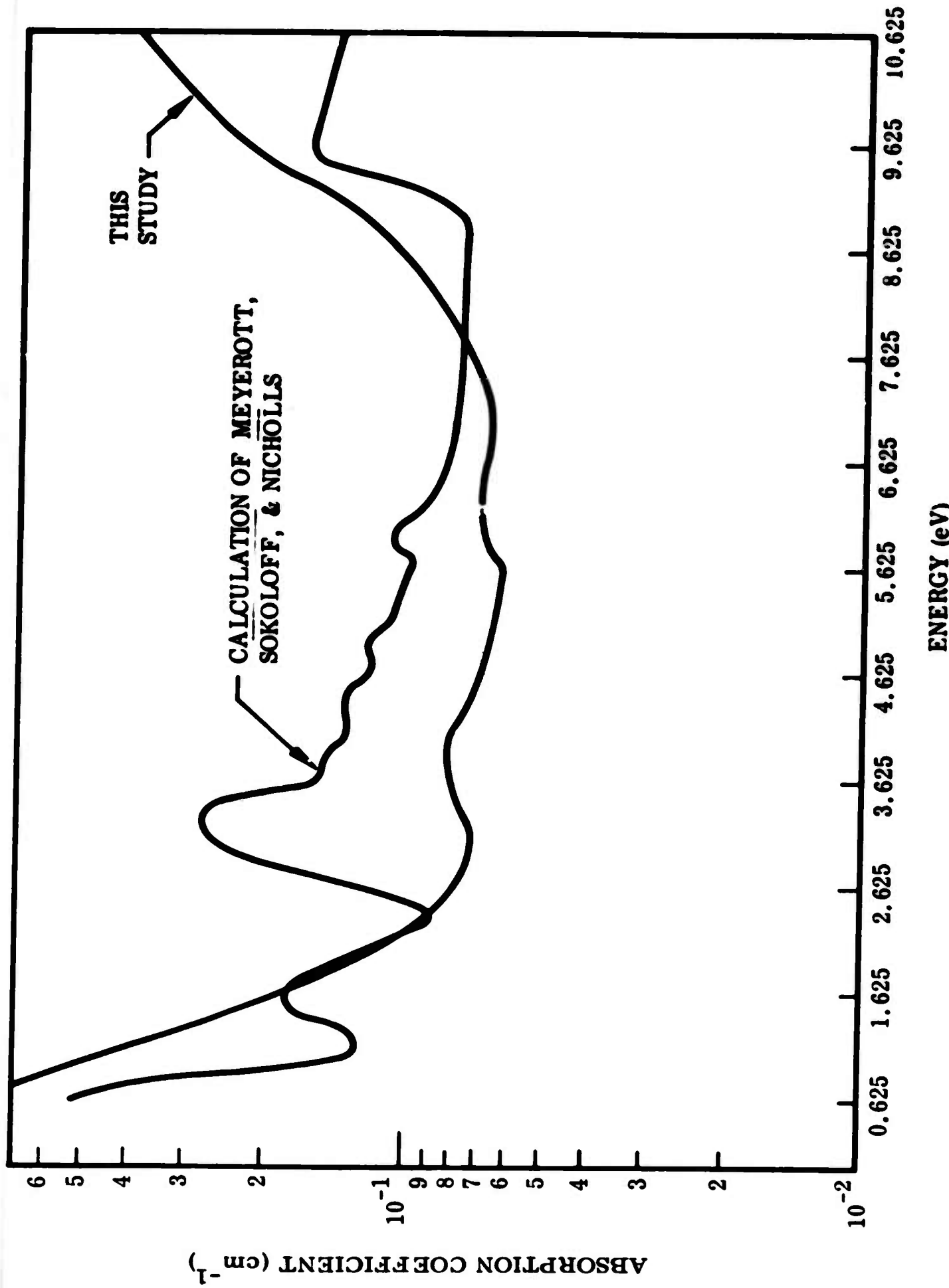


Figure 4 Absorption Coefficient of Heated Air vs. Photon Energy ($T = 12,000^\circ\text{K}$. $\rho/\rho_0 = 1$)

in absorption in the infrared is due to the larger nitrogen photoionization given by the present computations.

5.3 THE ATOMIC PHOTOIONIZATION CONTRIBUTION

A very brief comparison with experiment of the PIC code results was performed in Ref. 5. In the context of the present work, it is instructive to compare also with the previous tabulation of MSN and with the more recent calculation due to Ashley (Ref. 48). The photoelectric contribution was neglected in the MSN calculation for temperatures $T < 12,000^{\circ}\text{K}$. Since $12,000^{\circ}\text{K}$ is, in fact, the upper limit of their tabulation, comparison is possible only at this one temperature. Figure 5 shows this comparison for nitrogen. The centers of the squares represent the MSN points, and the centers of the circles show the results of the present calculation utilizing the PIC code. It should be noted that the PIC code result lumps all contributing stages of ionization, whereas the MSN calculation included only the contribution of the neutral atom.

The simple hydrogenic model utilized by MSN is seen to overestimate the present results (except at the very shortest wavelengths) by an amount varying from agreement to about a factor of four. This is somewhat reminiscent of the comparison of the unit-gaunt factor-hydrogenic and PIC results in Ref. 5, where the hydrogenic result for the 2p-edges was also shown to be high at low photon energies (~ 4 eV or less). In the present case, since we are considering more edges, the behavior is more complicated, but toward $\lambda \sim 0.14 \mu$ and less the PIC results have increased over the MSN hydrogenic values. Just prior to the lower wavelength limit of the calculation, the lowest nitrogen 2p-edge enters the range, which causes the absorption coefficient to shoot up markedly.

Also shown on the figure are the results of Ashley for the more limited wavelength range $\lambda = 0.38$ to 0.65μ . The remaining figures show further comparisons with Ashley's results. Figure 6 is for nitrogen at $6,000^{\circ}\text{K}$ and relative density $\rho/\rho_0 = 10^{-4}$. Figures 7 and 8 show oxygen at $T = 8,000^{\circ}\text{K}$ and at relative densities $\rho/\rho_0 = 1$ and 10^{-6} , respectively. Finally, Figure 9 compares the present results with those

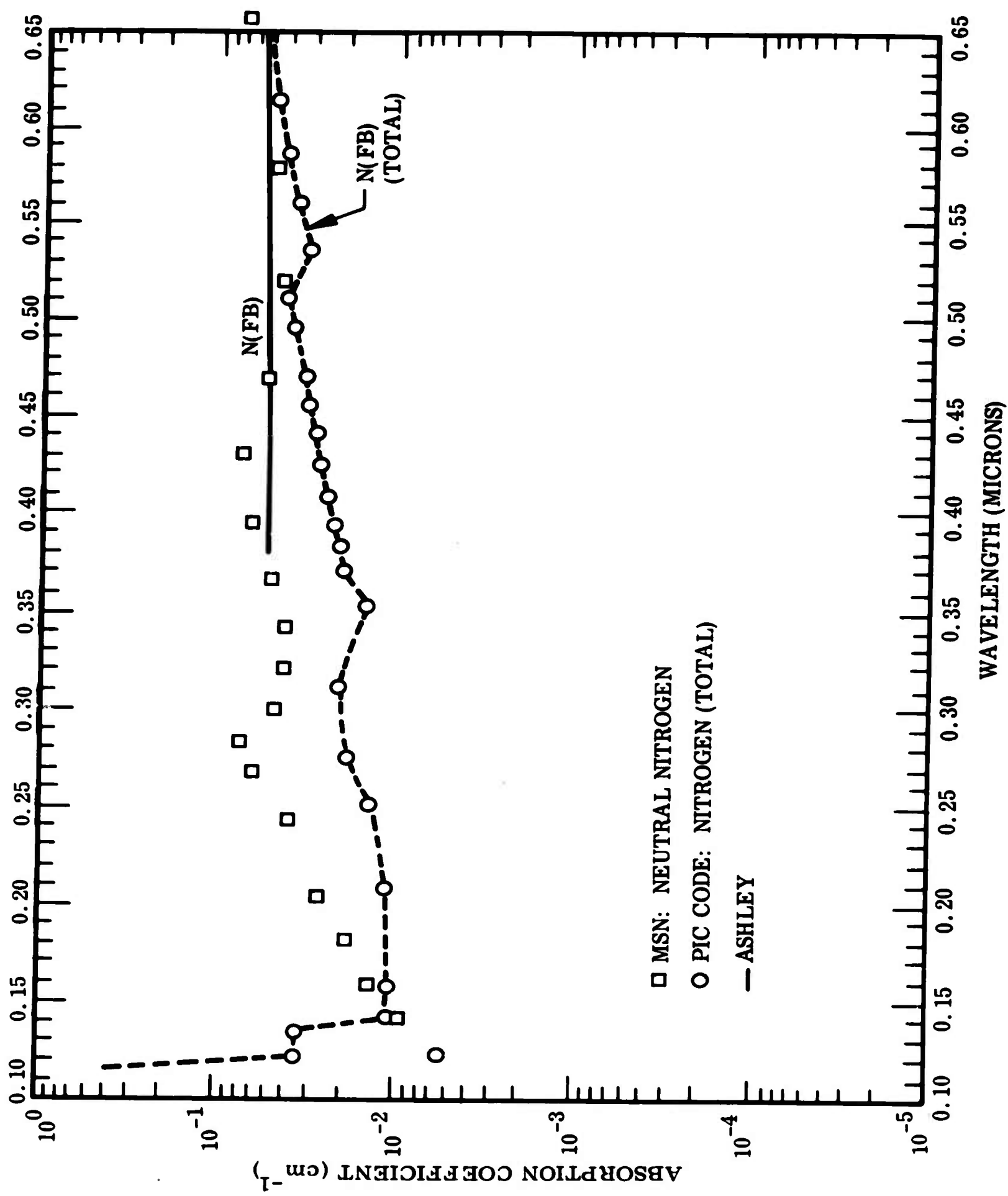


Figure 5 Linear Spectral Absorption Coefficient of Air vs. Wavelength ($T = 12,000^\circ\text{K}$, $\rho/\rho_0 = 10^0$)

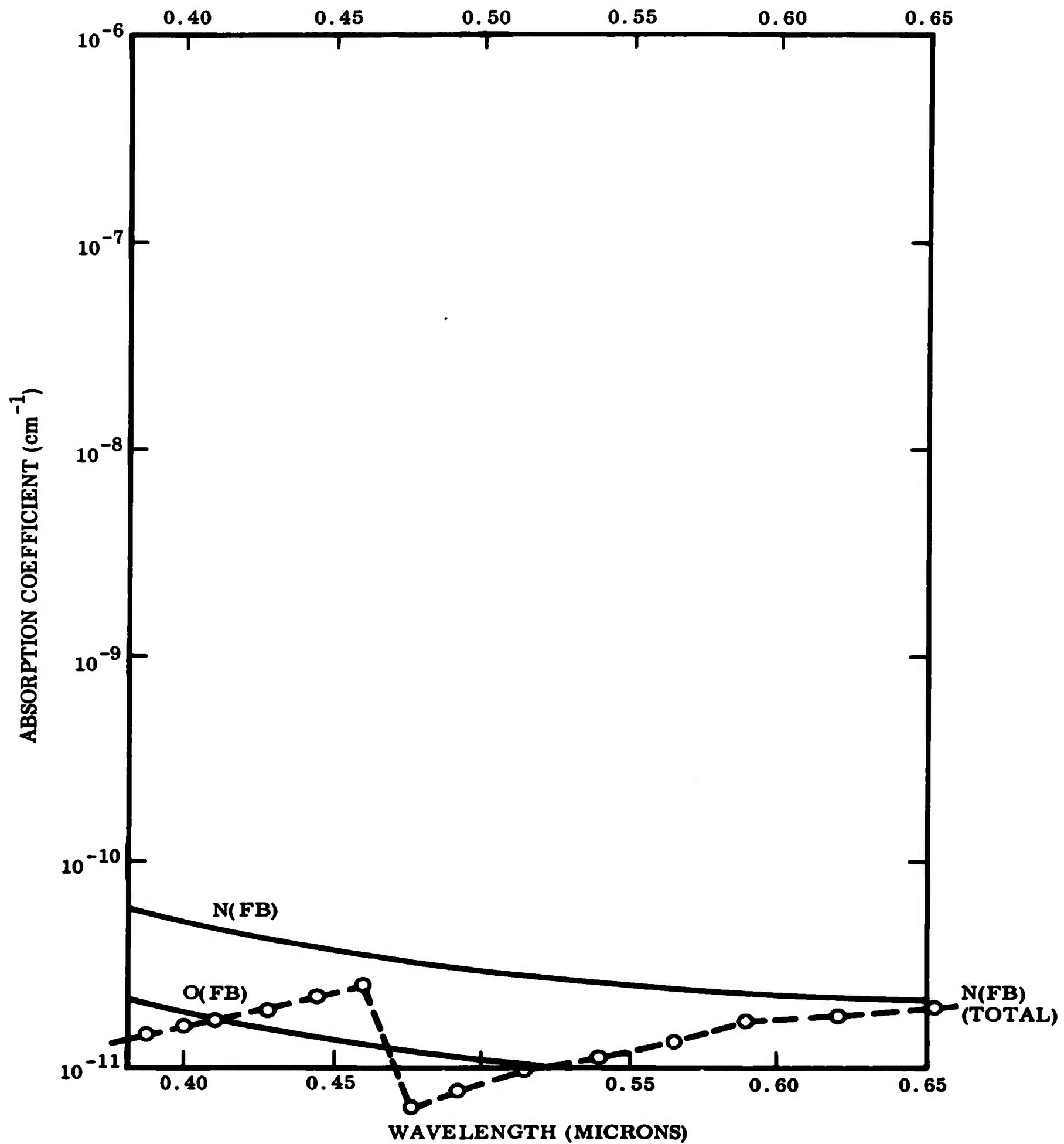


Figure 6 Linear Spectral Absorption Coefficient of Air vs. Wavelength
 $(T = 6000^\circ\text{K}, \rho/\rho_0 = 10^{-4})$

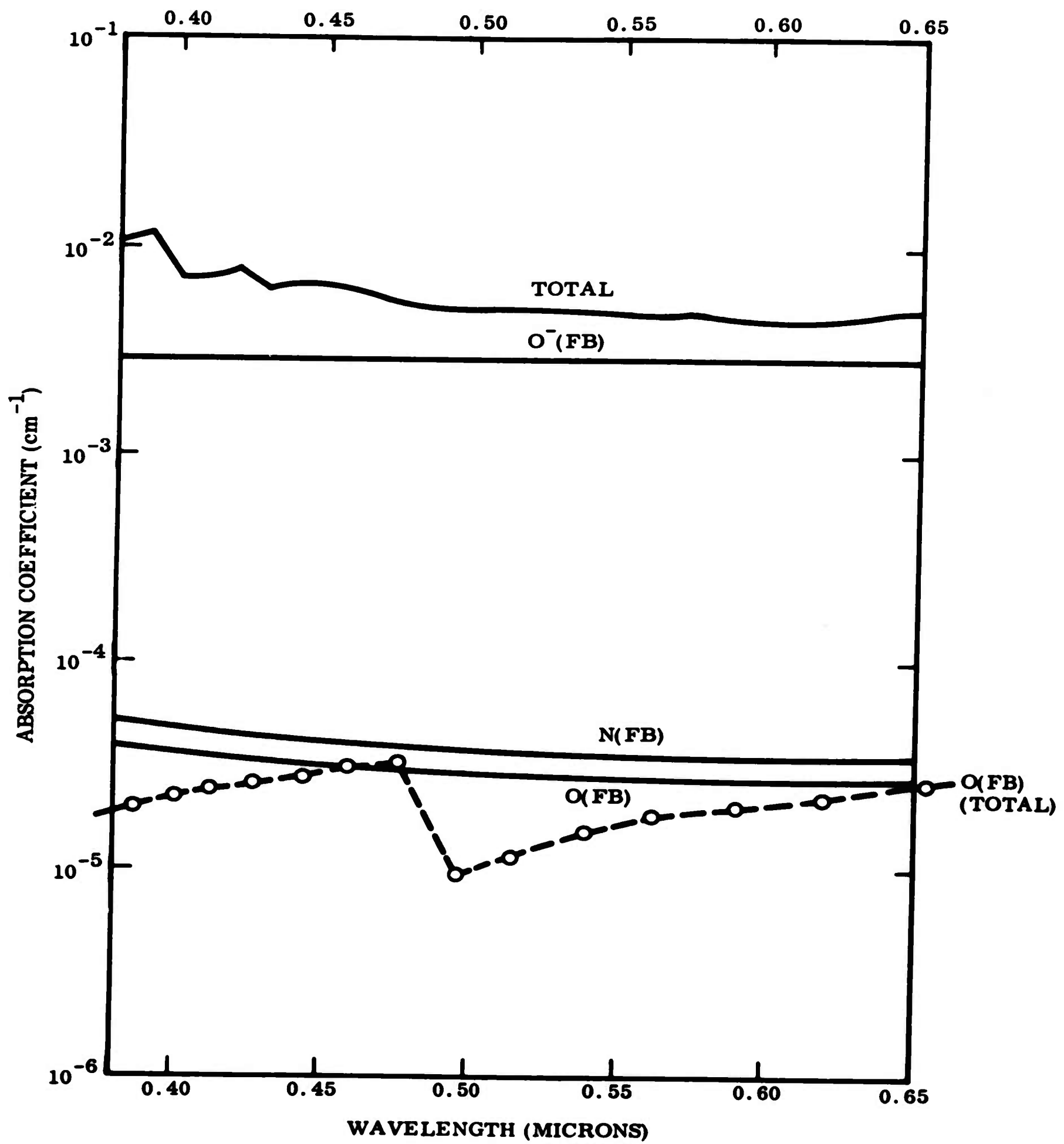
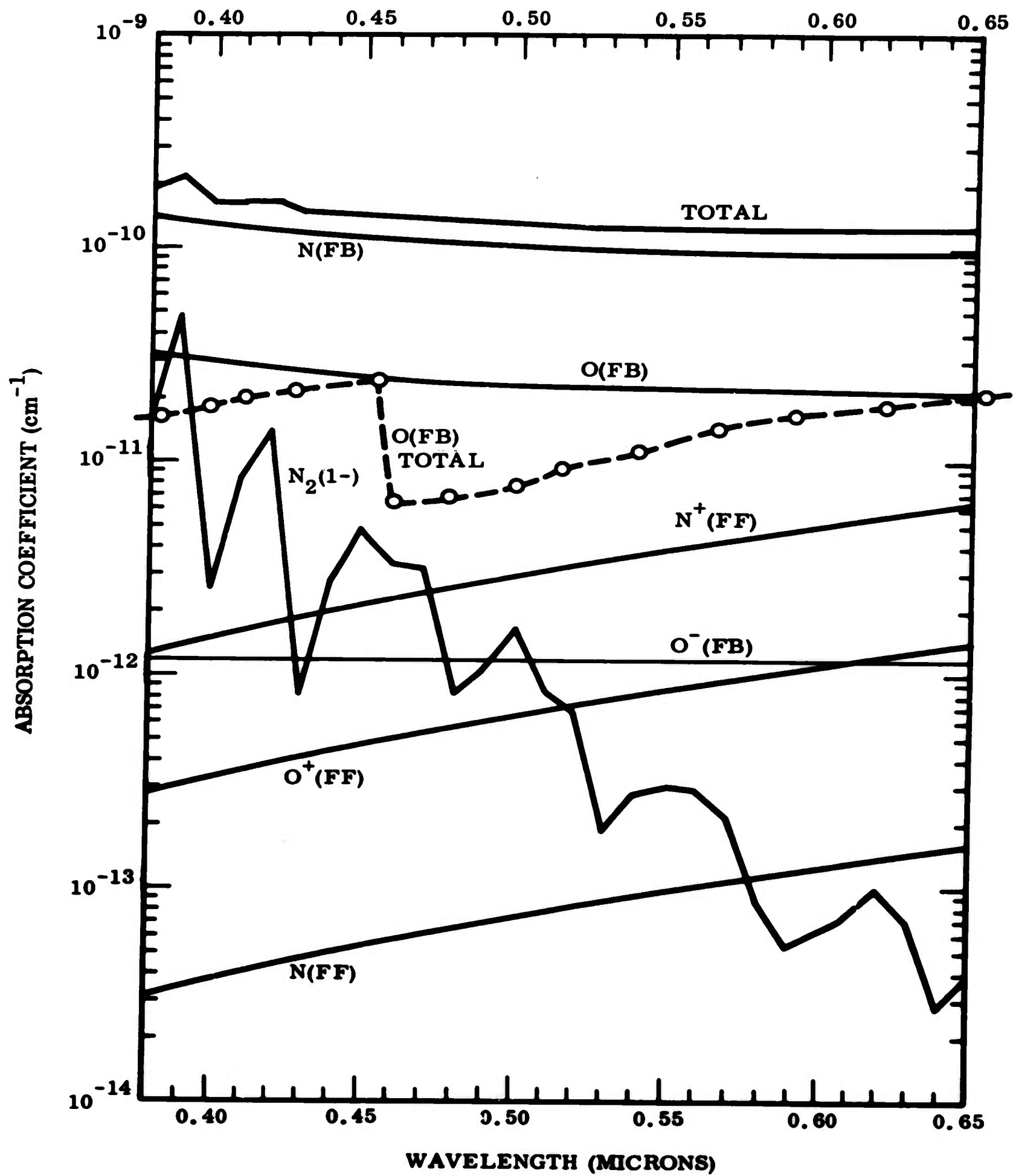


Figure 7 Linear Spectral Absorption Coefficient of Air vs. Wavelength
 $(T = 8000^\circ\text{K}, \rho/\rho_0 = 10^0)$



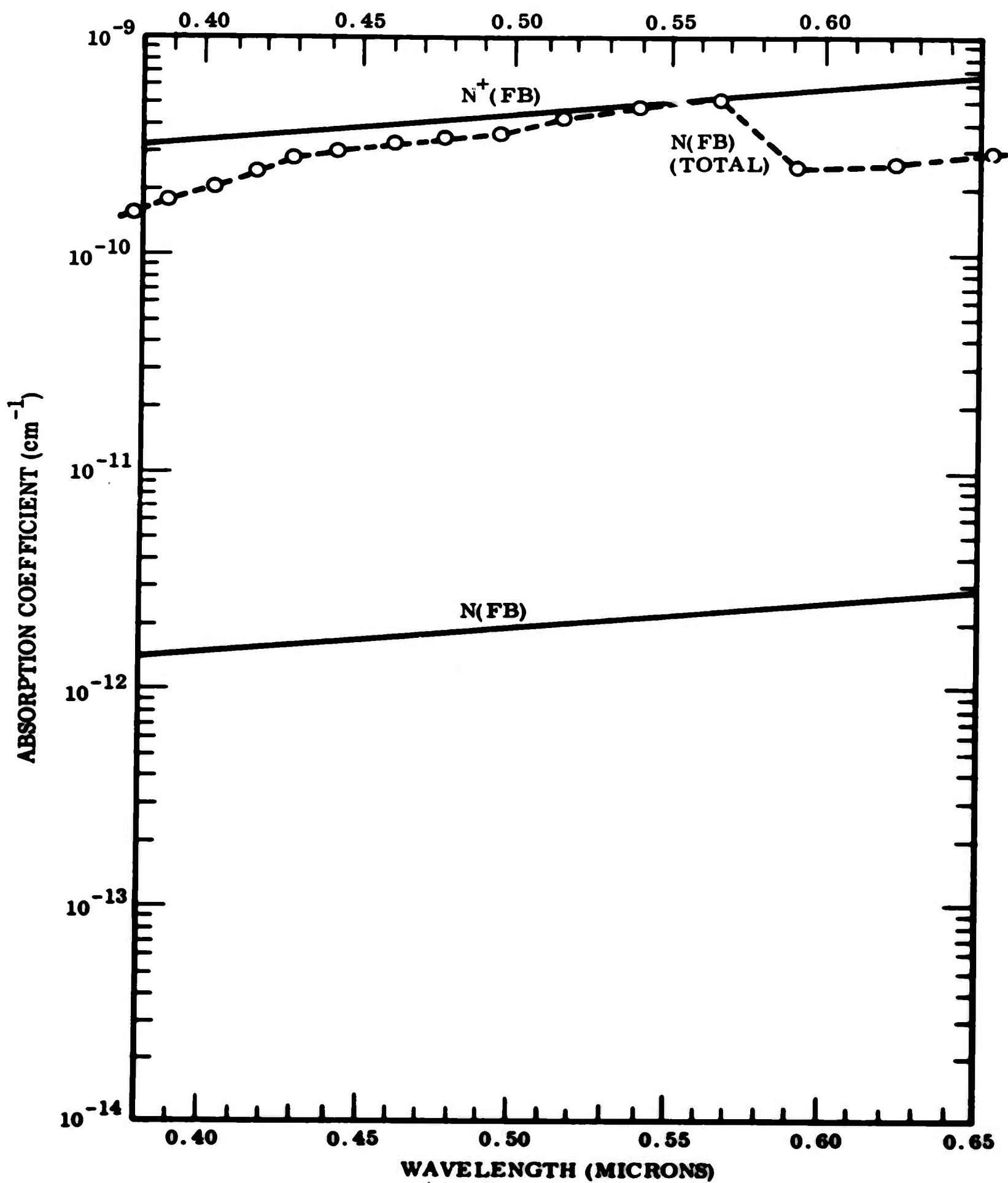


Figure 9 Linear Spectral Absorption Coefficient of Air vs. Wavelength
 $(T = 24,000^\circ\text{K}, \rho/\rho_0 = 10^{-6})$

of Ashley at $24,000^{\circ}\text{K}$ and relative density 10^{-6} . These conditions have been chosen to span, to a limited extent, the range of conditions covered. It should be noted that Ashley lists separately the contribution from each stage of ionization, rather than lumping them together as in the PIC results. Ashley's calculations, like those of MSN, were based on the hydrogenic cross sections with unit gaunt factor. However, Ashley employed a strong simplification over the ordinary hydrogenic approximation in that he treats the principal quantum number n as a continuous variable. His photoelectric cross section is therefore evaluated as though it arose from a continuous distribution of photoelectric edge strength, and is correct (hydrogenically speaking) at the thresholds, or edges, but not in between. His cross section has the behavior shown in Figure 10 where the correct hydrogenic edges are indicated and Ashley's

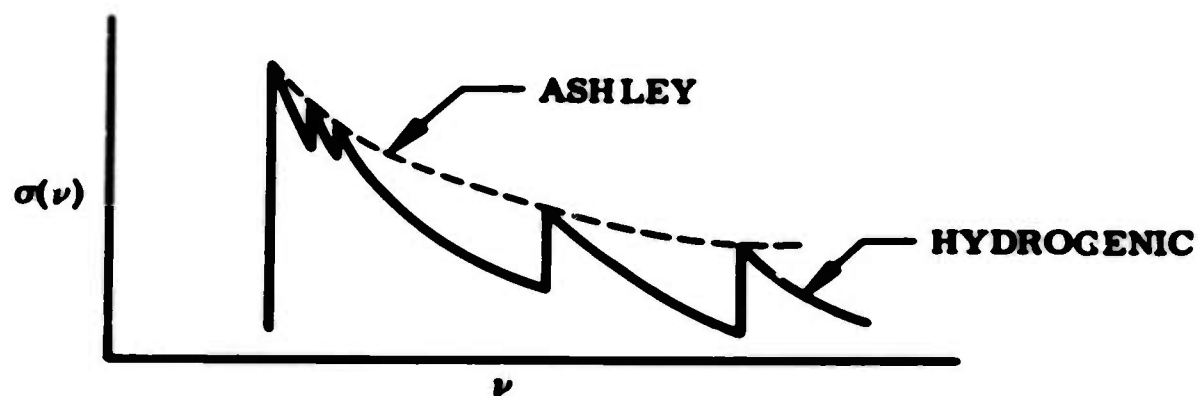


Figure 10 Photoelectric Cross Section (Sketch)

cross section, the dotted line, interpolates between them. The filling-in between the edges has the effect of including a "line contribution" and is at least partly desirable. However, this additional contribution enters in an uncontrolled fashion. The extra oscillator strength thereby introduced is not correlated with the correct additional oscillator strength needed, and is, in fact, divergent. (One can vary this by noting that $\int \sigma(\nu) d\nu$ would be infinite for Ashley's cross section.) On the other hand, this defect is partly compensated by the fact that Ashley concomitantly treats the occupation numbers as continuously distributed, but with the proper totals. This has the

effect of reducing the absorption coefficient $N\sigma$ in partial compensation for the increased oscillator strength which has been introduced. The general behavior indicated in our diagram for $\sigma(\nu)$, however, still persists in $\mu(\nu)$ even after this compensation, as can be seen in Figures 5 through 9. One would expect Ashley's method to be good for large n where the edges are closely spaced. However, the spectral region ($\lambda = 0.38$ to 0.65μ) of his calculation is primarily the region between the $n = 2$ and $n = 4$ edges of N and O, and these edges are quite widely spaced.

5.4 RECOMMENDED IMPROVEMENTS FOR FUTURE COMPILATIONS

Some of the less prominent bands of the O_2 Schumann-Runge and the N_2^+ first negative systems were not included in the calculations because of the lack of band strength information for those bands. There were, consequently, too few lines for these systems contained in the computation (see Table II). Omission of these lines has the effect of producing fictional "windows" in the associated spectrum. In the case of the O_2 Schumann-Runge system, this leads to the lack of a tabulated average absorption coefficient from 5.1 to 5.5 eV. For O_2 in air this gap is, of course, filled in by absorption arising from other mechanisms. Future compilations, however, should include the weaker bands.

In addition, there is a growing concern over possible inaccuracies in the band strengths due to the use of Franck-Condon factors based on the Morse potential. Franck-Condon factors based on more realistic potentials are now provided with the aid of larger digital computer programs and so those factors should be utilized (Refs. 49 and 50).

Also, more of the ultraviolet band systems of N_2 should be included in future compilations, particularly when better spectroscopic constants and band strengths become available. Gilmore (Ref. 22) attributes most of the N_2 absorption in this region to the Birge-Hopfield No. 2 system. His argument is based on an experiment by Wray and Teare (Ref. 51). We feel that both Birge-Hopfield systems should be included and that their relative importance, as well as that of other N_2 systems, needs further investigation. It should be noted here, however, that in problems of practical interest

connected with heated air absorption, the actual ultraviolet absorbing mechanism is of interest only as a matter of detail, since any band system covering the same energy interval as that of either Birge-Hopfield system causes the air to be relatively opaque in that interval.

In the case of the photoionization calculation, the most significant improvement that might ultimately be desired would be to assign energies of spectroscopic accuracy to the input energy levels. As noted in Sec. 3.1, the average energies used by Gilmore have been employed, and this approximation limits the spectral accuracy of the results. For further discussion of the limitations of the theory involved, the reader should consult Ref. 5.

Section VI
REFERENCES

1. R. E. Meyerott, J. Sokoloff, and R. W. Nicholls, Absorption Coefficients of Air, Air Force Cambridge Research Center, Bedford, Mass. 1960, Geophysics Research Paper No. 68
2. D. R. Churchill, S. A. Hagstrom, J. D. Weisner, and B. H. Armstrong, The Spectral Absorption Coefficient of Heated Air, Lockheed Missiles & Space Company, DASA Report Control No. 1348, Nov 1962
3. D. R. Churchill, S. A. Hagstrom, and R. K. M. Landshoff, The Calculations of Spectral Absorption in Heated Air, Lockheed Missiles & Space Company, DASA Report Control No. 1465, Dec 1963. See also D. R. Churchill, S. A. Hagstrom, and R. K. M. Landshoff, J. Quant. Spectrosc. Radiat. Transfer, Vol. 4, p. 291, 1964
4. D. R. Churchill and S. A. Hagstrom, Infrared Absorption in Heated Air From Vibration-Rotation Bands of Nitric Oxide, Lockheed Missiles & Space Company, 2-12-64-2, Dec 1964
5. B. H. Armstrong, R. R. Johnston, and P. S. Kelly, Opacity of High Temperature Air, Air Force Weapons Laboratory, AFWL-TR-65-17, Jun 1965
6. K. G. Mueller, The Absorption Coefficient of NO₂, Lockheed Missiles & Space Company, DASA Report Control No. 1416, Aug 1963
7. S. Chandrasekhar, An Introduction to the Theory of Stellar Structure, New York, Dover, 1957
8. G. Herzberg, Spectra of Diatomic Molecules, New York, Van Nostrand, 1950
9. S. S. Penner, Quantitative Molecular Spectroscopy and Gas Emissivities, Reading, Massachusetts, Addison-Wesley, 1959

10. R. W. Nicholls and A. L. Stewart, "Allowed Transitions," in Atomic and Molecular Processes, ed. D. R. Bates, New York, Academic Press, 1962
11. J. W. Chamberlain, Conversation with R. W. Nicholls, 1961
12. P. A. Fraser, Can. J. Phys., Vol. 32, p. 515, 1954
13. R. W. Nicholls and W. R. Jarman, Proc. Phys. Soc., Vol. A69, p. 253, 1956
14. R. W. Nicholls, Ann. Geophys., Vol. 20, p. 144, 1964
15. N. Davidson, Statistical Mechanics, New York, McGraw-Hill, 1962
16. H. A. Bethe, The Specific Heat of Air up to 25,000°C, OSRD Report 369, 1942
17. S. R. Brinkley, Jr., J. G. Kirkwood, and J. M. Richardson, Tables of the Properties of Air Along the Hugoniot Curve and the Adiabatic Terminating in the Hugoniot, OSRD Report 3550, 1944
18. R. G. Breene, Jr., The Shift and Shape of Spectral Lines, London, Pergamon, 1961
19. S. G. Tilford and P. G. Wilkinson, J. Mol. Spectroscopy, Vol. 12, p. 231, 1964
20. A. Lofthus, The Molecular Spectrum of Nitrogen, Spectroscopic Report Number 2, Dept. of Physics, University of Oslo, Blindern, Norway, Dec 1960
21. R. W. Nicholls, private communication
22. F. R. Gilmore, J. Quant. Spectrosc. Radiat. Transfer, Vol. 5, p. 125, 1965
23. J. S. Evans and C. J. Schexnayder, Jr., An Investigation of the Effect of High Temperature on the Schumann-Runge Ultraviolet Absorption Continuum of Oxygen, National Aeronautics and Space Administration, NASA TR R-92, 1961
24. B. H. Armstrong, D. H. Holland, and R. E. Meyerott, Absorption Coefficients of Air from 22,000° to 220,000°, Air Force Special Weapons Center, AFSWC-TR-58-36, Aug 1958
25. B. H. Armstrong, D. E. Buttrey, L. Sartori, A. J. F. Siegert, and J. D. Weisner, Radiative Properties of High-Temperature Gases, Air Force Special Weapons Center, AFSWC-TR-61-72

26. F. R. Gilmore, Energy Levels, Partition Functions, and Fractional Electronic Populations for Nitrogen and Oxygen Atoms and Ions to 25,000°K, RAND Corp. RM-3748-PR, Aug 1963
27. B. H. Armstrong, Proc. Phys. Soc. (London), Vol. 74, p. 136, 1959
28. A. R. Edmonds, Angular Momentum in Quantum Mechanics, Princeton University Press, 1957
29. J. C. Stewart and K. D. Pyatt, Jr., Theoretical Studies of Optical Properties, Air Force Special Weapons Center, AFSWC-TR-61-71, Sep 1961
30. H. Mayer, Methods of Opacity Calculations, Los Alamos Scientific Laboratory, LA 647, Oct 1947
31. B. H. Armstrong, J. Quant. Spectrosc. Radiat. Transfer, Vol. 4, p. 207, 1964
32. A. Burgess and M. J. Seaton, Mon. Not. Roy. Astron. Soc., Vol. 120, p. 121, 1960
33. D. R. Bates and A. Damgaard, Phil. Trans. Roy. Soc., Vol. A242, p. 101, 1949
34. M. J. Seaton, Mon. Not. Roy. Astron. Soc., Vol. 118, p. 504, 1958
35. B. L. Moiseiwitsch, Proc. Phys. Soc. (London), Vol. 81, p. 35, 1963
36. A. Dalgarno, R. Henry, and A. Stewart, Planetary and Space Science, Vol. 12, p. 235, 1964
37. P. Kabir and E. Salpeter, Phys. Rev., Vol. 108, p. 1256, 1957
38. H. A. Bethe and E. E. Salpeter, Quantum Mechanics of One- and Two-Electron Atoms, New York, Academic Press, 1957
39. F. Hermann and S. Skillman, Atomic Structure Calculations, New Jersey, Prentice-Hall, 1963
40. S. Chandrasekhar, Rev. Mod. Phys., Vol. 16, p. 301, 1944
41. W. H. Wurster and P. V. Marrone, Study of Infrared Emission in Heated Air, Cornell Aeronautical Laboratory, Report QM-1373-A-4, 1961

42. F. R. Gilmore, Approximate Radiation Properties of Air Between 2000° and 8000°K, RAND Corp., Memorandum RM-3997-ARPA, 1964
43. S. J. Smith, Proc. IV Int. Conf. Ionization Phenomena in Gases, Uppsala, North Holland Publishing Co., p. 219, 1960
44. M. M. Klein and K. A. Brueckner, Phys. Rev., Vol. 111, p. 1115, 1958
45. J. B. Martin and J. Cooper, Phys. Rev., Vol. 126, p. 1482, 1962
46. D. R. Bates and H. S. W. Massey, Trans. Roy. Soc. (London), Vol. A239, p. 269, 1943
47. W. J. Karzas and R. Latter, Astrophys. J., Suppl., Vol. 6, p. 167, 1961
48. E. N. Ashley, Jr., Radiant Properties of High Temperature Equilibrium Air, Boston, Mass., Edgerton, Germeshausen, and Grier, Inc., EG&G Report No. B-2782, May 1964
49. R. N. Zare, E. O. Larsson, and R. A. Berg, J. Mol. Spectry., Vol. 15, p. 117, 1965
50. D. J. Flinn, R. J. Spindler, S. Fifer, and M. Kelly, J. Quant. Spectrosc. Radiat. Transfer, Vol. 4, p. 271, 1964
51. K. L. Wray and J. D. Teare, J. Chem. Phys., Vol. 36, p. 2582, 1962

Appendix A
AN EQUILIBRIUM CODE

H. R. McChesney
K. G. Mueller

Appendix A AN EQUILIBRIUM CODE

A. 1 INTRODUCTION

An important step in the calculation of the radiative properties of high-temperature air is a determination of the particle concentration of those species which contribute significantly to the radiation processes. In general, at the temperatures under consideration, air can be a mixture of molecules, atoms, and ions which are formed by various chemical reactions from the low-temperature composition normally comprising the terrestrial atmosphere. By adopting the criterion that the composition of heated air can be fully determined by the methods of chemical equilibrium, it is possible to establish the required specie concentrations in terms of two independent thermodynamic properties.

Beginning with Brinkley (Refs. A-1 and A-2), several methods have been developed for calculating the equilibrium composition of a chemically reacting system. Of these, Brinkley adopted the technique of defining his system in terms of the independent parameters temperature T and pressure P . On applying the principles of chemical thermodynamics, he resolved his solution into a set of algebraic equations which on linearization were solved using an iteration procedure. Using this same method as a basic technique, Fickett (Ref. A-3) developed a computer code that later evolved as part of a more general HUG code (Ref. A-4) which has been used extensively for solving shock and detonation wave problems. Hilsenrath, Klein, Woolley and Sumida (Refs. A-5 and A-6) used a different set of independent properties in calculating the equilibrium composition and thermodynamic properties of a gaseous system. Selecting the parameters temperature T and density ρ , a solution was obtained without linearization by adopting a method based on the convergence scheme of Wegstein (Ref. A-7).

In essence, the determination of the composition of a reacting gaseous system varies as to the selection of independent properties and the method used to solve the resultant set of nonlinear simultaneous equations. For the present study, the composition of high-temperature air has been defined in terms of temperature and density. The solution of the algebraic relations has been iteratively solved using the techniques similar to those of Refs. A-6 and A-7, and in addition several organizational features of the HUG code have been adopted. The derivation of the equilibrium relations in terms of T and ρ will be described using a generalized notation. In turn, the method of solution will be indicated and the particular application for the composition of high-temperature air will be discussed.

A. 2 DESCRIPTION OF THE CHEMICAL SYSTEM

Let the system be defined in terms of s different gaseous species $Y^{(t)}$, which may be formed from \bar{c} elements $X^{(k)}$ according to the chemical reaction:

$$Y^{(t)} = \sum_{k=1}^{\bar{c}} \alpha_{tk} X^{(k)} \quad 1 \leq t \leq s \quad (A. 1)$$

The chemical formula of $Y^{(t)}$ is written symbolically as:

$$Y^{(t)} = X_{\alpha_{t1}}^{(1)} X_{\alpha_{t2}}^{(2)} \dots X_{\alpha_{tk}}^{(k)} \dots X_{\alpha_{t\bar{c}}}^{(\bar{c})} \quad 1 \leq t \leq s \quad (A. 2)$$

Once the set of elements $X^{(k)}$ is selected, applicable to a particular gaseous system, the chemical formula of the specie $Y^{(t)}$ can then be described by the vector

$$y_t = (\alpha_{t1}, \alpha_{t2}, \dots, \alpha_{tk}, \dots, \alpha_{t\bar{c}}) \quad (A. 3)$$

The components of all y_t vectors form an α matrix which provides a means of defining the elemental composition of all species $Y^{(t)}$.

It is now possible to choose a set of $c \leq \bar{c}$ independent vectors y_j [corresponding to the set of independent species $Y^{(j)}$] and assume an order of the $y^{(t)}$ such that the first c species are the independent ones. In this manner, the remaining dependent species $Y^{(i)}$ can be written in terms of the independent species according to the reaction:

$$Y^{(i)} = \sum_{j=1}^c \nu_{ij} Y^{(j)} \quad c + 1 \leq i \leq s \quad (A.4)$$

Expressing the species $Y^{(i)}$ and $Y^{(j)}$ in the above reaction by the reaction (A.1), we find a relation between the α and ν matrices as

$$\alpha_{ik} = \sum_{j=1}^c \nu_{ij} \alpha_{jk} \quad \begin{matrix} 1 \leq k \leq \bar{c} \\ c + 1 \leq i \leq s \end{matrix} \quad (A.5)$$

It is noted that only for the case $\bar{c} = c$ are the equations (A.5) independent. If $\bar{c} > c$, it is necessary to omit the extraneous equations. In this case, it is possible to introduce c independent elements and $(\bar{c} - c)$ dependent elements.

Let n_t be defined as the mole number of the t -th species at some prescribed thermodynamic state defined by T and ρ . In addition, let n be the total number of moles of gas at T and ρ . The chemical composition of the system can then be described in terms of the mole fraction X_t or the mole number per original moles c_t as

$$X_t = \frac{n_t}{n} \quad \text{where} \quad \sum_{t=1}^s X_t = 1 \quad (A.6a)$$

and

$$c_t = \frac{n_t}{n_o} \quad \text{where} \quad \sum_{t=1}^s c_t = \frac{n}{n_o} \quad (A.6b)$$

Here n_o is defined as the total number of moles at selected standard conditions of T_o and ρ_o . Further reference to X_t and c_t will more generally denote the concentration of the t -th specie.

The size of the chemical system can be specified either in terms of the total amounts of elements or in terms of the set of independent species. Thus, for the elements $X^{(k)}$ we have:

Q_k GRAM ATOMS OF THE ELEMENT $X^{(k)}$ $1 \leq k \leq c$

Similarly, using the independent species $Y^{(j)}$ the size of the system can be expressed as:

q_j MOLES OF INDEPENDENT SPECIES $Y^{(j)}$ $1 \leq j \leq c$

where the system is considered to be composed of only the independent species. The quantities Q_k and q_j are thus seen to be related by the expression:

$$Q_k = \sum_{j=1}^c \alpha_{jk} q_j \quad 1 \leq k \leq c \quad (A.7)$$

It is noted that Q_k and q_j are conserved in the course of all possible chemical reactions that may occur in the system. For a given set of Q_k , we can obtain the number of moles n_o at T_o and ρ_o by

$$n_o = \sum_{k=1}^c Q_k \beta_k \quad (A.8)$$

The set β_k is determined from the known elemental or molecular composition of the gaseous mixture.

A. 3 THERMODYNAMIC RELATIONS

As a basic assumption of the analysis, we assume that all reaction products $Y^{(t)}$ exhibit the characteristics of an ideal gas. Thus, the ideal gas law

$$PV = nRT \quad (A.9)$$

holds and relates the pressure P , and the volume V to the absolute temperature T . R is the molar gas constant and n is the number of moles.

The average molecular weight M of the gaseous system can be defined using the molecular weights M_t of the species $Y^{(t)}$ as

$$M = \frac{1}{n} \sum_{t=1}^s n_t M_t = \frac{n_o}{n} \sum_{t=1}^s c_t M_t \quad (A.10)$$

where the composition in terms of c_t has been expressed using Eq. (A.6b).

From the basic definition of mass density ρ and the above relation for M , the volume of the system V is written as

$$V = \frac{nM}{\rho} = \frac{n_o}{\rho} \sum_{t=1}^s c_t M_t \quad (A.11)$$

Thus, Eq. (A.9) may be rewritten in terms of ρ giving

$$P = \frac{\rho RT}{M} \quad (A.12)$$

For convenience, the compressibility factor Z is often introduced into the equation of state. This quantity is defined by the relation

$$Z = \frac{M_0}{M} \quad (A.13)$$

where M_0 is the molecular weight of the unreacted gas mixture at standard conditions. Now the mass of a closed system is conserved when chemical reactions occur. This is stated by the expression

$$nM = n_0 M_0 \quad (A.14)$$

Hence, the compressibility factor is also given as

$$Z = \frac{n}{n_0} \quad (A.15)$$

and denotes the increase in the number of moles in the system due to the occurrence of dissociation and ionization. The equation of state may therefore be alternately expressed in the following form

$$P = \frac{\rho Z RT}{M_0} \quad (A.16)$$

The particle or number density is often used to express the specific concentrations of gaseous mixtures and has the units of particles per cm^3 . Using Eqs. (A.9) and (A.11) and introducing Avogadro's number N^0 , the total particle density of the system N is given by

$$N = \frac{PN^0}{RT} = \frac{nN^0}{V} = \frac{N^0 \rho}{M} \quad (A.17)$$

In a similar manner, using the definition of the mole fraction X_t , the specie particle density N_t is found to be

$$N_t = X_t N \quad (A. 18)$$

A more convenient expression for the total particle density is found by taking the ratio of this quantity at T and ρ to that at standard conditions. Use of Eqs. (A. 13) and (A. 17) gives the expression

$$\frac{N(T, \rho)}{N(T_0, \rho_0)} = Z(\rho/\rho_0) \quad (A. 19)$$

$N(T_0, \rho_0)$ is recognized as Loschmidt's number L_0 . Thus, Eq. (A. 19) becomes

$$N = N(T, \rho) = ZL_0(\rho/\rho_0) \quad (A. 20)$$

From Eq. (A. 18), the specie number density in terms of the concentrations X_t and c_t is

$$N_t = ZX_t L_0(\rho/\rho_0) \quad (A. 21a)$$

$$N_t = c_t L_0(\rho/\rho_0) \quad (A. 21b)$$

where the relation $c_t = ZX_t$ is found from Eqs. (A. 6a) and (A. 6b).

A.4 EQUILIBRIUM COMPOSITION

For a gaseous system in chemical equilibrium, the concentration of the dependent species X_i and c_i can be obtained from the independent species X_j and c_j by applying the law of mass action to the reactions as given by Eq. (A. 4).

$$x_i = k_i^a \prod_{j=1}^c x_j^{\nu_{ij}} \quad (A. 22a)$$

$c + 1 \leq i \leq s$

$$c_i = k_i^b \prod_{j=1}^c c_j^{\nu_{ij}} \quad (A. 22b)$$

The equilibrium constants k_i^a and k_i^b are defined in terms of the standard free energies F_t^0 for each component in the reaction. These quantities, expressed in alternative form suitable for either of Eqs. (A. 22), are:

$$\ln k_i^a = \sum_{j=1}^c \left[\nu_{ij} \frac{F_j^0}{RT} \right] - \frac{F_i^0}{RT} + \left[\left(\sum_{j=1}^c \nu_{ij} \right) - 1 \right] \ln P \quad (A. 23a)$$

$$\ln k_i^b = \sum_{j=1}^c \left[\nu_{ij} \frac{F_j^0}{RT} \right] - \frac{F_i^0}{RT} + \left[\left(\sum_{j=1}^c \nu_{ij} \right) - 1 \right] \ln \left(\frac{P}{P_0 T_0} \right) \quad (A. 23b)$$

The mass balance equations, based on the conservation of q_j moles of independent components $Y^{(j)}$, are written as:

$$n_j + \sum_{l=c+1}^s \nu_{lj} n_l = q_j \quad 1 \leq j \leq c \quad (A. 24)$$

On introducing the concentrations x_l and c_l of Eqs. (A. 6), the mass balance equations become

$$x_j + \sum_{i=1}^s \nu_{ij} x_i = \frac{q_j}{n_0 Z} \quad (A. 25a)$$

$$1 \leq j \leq c$$

$$c_j + \sum_{i=c+1}^s \nu_{ij} c_i = \frac{q_j}{n_0} \quad (A. 25b)$$

The companion relations of Eqs. (A. 6) can also be reexpressed as

$$\sum_{i=1}^s x_i = 1 \quad (A. 26a)$$

$$\sum_{i=1}^s c_i = Z \quad (A. 26b)$$

The solution to the problem of determining the equilibrium composition of a reacting gas mixture for the formulation presented here is most readily accomplished by adopting the relations in terms of the concentration c_i . It is noted that the dependent specie concentrations shown in Eq. (A. 25b) can be eliminated by Eqs. (A. 22b). Thus, the problem is reduced to finding the nonnegative set of independent specie concentrations c_i from the set of c mass balance relations given by Eq. (A. 25b). Once the c_i are known, the x_i are readily determined and the related component number densities and compressibility factor are then calculable.

The standard free energies F_i^0 are generally available in tabular form as found in the literature. For practical problems, it is sufficiently accurate to represent these data by an empirical relation as a function of temperature. The representation of F_i^0 used in this work is given by

$$\frac{F_i^0}{RT} = \frac{\Delta H_i^0}{RT} + A_i(1 - \ln T) - B_i T - \frac{C_i}{2} - 2 - \frac{D_i}{3} T^3 - \frac{E_i}{4} T^4 - k_i \quad (A. 27)$$

ΔH_f^0 represents the standard heat of formation, which is the increment in enthalpy associated with the reaction of forming the given compound from its elements, with each substance in its thermodynamic standard state at the given temperature. The coefficients A_t , B_t , c_t , D_t , E_t , and k_t are determined by the curve fitting of tabulated data.

A. 5 EQUILIBRIUM CODE

The application of the equilibrium relations previously discussed are facilitated by certain organizational features. The code offers provisions for investigating different chemical subsystems which are parts of a larger chemical system. The overall system can be considered to be composed of r different species $\bar{Y}^{(m)}$ which include the above described s species $Y^{(j)}$ and $Y^{(i)}$ as a subset. This subset can then be defined by m_j and m_i , which are the m numbers of the j^{th} and i^{th} components. With this nomenclature, the following identities can be stated:

$$Y^{(j)} = \bar{Y}^{(m_j)} \quad 1 \leq j \leq s \quad (\text{A. 28})$$

$$Y^{(i)} = \bar{Y}^{(m_i)} \quad c + 1 \leq i \leq s \quad (\text{A. 29})$$

Similarly, a subset of \bar{c} elements $X^{(k)}$ can be associated with a larger set of c elements $X^{(l)}$ with the identity

$$X^{(k)} = \bar{X}^{(l_k)} \quad 1 \leq k \leq \bar{c} \quad (\text{A. 30})$$

With these identities, the description of the chemical system given in Section B. 2 holds for every subset as well as for the total system. Thus, all the relations of that section are valid for the quantities characterized by a bar shown above. In addition, the related quantities furnish the further identities

$$\alpha_{ik} = \bar{\alpha}_{m_j l_k} \quad (\text{A. 31})$$

$$Q_k = \bar{Q}_{L_k} \quad (A.32)$$

$$\beta_k = \bar{\beta}_{L_k} \quad (A.33)$$

The use of this organizational feature in the equilibrium code is obtained by providing for two sets of input data. The first set comprises the data which define the total overall system of the r species and e elements. Individual cases are then specified by additional sets of input, each of which defines the thermodynamic state by the independent variables T and ρ and the subsets of gaseous components and elements of the subsystem.

The iteration scheme used to determine the c independent species concentrations c_j has been adapted in part from the work of Refs. A-6 and A-7. It has been found that convergence is facilitated by selecting the X_j 's which will have dominant concentrations. Thus, in individual cases, various subsystems can be defined at desired temperatures and densities which exclude species that may not exist or for which thermodynamic data are incomplete. In turn, this allows convenient changes in the selected independent species during any one computer run.

The high-temperature composition of air determined by the equilibrium code for this study, is based on the molecular composition of dry air compiled by Glueckauf and as given by Gilmore in Ref. A-8. These data are shown in Table A-I and have been used to calculate the \bar{Q}_{L_k} for the total system.

Table A-I. Molecular Composition of Dry Air

| Component | Mole Percent |
|-----------|--------------|
| N | 78.084 |
| O | 20.946 |
| A | 0.934 |
| C | 0.033 |
| No | 0.003 |

The thermodynamic data used to define the standard free energy of the gaseous components have been obtained from several sources. The values of the heats of formation ΔH_{mt}^0 used and their data sources are listed in Table A-II. Additionally, the data sources are also given from which the coefficients shown in Eq. (A.27) have been derived. The 34 gaseous species shown in this table comprise the full set of r species $\bar{X}^{(m)}$.

A.6 REFERENCES

- A-1 S. R. Brinkley, J. Chem. Phys., Vol. 14, p. 563, 1946
- A-2 S. R. Brinkley, J. Chem. Phys., Vol. 15, p. 107, 1947
- A-3 W. Fickett, Detonation Properties of Condensed Explosives Calculated With an Equation of State Based on Intermolecular Potentials, Los Alamos Scientific Laboratory, LA-2712, May 1962
- A-4 P. F. Bird, R. E. Duff, and G. L. Schott, HUG, a Fortran-FAP Code for Computing Normal Shock and Detonation Wave Parameters in Gases, Los Alamos Scientific Laboratory, LA-2980, Feb 1964
- A-5 J. Hilsenrath, M. Klein, and H. W. Wooley, Arnold Engineering Development Center, AEDC TR-59-20 (National Bureau of Standards OSS 59-24), 1959
- A-6 J. Hilsenrath, M. Klein, and D. Y. Sumida, "Mechanized Computation of Thermodynamic Tables at the NBS. I. The Calculation of the Equilibrium Composition and Thermodynamic Properties of Dissociated and Ionized Gaseous Systems," Thermodynamic and Transport Properties of Gases, Liquids and Solids, New York, The American Society of Mechanical Engineers, 1959
- A-7 J. H. Wegstein, Comm. Assoc. of Comp. Mach., Vol. 1, p. 9, 1958
- A-8 F. R. Gilmore, Equilibrium Composition and Thermodynamic Properties of Air to 24,000°K, Rand Corp., RM-1543, Aug 1955
- A-9 JANAF Thermochemical Tables, (D. R. Stull, ed.) Dow Chemical Company, Midland, Michigan, Sep 1961

Table A-II. Thermodynamic Data

| Component | Heat of Formation, ΔH_{mt}^0 at 0°K (kcal/mole) | Reference (Appendix A, Sec. A.6) | F_{mt}^0 Reference (Appendix A, Sec. A.6) |
|----------------------------|---|--|---|
| 1. CO_2 | -93.965 | 9 | 8, 9 |
| 2. NO_2 | 8.734 | 9 | 8, 9 |
| 3. O_3 | 34.739 | 9 | 8, 9 |
| 4. CO | -27.190 | 9 | 8, 9 |
| 5. CO^+ | 295.990 | 8 | 8 |
| 6. N_2 | 0.0 | 9 | 8, 9 |
| 7. N_2^+ | 359.310 | 8 | 8 |
| 8. NO | 21.480 | 9 | 8, 9 |
| 9. NO^+ | 234.880 | 8 | 8 |
| 10. O_2^- | -10.400 | 8 | 8 |
| 11. O_2^+ | 0.0 | 9 | 8, 9 |
| 12. O_2^\ddagger | 277.900 | 8 | 8 |
| 13. E^- | 0.0 | 8 | 8 |
| 14. C | 169.990 | 8 | 8, 9, 11 |
| 15. C^+ | 429.832 | 8 | 8, 9, 11 |
| 16. C^{++} | 992.125 | 8 | 8, 9, 11 |
| 17. C^{+++} | 2096.240 | 8 | 8, 10, 11 |
| 18. N | 112.535 | 8 | 8, 9, 11 |
| 19. N^+ | 448.051 | 8 | 8, 10, 11 |
| 20. N^{++} | 1130.970 | 8 | 8, 10, 11 |
| 21. N^{+++} | 2224.980 | 8 | 8, 10, 11 |
| 22. O^- | 25.310 | 8 | 8 |
| 23. O | 58.989 | 8 | 8, 9, 11 |
| 24. O^+ | 373.037 | 8 | 8, 10, 11 |
| 25. O^{\ddagger} | 1183.770 | 8 | 8, 10, 11 |
| 26. O^{+++} | 2450.970 | 8 | 8, 10, 11 |
| 27. A^- | 0.0 | 8 | 8, 11 |
| 28. A^+ | 363.436 | 8 | 8, 10, 11 |
| 29. A^{\ddagger} | 1000.530 | 8 | 8, 10, 11 |
| 30. A^{+++} | 1943.970 | 8 | 8, 10, 11 |
| 31. Ne | 0.0 | 8 | 8, 11 |
| 32. Ne^+ | 497.311 | 8 | 8, 10, 11 |
| 33. Ne^{\ddagger} | 1444.720 | 8 | 8, 10, 11 |
| 34. Ne^{+++} | 2914.790 | 8 | 8, 10, 11 |

A-10 J. W. Green, D. E. Poland, and J. L. Margrave, Thermodynamic Properties of Ions at High Temperatures, Univ. of Wisconsin, ARL 191, Dec 1961

A-11 H. W. Wooley, Thermodynamic Functions for Atomic Ions, Air Force Special Weapons Center, AFSWC-TR-56-34 (ASTIA No. AD 96302), Apr 1957

A. 7 DIGITAL COMPUTER PROGRAM LISTINGS

The following list is the Fortran compile listing and input data for the equilibrium code.

```

C EQUILIBRIUM CODE
DIMENSION YB(10),CUEB(10),BETA(10),MS(50),YA(50),ALF(10,50)
DIMENSION ETH(4,50),DTH(4,50),CTH(4,50),BTH(4,50),ATH(4,50),EKTH(4
1,50),HZZ(4,50)
DIMENSION FZ(50),ENU(10,50),EK(50),CUE(10),C(50),CB(10),AJJP(10,10
1),A(10,10),B(10),CP(50),MC(50),OA(9,54),TS(50),X(50),LS(10),MB(50)
DIMENSION DEL(50),ITER(9),KEY(50),CONVG(50),CBCP(50),SUMT(50)
DIMENSION PCC(50),OP(9,54)
DIMENSION CPLAST(10),CBLAST(10),QA(10),QQ(10)
EPS=1.0E-06
EPS2=1.E-20
QCONVG = 100.0
LIMIT = 300
REWIND 15
C INPUT I
READ INPUT TAPE 5,2213
1 READ INPUT TAPE 5,1000,NES,NSP,(YB(I),I=1,NES)
3 READ INPUT TAPE 5,1900,SSW1,SSW2,SSW3,SSW4,SSW5
I=NSP+4
READ INPUT TAPE 5,1001,(OA(1,J),J=5,1)
DO 650 J = 5, I
650 OP(1,J) = OA(1,J)
READ INPUT TAPE 5,1010,(CUEB(I),I=1,NES)
READ INPUT TAPE 5,1010,(BETA(I),I=1,NES)
DO 10 I=1,NSP
10 READ INPUT TAPE 5,1020,MS(I),YA(I),(ALF(L,I),L=1,NES)
READ INPUT TAPE 5,1030,R,ENL,RHOZ,TBZ
DO 5 I=1,4
READ INPUT TAPE 5,1100,(ETH(I,J),DTH(I,J),CTH(I,J),BTH(I,J),ATH(I,
1J),EKTH(I,J),HZZ(I,J),J=1,NSP)
5 CONTINUE
C INPUT II
100 CONTINUE
READ INPUT TAPE 5,1200,IJX,JKX,T,DT,RHORZ,DRH
IF(IJX-400)801,801,800
800 WRITE OUTPUT TAPE 15,2211,IJX
END FILE 15
REWIND 15
CALL COPY (15,6)
CALL UNLOAD(15)
CALL EXIT
801 CONTINUE
READ INPUT TAPE 5,1110,NC,NS,(LS(K),K=1,NC)
READ INPUT TAPE 5,1110,(MB(J),J=1,NC)
NC1=NC+1
READ INPUT TAPE 5,1110,(MB(I),I=NC1,NS)
1000 FORMAT(2I5.6(5XA5))
1001 FORMAT(12A6)
1010 FORMAT(10X,6E10.5)
1020 FORMAT(15,A5.6(E5.0,5X))
1030 FORMAT(7E10.5)
1100 FORMAT(7E10.5)
1110 FORMAT(14I5)
1200 FORMAT(2I5,4E12.4)

```

```

1900 FORMAT(10F5.0)
2213 FORMAT(10H
      DO 2 I=1,NS
      2 MC(I)=MB(I)
      CALL SORTMC(MC,NS)
      DO 600 IJ=1,IJX
      DO 6 I = 1, NC
      CP(I) = 0.1
      CPLAST(I) = 0.0
      6 CBLAST(I) = 0.0
      RT=R*T
      IF(T-1600.0)700,700,701
700 K=1
      GOTO 706
701 IF(T-6500.0)702,702,703
702 K=2
      GO TO 706
703 IF(T-9500.0)704,704,705
704 K=3
      GO TO 706
705 K=4
706 DO 22 I=1,NS
      M=MB(I)
      IF(ABSF(EKTH(K,M))-0.00001)707,707,708
707 WRITE OUTPUT TAPE 6,1201,T,M
      GO TO 100
708 EKON=-ATH(K,M)*(1.0-LOGF(T))+EKTH(K,M)
      TEMP=((((ETH(K,M)/4.0)*T+DTH(K,M)/3.0)*T+CTH(K,M)/2.0)*T+UTH(K,M))
      1*T+EKON
22 FZ(I)=-TEMP
      EQU.2
      DO 28 I1=NC1,NS
      MI=MB(I1)
      DO 24 K1=1,NC
      LK=LS(K1)
      DO 24 J1=1,NC
      MJ=MB(J1)
24 A(K1,J1)=ALF(LK,MJ)
      DO 26 I=1,NC
      LK=LS(I)
26 B(I)=ALF(LK,MI)
      CALL MATINV(A,NC,B,1,DET)
      IF(ABSF(DET)-EPS2)30,30,32
30 WRITE OUTPUT TAPE 6,3000,DET
      GO TO 100
32 DO 28 J=1,NC
28 ENU(J,I1)=B(J)
      EQU.4
      DO 38 J=1,NC
      LJ=LS(J)
      DO 38 KK=1,NC
      MK=MB(KK)
38 A(J,KK)=ALF(LJ,MK)
      DO 40 KK=1,NC

```

```

LK=LS(KK)
40 R(KK)=PUE(R(LK))
CALL MATINV(A,NC,B,1,DET)
IF(ABSF(DET)-EPS2)42,42,44
42 WRITE OUTPUT TAPE 6,3100,DET
GO TO 100
44 DO 46 J=1,NC
46 CUE(J)=B(J)
C
EQU.5
ENZ=0.
DO 48 KK=1,NC
L=LS(KK)
48 ENZ=ENZ+BETAL(L)*CUEB(L)
IF(SSW1-0.5)41,41,43
43 WRITE OUTPUT TAPE6,4003,(FZ(I),I=1,NS)
DO 45 J=NC1,NS
45 WRITE OUTPUT TAPE6,4002,(ENU(I,J),I=1,NC)
WRITE OUTPUT TAPE6,4006,(CUE(I),I=1,NC)
WRITE OUTPUT TAPE6,4008,ENZ
41 CONTINUE
RHO=RHOZR
DO 500 JK=1,JKX
DO 36 I=NC1,NS
TEMP=0.
TMPB=0.
DO 34 J=1,NC
M=MR(J)
TEMP=TEMP+ENU(J,I)*(HZZ(K,M)/RT+FZ(J))
34 TMPB=TMPB+ENU(J,I)
TMPB=(TMPB-1.)*LOGF(T/TBZ*RHO)
M=MB(I)
TEMP=TEMP-HZZ(K,M)/RT-FZ(I)+TMPB
36 EK(I)=TEMP
IF(SSW5-0.5)31,31,33
33 WRITE OUTPUT TAPE6,4004,(EK(I),I=NC1,NS)
31 CONTINUE
300 MN = 1
NCON = 0
C BEGIN LOOP TO CONVERGE INDEP. SPECIES FOR GIVEN T AND RHO/RHOZ
301 DO 332 L = 1, LIMIT
!TER(JK) = L
C DOUBLE LOOP TO CALC. DEPEND. CONCENTRATIONS
302 DO 304 I = NC1, NS
TMP = EK(I)
DO 303 J = 1, NC
303 TMP = TMP + LOGF(CP(J))*ENU(J,I)
304 C(I) = EXPF(TMP)
IF (MN - 2) 305, 305, 130
305 DO 299 J = 1, NC
299 KEY(J) = 3
NCON = 0
C LOOP TO CALC. CB(J) AND SET CONVG. LOGIC AS REQD.
DO 319 J = 1, NC
TMP = 0.0

```

```

C      OBTAIN CB(J) USING MOLE OR ELECTRON BALANCE
      DO 306 I = NC1, NS
      306 TMP = TMP + ENU(J,I)*C(I)
      SUMT(J) = TMP
C      CUE(J) = 0.0 DENOTES ELECTRON BAL. (NO. MOLES NOT FIXED)
C      CHECK NEG. CUE(J)
      IF (CUE(J)) 307, 307, 308
      307 CB(J) = - TMP
      CBCP(J) = CB(J)/CP(J)
      KEY(J) = 4
      GO TO 319
      308 CB(J) = ((CUE(J)/ENZ)*CP(J))/(CP(J) + TMP)
      309 CBCP(J) = CB(J)/CP(J)
      310 IF (ABSF(CBCP(J)) - QCONVG) 312, 312, 311
      311 C(J) = CP(J)*QCONVG
      GO TO 314
      312 IF (ABSF(CBCP(J)) - (1.0/QCONVG)) 313, 316, 316
      313 C(J) = CP(J)/QCONVG
      314 KEY(J) = 1
      GO TO 318
      316 IF (L - 1) 319, 317, 319
      317 KEY(J) = 2
      318 NOCON = 1
      319 CONTINUE
C      LOOP TO CALC. QQ(J) AND C(J) WHEN DATA IS AVAIL. (KEY(J) = 3)
      DO 322 J = 1, NC
      IF (KEY(J) - 2) 320, 321, 321
      320 QA(J) = 0.0
      QQ(J) = 0.0
      GO TO 322
      321 QA(J) = (CB(J) - CPLAST(J))/(CP(J) - CPLAST(J))
      IF (KEY(J) - 4) 349, 406, 349
      406 IF (NCON - (NC-1)) 351, 349, 351
      349 QQ(J) = QA(J)/(QA(J) - 1.0)
      IF (QQ(J) - 0.99) 350, 351, 351
      350 IF (QQ(J)) 351, 351, 352
      351 QQ(J) = 0.5
      352 C(J) = QQ(J)*CP(J) + (1.0-QQ(J))*CB(J)
      322 CONTINUE
C      LOOP TO CALCULATE CONVERGENCE PARAMETERS
      DO 323 J = 1, NC
      DEL(J) = C(J) - CP(J)
      323 CONVG(J) = ABSF(DFL(J)/C(J))
C      SKIP LOOP TO CHECK CONVERGENCE IF NOCON = 1
      IF (NOCON) 324, 324, 326
      324 NCON = 0
      DO 325 J = 1, NC
      IF (CONVG(J) - EPS) 407, 325, 325
      407 NCON = NCON + 1
      325 CONTINUE
      IF (NCON - NC) 326, 411, 326
      411 MN = 5
C      CHECK SSW2 FOR CONVERGENCE TRAPS
      326 IF (SSW2 - 0.5) 410, 410, 327

```

```

327 WRITE OUTPUT TAPE 6, 5010, L, T, RHO
WRITE OUTPUT TAPE 6, 4011, (SUMT(I)), I = 1, NC
WRITE OUTPUT TAPE 6, 4012, (CB(I)), I = 1, NC
WRITE OUTPUT TAPE 6, 4013, (CBLAST(I)), I = 1, NC
WRITE OUTPUT TAPE 6, 4014, (CP(I)), I = 1, NC
WRITE OUTPUT TAPE 6, 4015, (CPLAST(I)), I = 1, NC
WRITE OUTPUT TAPE 6, 4016, (QA(I)), I = 1, NC
WRITE OUTPUT TAPE 6, 4017, (QQ(I)), I = 1, NC
WRITE OUTPUT TAPE 6, 5011, (KEY(I)), I = 1, NC
WRITE OUTPUT TAPE 6, 4018, (CBCP(I)), I = 1, NC
WRITE OUTPUT TAPE 6, 4019, (DEL(I)), I = 1, NC
WRITE OUTPUT TAPE 6, 4020, (C(I)), I = 1, NC
WRITE OUTPUT TAPE 6, 4021, (CONVG(I)), I = 1, NC
C SKIP TRIAL VALUES IF LOOP DOES NOT CONVERGE
410 IF (L - LIMIT) 328, 332, 332
C SET-UP TRIAL VALUES FOR NEXT ITERATION OR INITIAL VALUES NEXT RHO
328 DO 331 J = 1, NC
IF (KEY(J) - 2) 330, 329, 330
329 CPLAST(J) = CP(J)
CP(J) = CR(J)
CBLAST(J) = CB(J)
GO TO 331
330 CPLAST(J) = CP(J)
CP(J) = C(J)
CBLAST(J) = CR(J)
331 CONTINUE
C IF CONVERGED, (MN = 5) RETURN TO 302 AND CALC. DEPEND. CONC. ONLY
IF (MN = 2) 332, 332, 302
C END OF CONVERGENCE LOOP
332 CONTINUE
C IF LIMIT EXCEEDED, PRINT CURRENT RESULTS
WRITE OUTPUT TAPE 6, 3300, T, RHO
WRITE OUTPUT TAPE 6, 4011, (SUMT(I)), I = 1, NC
WRITE OUTPUT TAPE 6, 4012, (CB(I)), I = 1, NC
WRITE OUTPUT TAPE 6, 4013, (CBLAST(I)), I = 1, NC
WRITE OUTPUT TAPE 6, 4014, (CP(I)), I = 1, NC
WRITE OUTPUT TAPE 6, 4015, (CPLAST(I)), I = 1, NC
WRITE OUTPUT TAPE 6, 4016, (QA(I)), I = 1, NC
WRITE OUTPUT TAPE 6, 4017, (QQ(I)), I = 1, NC
WRITE OUTPUT TAPE 6, 5011, (KEY(I)), I = 1, NC
WRITE OUTPUT TAPE 6, 4018, (CBCP(I)), I = 1, NC
WRITE OUTPUT TAPE 6, 4019, (DEL(I)), I = 1, NC
WRITE OUTPUT TAPE 6, 4020, (C(I)), I = 1, NC
WRITE OUTPUT TAPE 6, 4021, (CONVG(I)), I = 1, NC
C ZERO OUT OUTPUT ARRAY
GO TO 360
*****  

130 Z = 0.0
DO 132 J=1,NS
132 Z = Z + C(J)
P = Z*RHO*(T/TRZ)
ENV=RHO*Z*ENL
DO 134 J=1,NS
PCC(J) = C(J)*RHO*ENL
134 X(J)=C(J)/Z

```

```

C      STORE IN OUTPUT ARRAY  CA
      J3=JK+1
      OA(J3,1)=RHO
      OP(J3,1)=RHO
      OA(J3,2)=P
      OP(J3,2)=P
      OA(J3,3)=Z
      OP(J3,3)=Z
      OA(J3,4)=ENV
      OP(J3,4)=ENV
      DO 136 J=1,NS
      J1=MC(J)
      J2=MB(J1)+4
      OP(J3,J2) = PCC(J1)
136  OA(J3,J2)=X(J1)
500  RHO=RHO*DRH
360  M=JKX+1
      L=6
      K=1
      WRITE OUTPUT TAPE 6.2207
501  WRITE OUTPUT TAPE L.2213
      WRITE OUTPUT TAPE L.2200,T
      WRITE OUTPUT TAPE L.2202,(OA(I,1),I=2,M)
      WRITE OUTPUT TAPE L.2204,(OA(I,2),I=2,M)
      WRITE OUTPUT TAPE L.2206,(OA(I,3),I=2,M)
      WRITE OUTPUT TAPE L.2208,(OA(I,4),I=2,M)
      WRITE OUTPUT TAPE L.2212
      WRITE OUTPUT TAPE L.2209
      IF(K-2)503,507,507
503  DO 505 J=1,NSP
      J1=J+4
      IF(OA(2,J1))505,505,504
504  WRITE OUTPUT TAPE L.2210,(OA(I,J1),I=1,M)
505  CONTINUE
      M=JKX+1
      L=6
      K=1

```

WRITE OUTPUT TAPE 6.2207

6.1 WRITE OUTPUT TAPE L.2213

```

      WRITE OUTPUT TAPE L.2200,T
      WRITE OUTPUT TAPE L.2202,(OP(I,1),I=2,M)
      WRITE OUTPUT TAPE L.2204,(OP(I,2),I=2,M)
      WRITE OUTPUT TAPE L.2206,(OP(I,3),I=2,M)
      WRITE OUTPUT TAPE L.2208,(OP(I,4),I=2,M)
      WRITE OUTPUT TAPE L.2214
      WRITE OUTPUT TAPE L.2209
      IF(K-2)603,507,507
603  DO 605 J=1,NSP
      J1=J+4
      IF(OP(2,J1))605,605,604

```

```

604 WRITE OUTPUT TAPE L=2210, (OP(I,J1), I=1,M)
605 CONTINUE
    WRITE OUTPUT TAPE 6, 4023, (ITER(I), I = 1, JKX)
506 L=15
    K=5
    WRITE OUTPUT TAPE 15,2211,JKX
    GO TO 501
507 DO 508 J=1,NSP
    J1=J+4
508 WRITE OUTPUT TAPE L=2210, (OA(I,J1), I=1,M)
    DO 799 J=1,NSP
    DO 798 I = 2, M
    OP(I,J) = 0.0
798 OA(I,J) = 0.0
799 CONTINUE
600 T=T+DT
    GO TO 100
1201 FORMAT(43HOTHERMODYNAMIC FUNCTION NOT AVAILABLE T =1PE13.4,13H
1  SPECIES =13)
2200 FORMAT(6H0 T =F6.0)
2202 FORMAT(8H0 RHO ,(1P11E11.3))
2204 FORMAT(8H0 P ,(1P11E11.3))
2206 FORMAT(8H Z ,(1P11E11.3))
2207 FORMAT(1H1)
2208 FORMAT(8H NV ,(1P11E11.3))
2209 FORMAT(1H0)
2210 FORMAT(1A6,2X,(1P11E11.3))
2211 FORMAT(1H1,I4)
2212 FORMAT(45HOSPECIE CONCENTRATIONS IN MOLE FRACTIONS-P(S))
2214 FORMAT(48HOSPECIE CONCENTRATIONS IN PARTICLES/CM**3-PCC(S))
3000 FORMAT(1H0/28H0EQU.2 FAILURE DETERMINANT=,1PE11.4)
3100 FORMAT(1H0/28H0EQU.4 FAILURE DETERMINANT=,1PE11.4)
3300 FORMAT(21HONO CONVERGENCE T =1PE13.6,8H RHO =1PE13.6)
4000 FORMAT(7HOFZ(NS) /(1H 1P8E14.5))
4002 FORMAT(4H ENU /(1H 1P8E14.5))
4004 FORMAT(8H0EK(NS-1) /(1H 1P8E14.5))
4006 FORMAT(8H0CUE(NC) /(1H 1P8E14.5))
4008 FORMAT(5H0ENZ=1PF12.5)
4010 FORMAT(1X,1P8E14.5)
4011 FORMAT(7H SUMT ,(1P8E14.5))
4012 FORMAT(7H CB ,(1P8E14.5))
4013 FORMAT(7H CBLAST ,(1P8E14.5))
4014 FORMAT(7H CP ,(1P8E14.5))
4015 FORMAT(7H CPLAST ,(1P8E14.5))
4016 FORMAT(7H QA ,(1P8E14.5))
4017 FORMAT(7H QQ ,(1P8E14.5))
4018 FORMAT(7H CBCP ,(1P8E14.5))
4019 FORMAT(7H DEL ,(1P8E14.5))
4020 FORMAT(7H C ,(1P8E14.5))
4021 FORMAT(7H CONVG ,(1P8E14.5))
4023 FORMAT(6H0 ITER,2X, (9I11))
5010 FORMAT(1H0,9X,3HL = I4,7X,3MT = 0PF8.1,4H R= 1PE10.3)
5011 FORMAT(7H KEY ,(8I14))
END

```

```

C MATRIX INVERSION WITH ACCOMPANYING SOLUTION OF LINEAR EQUATIONS
C
C SUBROUTINE MATINV(A,N,B,M,DETERM)
C
C DIMENSION IPIVOT(10),A(10,10),B(10,1),INDEX(10,2),PIVOT(10)
C EQUIVALENCE (IROW,JROW), (ICOLUMN,JCOLUMN), (AMAX, T, SWAP)
C
C INITIALIZATION
C
10 DETERM=1.0
15 DO 20 J=1,N
20 IPIVOT(J)=0
30 DO 550 I=1,N
C
C SEARCH FOR PIVOT ELEMENT
C
40 AMAX=0.0
45 DO 105 J=1,N
50 IF (IPIVOT(J)-1) 60, 105, 60
60 DO 100 K=1,N
70 IF (IPIVOT(K)-1) 80, 100, 740
80 IF (ABSF(AMAX)-ABSF(A(J,K))) 85, 100, 100
85 IROW=J
90 ICOLUMN=K
95 AMAX=A(J,K)
100 CONTINUE
105 CONTINUE
110 IPIVOT(ICOLUMN)=IPIVOT(ICOLUMN)+1
C
C INTERCHANGE ROWS TO PUT PIVOT ELEMENT ON DIAGONAL
C
130 IF (IROW-ICOLUMN) 140, 260, 140
140 DETERM=-DETERM
150 DO 200 L=1,N
160 SWAP=A(IROW,L)
170 A(IROW,L)=A(ICOLUMN,L)
200 A(ICOLUMN,L)=SWAP
205 IF(M) 260, 260, 210
210 DO 250 L=1, M
220 SWAP=B(IROW,L)
230 B(IROW,L)=B(ICOLUMN,L)
250 B(ICOLUMN,L)=SWAP
260 INDEX(I,1)=IROW
270 INDEX(I,2)=ICOLUMN
310 PIVOT(I)=A(ICOLUMN,ICOLUMN)
320 DETERM=DETERM*PIVOT(I)
C
C DIVIDE PIVOT ROW BY PIVOT ELEMENT
C
330 A(ICOLUMN,ICOLUMN)=1.0
340 DO 350 L=1,N
350 A(ICOLUMN,L)=A(ICOLUMN,L)/PIVOT(I)
355 IF(M) 380, 380, 360
360 DO 370 L=1,M

```

```

370 B(ICOLUMN,L)=B(ICOLUMN,L)/PIVOT(I)
C
C      REDUCE NON-PIVOT ROWS
C
380 DO 550 L1=1,N
390 IF(L1-ICOLUMN) 400, 550, 400
400 T=A(L1,ICOLUMN)
420 A(L1,ICOLUMN)=0.0
430 DO 450 L=1,N
450 A(L1,L)=A(L1,L)-A(ICOLUMN,L)*T
455 IF(M) 550, 550, 460
460 DO 500 L=1,M
500 B(L1,L)=B(L1,L)-B(ICOLUMN,L)*T
550 CONTINUE
C
C      INTERCHANGE COLUMNS
C
600 DO 710 I=1,N
610 L=N+1-I
620 IF (INDEX(L,1)-INDEX(L,2)) 630, 710, 630
630 JROW=INDEX(L,1)
640 JCOLUMN=INDEX(L,2)
650 DO 705 K=1,N
660 SWAP=A(K,JROW)
670 A(K,JROW)=A(K,JCOLUMN)
700 A(K,JCOLUMN)=SWAP
705 CONTINUE
710 CONTINUE
740 RETURN
END
SUBROUTINE SORTMC(MC,NS)
DIMENSION MC(1),MD(50)
DO 2 I=1,NS
2 MD(I)=I
K1=NS-1
DO 20 J1=1,K1
I2=J1+1
DO 20 I1=I2,NS
IF(MC(J1)-MC(I1))20,20,10
10 IT=MC(J1)
MC(J1)=MC(I1)
MC(I1)=IT
IT2=MD(J1)
MD(J1)=MD(I1)
MD(I1)=IT2
20 CONTINUE
DO 30 I=1,NS
30 MC(I)=MD(I)
RETURN
END

```

| DATA | DRY AIR | 34 | C | 0 | 0 | N | 0 | CO | CO ₂ | N ₂ | NO ₂ | NO | 02 ⁺ | 02 ⁻ | 02 | 02 ⁺ | 02 ⁻ | 0 | 0 | NE | NE | |
|-------------------|-------------------|---------|---------|---------|---------|---------|---------|-----|-----------------|-----------------|-----------------|-----------------|-----------------|-----------------|-----------------|-----------------|-----------------|-----|-----|-----|-----|-----|
| 1 | 0 | 0 | 0 | 0 | 0 | 0 | 0 | C | C ⁺⁺ | N | N ⁺⁺ | 0 | 0 | 0 | 0 | |
| CO ₂ | NO ₂ | 0.9 | 0.9 | 0.9 | 0.9 | 0.9 | 0.9 | C | C ⁺⁺ | N | N ⁺⁺ | 0 | 0 | 0 | 0 | |
| O ⁺⁺ | O ⁺⁺ | 0.00033 | 0.00033 | 0.00033 | 0.00033 | 0.00033 | 0.00033 | A | A ⁺⁺ | 0.0 | 0.0 | 0.0 | 0.0 | |
| E- | E- | 1.0 | 1.0 | 1.0 | 1.0 | 1.0 | 1.0 | 1.0 | 1.0 | 1.0 | 1.0 | 1.0 | 1.0 | 1.0 | 1.0 | 1.0 | 1.0 | 1.0 | 1.0 | 1.0 | 1.0 | 1.0 |
| 1002 | 2N ₂ | 1 | 1 | 1 | 1 | 1 | 1 | 1 | 1 | 1 | 1 | 1 | 1 | 1 | 1 | 1 | 1 | 1 | 1 | 1 | 1 | 1 |
| 1002 | 9NO | 1 | 1 | 1 | 1 | 1 | 1 | 1 | 1 | 1 | 1 | 1 | 1 | 1 | 1 | 1 | 1 | 1 | 1 | 1 | 1 | 1 |
| 1002 | 9NO ₂ | 1 | 1 | 1 | 1 | 1 | 1 | 1 | 1 | 1 | 1 | 1 | 1 | 1 | 1 | 1 | 1 | 1 | 1 | 1 | 1 | 1 |
| 1002 | 1002 | 1 | 1 | 1 | 1 | 1 | 1 | 1 | 1 | 1 | 1 | 1 | 1 | 1 | 1 | 1 | 1 | 1 | 1 | 1 | 1 | 1 |
| 1002 | 1102 | 1 | 1 | 1 | 1 | 1 | 1 | 1 | 1 | 1 | 1 | 1 | 1 | 1 | 1 | 1 | 1 | 1 | 1 | 1 | 1 | 1 |
| 1002 | 1202 | 1 | 1 | 1 | 1 | 1 | 1 | 1 | 1 | 1 | 1 | 1 | 1 | 1 | 1 | 1 | 1 | 1 | 1 | 1 | 1 | 1 |
| 13E- | 13E- | 1 | 1 | 1 | 1 | 1 | 1 | 1 | 1 | 1 | 1 | 1 | 1 | 1 | 1 | 1 | 1 | 1 | 1 | 1 | 1 | 1 |
| 14C | 14C | 1 | 1 | 1 | 1 | 1 | 1 | 1 | 1 | 1 | 1 | 1 | 1 | 1 | 1 | 1 | 1 | 1 | 1 | 1 | 1 | 1 |
| 15C ⁺ | 15C ⁺ | 1 | 1 | 1 | 1 | 1 | 1 | 1 | 1 | 1 | 1 | 1 | 1 | 1 | 1 | 1 | 1 | 1 | 1 | 1 | 1 | 1 |
| 16C ⁺⁺ | 16C ⁺⁺ | 1 | 1 | 1 | 1 | 1 | 1 | 1 | 1 | 1 | 1 | 1 | 1 | 1 | 1 | 1 | 1 | 1 | 1 | 1 | 1 | 1 |
| 17C ⁺⁺ | 17C ⁺⁺ | 1 | 1 | 1 | 1 | 1 | 1 | 1 | 1 | 1 | 1 | 1 | 1 | 1 | 1 | 1 | 1 | 1 | 1 | 1 | 1 | 1 |
| 18N ⁺ | 18N ⁺ | 1 | 1 | 1 | 1 | 1 | 1 | 1 | 1 | 1 | 1 | 1 | 1 | 1 | 1 | 1 | 1 | 1 | 1 | 1 | 1 | 1 |
| 19N ⁺ | 19N ⁺ | 1 | 1 | 1 | 1 | 1 | 1 | 1 | 1 | 1 | 1 | 1 | 1 | 1 | 1 | 1 | 1 | 1 | 1 | 1 | 1 | 1 |
| 20N ⁺⁺ | 20N ⁺⁺ | 1 | 1 | 1 | 1 | 1 | 1 | 1 | 1 | 1 | 1 | 1 | 1 | 1 | 1 | 1 | 1 | 1 | 1 | 1 | 1 | 1 |
| 21N ⁺⁺ | 21N ⁺⁺ | 1 | 1 | 1 | 1 | 1 | 1 | 1 | 1 | 1 | 1 | 1 | 1 | 1 | 1 | 1 | 1 | 1 | 1 | 1 | 1 | 1 |
| 220- | 220- | 1 | 1 | 1 | 1 | 1 | 1 | 1 | 1 | 1 | 1 | 1 | 1 | 1 | 1 | 1 | 1 | 1 | 1 | 1 | 1 | 1 |
| 230 | 230 | 1 | 1 | 1 | 1 | 1 | 1 | 1 | 1 | 1 | 1 | 1 | 1 | 1 | 1 | 1 | 1 | 1 | 1 | 1 | 1 | 1 |
| 240 ⁺ | 240 ⁺ | 1 | 1 | 1 | 1 | 1 | 1 | 1 | 1 | 1 | 1 | 1 | 1 | 1 | 1 | 1 | 1 | 1 | 1 | 1 | 1 | 1 |
| 250 ⁺⁺ | 250 ⁺⁺ | 1 | 1 | 1 | 1 | 1 | 1 | 1 | 1 | 1 | 1 | 1 | 1 | 1 | 1 | 1 | 1 | 1 | 1 | 1 | 1 | 1 |
| 260 ⁺⁺ | 260 ⁺⁺ | 1 | 1 | 1 | 1 | 1 | 1 | 1 | 1 | 1 | 1 | 1 | 1 | 1 | 1 | 1 | 1 | 1 | 1 | 1 | 1 | 1 |
| 27A | 27A | 1 | 1 | 1 | 1 | 1 | 1 | 1 | 1 | 1 | 1 | 1 | 1 | 1 | 1 | 1 | 1 | 1 | 1 | 1 | 1 | 1 |
| 28A ⁺ | 28A ⁺ | 1 | 1 | 1 | 1 | 1 | 1 | 1 | 1 | 1 | 1 | 1 | 1 | 1 | 1 | 1 | 1 | 1 | 1 | 1 | 1 | 1 |
| 29A ⁺⁺ | 29A ⁺⁺ | 1 | 1 | 1 | 1 | 1 | 1 | 1 | 1 | 1 | 1 | 1 | 1 | 1 | 1 | 1 | 1 | 1 | 1 | 1 | 1 | 1 |
| 30A ⁺⁺ | 30A ⁺⁺ | 1 | 1 | 1 | 1 | 1 | 1 | 1 | 1 | 1 | 1 | 1 | 1 | 1 | 1 | 1 | 1 | 1 | 1 | 1 | 1 | 1 |

-849307-16+173245-11-140657-07+594282-04+318229+00+521173+00-271900+04
 C0+ G HUG
 +460833-12-616285-08+370220-04+338724+00+82497+00+295990+05
 C0+ G HUG
 -746882-16+156618-1-131173-07+575350-04+315780+00+463502+00
 N2+ HUG
 +112500-15-197500-11+101875-07+487500-05+350300+00+326360+00+359310+05
 N2+ HUG
 -799242-16+160889-11-128693-07+534354-04+136193+00+534000+00+234880+05
 N0+ HUG
 -506723-16+919526-12-790161-08+450077-04+362972+00+543600+00-104000+04
 07- HUG
 -458333-16+107500-11-965042-08+446063-04+348223+00+450240+00+277900+05
 02+ HUG
 +187066-16-461230-12+394596-08-110584-04+262088+00+409580+00+169990+05
 C+ ARL
 -283335-13+475717-09-281739-05+256976+00+391190+00+429832+05
 C+ ARL

 -349970-16+656694-12-329578-08+646177-05+245587+00+439243+00+112535+05
 N+ HUG
 +208333-17-125833-12+189792-08-904416-09+267780+00+390040+00+48050406
 N+ HUG
 +187066-16-461230-12+394596-08-110584-04+262088+00+409580+00+169990+05
 C+ ARL

 -349970-17-102418-12+154998-08-740637-05+764639+00+429018+00+589890+04
 0- HUG
 +358333-17+208333-13-314083-09+949667-06+249133+00+442384+00+373000+05
 0+ HUG

 +250000+00+436539+00
 +250000+00+334163+00
 +408332-13-387855-09-672983-06+268178+00+473701+00+363436+05
 A+ ARL

 -524998-13+952140-09-662963-05+272338+00+361947+00+497311+05
 NE+ ARL

 -154101-07+227960-03
 +275398+01-939650+04
 C02 G
 -137572-07+105309-03
 +323681+01+873400+03
 N02 G
 -134856-07+190882-03
 +323038+01+347390+04
 01 G
 +797505-09-652278-05+442597+00-21177+00-271900+04
 CU G
 -380599-09+183105-04+347267+00+462605+00+295990+05
 C0+ G
 +342516-09-518341-06+420387+00-148402+00
 N2 G
 -120571-08+269412-04+372503+00+188903+00+359310+05
 N2+ G
 +875835-10+263325-05+418585+00+100750+0; +214800+04
 NO G

Unclassified

Security Classification

DOCUMENT CONTROL DATA - R&D

(Security classification of title, body of abstract and indexing annotation must be entered when the overall report is classified)

| | | | |
|--|--|---|-----------------|
| 1. ORIGINATING ACTIVITY (Corporate author) | | 2a. REPORT SECURITY CLASSIFICATION | |
| Lockheed Palo Alto Research Laboratory Lockheed Missiles & Space Company Palo Alto, California | | Unclassified | |
| 3. REPORT TITLE | | 2b. GROUP | |
| ABSORPTION COEFFICIENTS OF HEATED AIR: A COMPILATION TO 24,000°K Volume I | | | |
| 4. DESCRIPTIVE NOTES (Type of report and inclusive dates) | | | |
| Final Report 1 April 1964 to 30 July 1965 | | | |
| 5. AUTHOR(S) (Last name, first name, initial) | | | |
| Churchill, D.R.; Armstrong, B.H.; and Mueller, K.G. | | | |
| 6. REPORT DATE | | 7a. TOTAL NO. OF PAGES | 7b. NO. OF REFS |
| September 1965 | | 120 | 62 |
| 8a. CONTRACT OR GRANT NO. | | 9a. ORIGINATOR'S REPORT NUMBER(S) | |
| AF 29(601)-6320 | | AFWL-TR-65-132, Vol. I | |
| b. PROJECT NO. | | 9b. OTHER REPORT NO(S) (Any other numbers that may be assigned this report) | |
| c. Subtask 07.003 | | Lockheed Report No. 4-77-65-1 | |
| d. | | | |
| 10. AVAILABILITY/LIMITATION NOTICES | | | |
| DDC release to OTS is authorized. | | | |
| 11. SUPPLEMENTARY NOTES | | 12. SPONSORING MILITARY ACTIVITY | |
| | | Air Force Weapons Laboratory (WLRTH) Kirtland Air Force Base, New Mexico | |
| 13. ABSTRACT | | | |
| An extensive tabulation of absorption coefficients of heated air has been carried out with the aid of several large digital computer programs. These tables supersede the previous ones computed at Lockheed by Meyerott, Sokoloff, and Nicholls in 1959. Tables are presented for temperatures at every 1000°K between 1000°K and 24,000°K and for eight densities between ten times normal atmospheric to 10^{-6} times normal. Absorption coefficients are individually listed for each of 14 contributing absorbers. The photon energy range is 0.6-10.7 eV with a partition interval of 0.1 eV. | | | |

Unclassified

Security Classification

| 14 KEY WORDS | LINK A | | LINK B | | LINK C | |
|---|--------|----|--------|----|--------|----|
| | ROLE | WT | ROLE | WT | ROLE | WT |
| Absorption coefficients of heated air | | | | | | |
| Spectral absorption of air diatomic molecules | | | | | | |
| Spectral absorption of air atoms | | | | | | |
| Air thermal radiation | | | | | | |

INSTRUCTIONS

1. ORIGINATING ACTIVITY: Enter the name and address of the contractor, subcontractor, grantee, Department of Defense activity or other organization (corporate author) issuing the report.

2a. REPORT SECURITY CLASSIFICATION: Enter the overall security classification of the report. Indicate whether "Restricted Data" is included. Marking is to be in accordance with appropriate security regulations.

2b. GROUP: Automatic downgrading is specified in DoD Directive 5200.10 and Armed Forces Industrial Manual. Enter the group number. Also, when applicable, show that optional markings have been used for Group 3 and Group 4 as authorized.

3. REPORT TITLE: Enter the complete report title in all capital letters. Titles in all cases should be unclassified. If a meaningful title cannot be selected without classification, show title classification in all capitals in parenthesis immediately following the title.

4. DESCRIPTIVE NOTES: If appropriate, enter the type of report, e.g., interim, progress, summary, annual, or final. Give the inclusive dates when a specific reporting period is covered.

5. AUTHOR(S): Enter the name(s) of author(s) as shown on or in the report. Enter last name, first name, middle initial. If military, show rank and branch of service. The name of the principal author is an absolute minimum requirement.

6. REPORT DATE: Enter the date of the report as day, month, year; or month, year. If more than one date appears on the report, use date of publication.

7a. TOTAL NUMBER OF PAGES: The total page count should follow normal pagination procedures, i.e., enter the number of pages containing information.

7b. NUMBER OF REFERENCES: Enter the total number of references cited in the report.

8a. CONTRACT OR GRANT NUMBER: If appropriate, enter the applicable number of the contract or grant under which the report was written.

8b, 8c, & 8d. PROJECT NUMBER: Enter the appropriate military department identification, such as project number, subproject number, system numbers, task number, etc.

9a. ORIGINATOR'S REPORT NUMBER(S): Enter the official report number by which the document will be identified and controlled by the originating activity. This number must be unique to this report.

9b. OTHER REPORT NUMBER(S): If the report has been assigned any other report numbers (either by the originator or by the sponsor), also enter this number(s).

10. AVAILABILITY/LIMITATION NOTICES: Enter any limitations on further dissemination of the report, other than those

imposed by security classification, using standard statements such as:

- (1) "Qualified requesters may obtain copies of this report from DDC."
- (2) "Foreign announcement and dissemination of this report by DDC is not authorized."
- (3) "U. S. Government agencies may obtain copies of this report directly from DDC. Other qualified DDC users shall request through _____."
- (4) "U. S. military agencies may obtain copies of this report directly from DDC. Other qualified users shall request through _____."
- (5) "All distribution of this report is controlled. Qualified DDC users shall request through _____."

If the report has been furnished to the Office of Technical Services, Department of Commerce, for sale to the public, indicate this fact and enter the price, if known.

11. SUPPLEMENTARY NOTES: Use for additional explanatory notes.

12. SPONSORING MILITARY ACTIVITY: Enter the name of the departmental project office or laboratory sponsoring (paying for) the research and development. Include address.

13. ABSTRACT: Enter an abstract giving a brief and factual summary of the document indicative of the report, even though it may also appear elsewhere in the body of the technical report. If additional space is required, a continuation sheet shall be attached.

It is highly desirable that the abstract of classified reports be unclassified. Each paragraph of the abstract shall end with an indication of the military security classification of the information in the paragraph, represented as (TS), (S), (C), or (U).

There is no limitation on the length of the abstract. However, the suggested length is from 150 to 225 words.

14. KEY WORDS: Key words are technically meaningful terms or short phrases that characterize a report and may be used as index entries for cataloging the report. Key words must be selected so that no security classification is required. Identifiers, such as equipment model designation, trade name, military project code name, geographic location, may be used as key words but will be followed by an indication of technical context. The assignment of links, rules, and weights is optional.